CELL CYCLE DEPENDENT ASSOCIATION AND ACTIVATION OF A HISTONE H1.3-HDAC3 COMPLEX

A DISSERTATION

SUBMITTED IN PARTIAL FULFILLMENT OF THE REQUIREMENTS FOR THE DEGREE OF DOCTOR OF PHILOSOPHY

IN THE GRADUATE SCHOOL OF THE

TEXAS WOMAN'S UNIVERSITY

COLLEGE OF ARTS AND SCIENCES

BY

HEMANGI PATIL, B.S.

DENTON, TEXAS

DECEMBER 2009

TEXAS WOMAN'S UNIVERSITY
DENTON, TEXAS

November 10, 2009

To the Dean of the Graduate School:

I am submitting here with a dissertation written by Hemangi Patil entitled "Cell Cycle Dependent Association and Activation of A Histone H1.3-HDAC3 Complex." I have examined this dissertation for form and content and recommend that it be accepted in partial fulfillment of the requirements for the degree of Doctor of Philosophy with a major in Molecular Biology.

Dr. Michael Bergel, Major Professor

We have read this dissertation and recommend its acceptance:

Heather Conrad Webb

Nathaniel Mills

Department Chair

Accepted:

Jennifer Martin

Dean of the Graduate School

ACKNOWLEDGMENTS

I am grateful to Dr. Michael Bergel for his continuous support and guidance for this project. I am also grateful to Dr. Heather Conrad-Webb, Dr. DiAnna Hynds, Dr. Nathaniel Mills, and Dr. Douglas Root for serving on my PhD committee. I thank them for their input and critical evaluation of this research.

I also thank Dr. Michael Bustin (National Institutes of Health) for the anti-histone H1 antibody, Dr. Lon Turnbull (University of North Texas) for help with confocal imaging and Dr. Weihang Chai (Washington State University) for the HeLa cells.

I thank my lab colleague and friend Ms. Mangalam Subramanian and Mrs. Rhiannon Wold Gonzales for their collaboration and help with histone deacetylase (HDAC) assay. I also thank my lab colleagues for their friendship and encouragement throughout this project.

I would also like to thank my loving and caring husband, Mr. Mangesh Patil, for his support and patience through out this entire journey. I am also thankful to my family for their support.

Finally, I would like to thank Ms. Michan Chowritmootoo for her help in formatting this document.

ABSTRACT

HEMANGI PATIL

CELL CYCLE DEPENDENT ASSOCIATION AND ACTIVATION OF A HISTONE H1.3-HDAC3 COMPLEX

DECEMBER 2009

Eukaryotic DNA is organized with nucleoproteins into a dynamic structure named chromatin. Chromatin compaction and decompaction plays an important role in modulation of various DNA-dependent functions in the cell. Histone deacetylases (HDACs), which remove acetyl groups from core histone proteins, regulate the compaction of the chromatin fiber, thus modulating gene transcription levels. Chromatin binding proteins, such as linker histone H1, are also known to cause chromatin compaction. Histone H1 and HDAC3 were independently reported to be involved in the regulation of mitosis. The hypothesis of this study was that histone H1 and HDAC3 could form a complex that will be involved in chromatin condensation and mitosis regulation. Co-immunoprecipitation assay results demonstrated the formation of stable complexes between HDAC3 and histone H1.3 in HeLaS3 human cervical carcinoma epithelial cells. Although the amount of complex increased during the late-G_2 and mitosis phases of the cell cycle, the complex was activated for chromatin deacetylation only in mitosis. Studies *in vitro* demonstrated that HDAC3 was highly phosphorylated on Ser-424 in the mitotic complex but not the

G_2 complex. Further studies also showed that HDAC3 from late-G_2 complex can be activated *in vitro* by phosphorylating on Ser-424 with casein kinase II (CK2). Based on the immunocytochemistry and confocal imaging studies, the HDAC3-H1.3 complexes co-localized with mitotic polar microtubules. The complex included also silencing mediator of retinoic acid receptor and thyroid hormone receptor (SMRT), glyceraldehyde 3-phosphate dehydrogenase (GAPDH) and annexin I. GAPDH, annexin I and histone H1 are known to bind tubulins and thus increases confidence that they may tether HDAC3 to the polar spindle mitotic microtubules. This report is the first, to the best of our knowledge, in which histone H1 and a class I HDAC are shown to form a complex. This is also the first record of a co-localization of histone H1 with microtubules in an animal kingdom.

TABLE OF CONTENTS

Page

LIST OF TABLES

LIST OF FIGURES

CHAPTER I

INTRODUCTION

Cell Cycle Regulation

The eukaryotic cell cycle is a highly regulated by series of events composed of four main phases—Gap 1 (G_1 phase), Synthesis (S phase), Gap 2 (G_2 phase), and mitosis (M phase) (Karp, 2005). The correct order and timing of events during the cell division process is tightly regulated and coordinated. In eukaryotic cells, the order of the cell division events is reinforced by the dependence of one event on another and by the networking of the cell cycle machinery with the control system. Different types of regulatory proteins, called cyclins, are synthesized at a specific cell cycle phases. The major components of the cell cycle control system are the family of enzymes called as cyclin-dependent kinases (Cdks). Cdks are activated by binding to cyclins (Karp, 2005). The cyclins form the regulatory subunit, whereas Cdks form the catalytic subunit of an active cyclin-Cdk complex which phosphorylates the components of the cell cycle machinery resulting in the initiation of the cell cycle event (Karp, 2005). During cell division, the cell passes through regulatory transition points called cell cycle checkpoints (Lodish, 2004). The known eukaryotic cell cycle checkpoints are—the DNA damage checkpoints between G_1 phase and S phase and between G_2 and M phase, DNA damage checkpoint in G_1 and S phases,

unreplicated DNA checkpoint at the entry of M phase, spindle assembly checkpoint at metaphase, and chromosome-segregation checkpoint at telophase (Fig. 1) (Lodish, 2004).

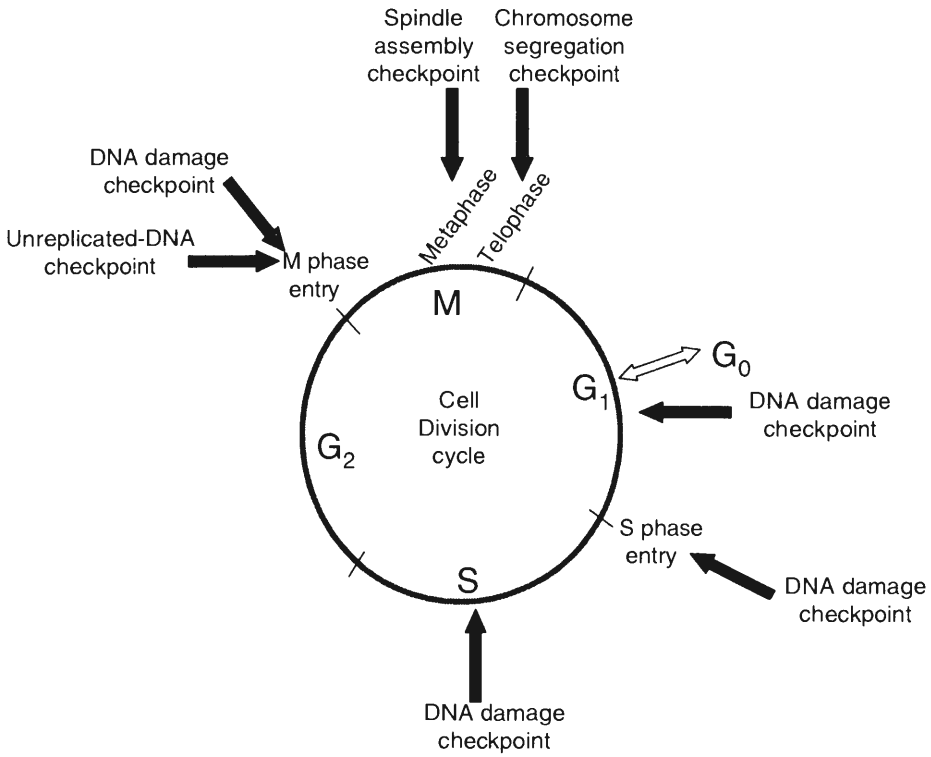

Figure 1: Cell cycle and cell cycle checkpoints.

The DNA damage checkpoints activate ataxia telangiectasia mutated (ATM) or ataxia telangiectasia Rad3-related (ATR) kinases, which can initiate Chk1/2-Cdc25A and p53-p21 pathways causing arrest in the cell cycle. At the entry of M phase the transition into mitosis is regulated by DNA damage and completion of DNA replication. At the end of metaphase the initiation of sister-chromatid separation can be blocked if the mitotic spindles are not fully

assembled. Telophase events can be stopped by blocking activation of cdh1 due to abnormal chromosome-segregation (Lodish, 2004). Among all the checkpoints, mitotic checkpoints are considered vital.

Regulation of Mitosis

The onset of mitosis is triggered by activation of the mitotic Cdk1-cyclinB (cdc2-cyclinB) complex, which in turn is involved in phosphorylation of lamins, kinesin related motor proteins, microtubule binding proteins, condensins and golgi matrix components (Kimura, 1998; Lowe, 1998; Nigg, 1995). When activated these complexes trigger chromosome condensation and mitotic spindle assembly. During the early mitosis, Polo-like kinases (Plks) regulate centrosome maturation in human cells (Lane, 1996); while the separation of centrosomes is regulated by NIMA-related kinase 2 (Nek2) that phosphorylates centrosomal protein, and by centrosomal Nek2-associated protein 1 (C-Nap1) that dissolves structural complexes that tethers duplicated centrosomes (Fry, 1998). Kinesin-related motor proteins like Eg5 (Sawin, 1995a), and aurora A family members (Bischoff, 1999) are also involved in centrosome separation and activation. During early mitosis histone H1 is heavily phosphorylated by Cdk1-cyclin B and histone H3 serine 10 (H3S10) is phosphorylated by Aurora (Li, 2006) and never in mitosis A (NIMA) related kinases (De Souza, 2000). Prior to the metaphase checkpoint securin prevents the protease, separase, from degrading the multiprotein complex cohesin that keeps sister-chromatids together (Karp, 2005; Lodish, 2004). Anaphase starts by separation of the sister-chromatids, which is

triggered by the degradation of an inhibitor securin. Even though many protein complexes are linked to mitosis, the mitosis progression is not completely understood. Along with the mitotic checkpoint system, the progress of mitosis is highly coordinated with the dynamic changes in the mitotic spindle fibers, which is discussed next.

Spindle fiber dynamics during mitosis. The mitotic spindle is a bipolar array of microtubules. The basic building block of microtubules is a tubulin dimer of α-tubulin and β-tubulin attached with non-covalent interactions. Tubulin dimers join head to tail in the same orientation forming a linear protofilament. A microtubule is formed by thirteen parallel protofilaments forming a hollow cylinder. Because all the tubulin dimers in the microtubule filaments orient in the same way, microtubules form one end called minus-end where α-tubulin is exposed and is embedded in a spindle pole; while the other end, called as plus-end pointing outwards from the pole where β-tubulin is exposed (Lodish, 2004). The spindle assembly during mitosis depends on the instability and treadmilling of microtubule polymers, the microtubule stabilizing and destabilizing proteins, and the dynein and kinesin family proteins (Lodish, 2004). During mitosis three distinct types of microtubules—polar, astral and kinetochore are formed in the spindle (Fig. 2). When the plus-end of microtubules from two opposite poles overlap with each other, that results in antiparrallel arrays of microtubules; these are called as polar microtubules. The microtubules that form asters radiating out from centrosome towards the cell cortex and helping position the mitotic

apparatus are called astral microtubules. Microtubules that attach to the kinetochore of the chromosomes are kinetochore microtubules (Lodish, 2004).

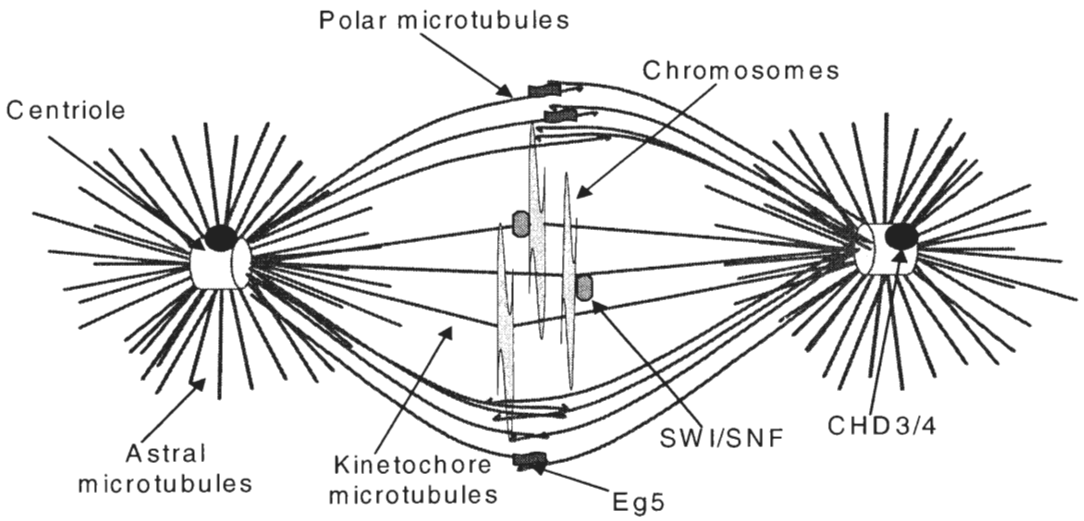

Figure 2: Mitotic spindle microtubules.

Chromosomes as well as centrosomes participate in spindle assembly. Chromosomes help to organize mitotic spindles (Li, 2004); while centrosomes provide site for nucleation and organization of the microtubules (Karp, 2005). Many transcription factors and components of chromatin remodeling complexes have been shown to localize to mitotic centrosomes, mitotic spindles and poles. The human switch/sucrose nonfermentable-B (SWI/SNF-B) chromatin-remodeling complex is seen to localize at kinetochore during mitosis (Xue, 2000). DNA binding proteins—CHD3 and CHD4 are also shown to be required for anchoring of γ–tubulin to the centrosomes (Sillibourne, 2007). A regulatory motor

protein—Eg5 organizes the polar microtubule meshwork by crosslinking the antiparrallel polar microtubules (Valentine, 2006).

Chromatin Regulation Along the Cell Cycle

In the eukaryotic cells, the higher-order condensed chromatin structure is poorly understood. The chromatin structure undergoes dynamic changes throughout the cell cycle with the highest compaction in metaphase chromosome and the least compaction during interphase. The most recent proposal is that the mitotic chromosomes condense by the gradual folding of chromatin fibers from a 30 nm fiber to more compact structures (Kireeva, 2004). A progressive decondensation of chromatin follows from G_1 to S phase (Zhao, 2001); while a progressive condensation follows during late S phase and G_2 phase (Barlow, 1977; Colomb, 1992).

Changes in the intranuclear chromatin location occur with the change in the cell cycle stages. The early replicating regions preferably locate to the nuclear interior while the late replicating regions are localized to nuclear periphery. This pattern is established during early G_1 phase (Tumbar, 1999). The decondensation of the chromatin is accompanied by re-localization of the chromatin region from the nuclear periphery to the nuclear interior (Tumbar, 1999). According to the cell cycle stages the chromosome structure and its organization shows dynamic changes. A short discussion of chromatin and its organization is given in the following topics.

Chromatin

The human genome is compacted over 10,000 fold in a eukaryotic nucleus. This is achieved by organizing the double stranded DNA in association with proteins, in a complex structure, termed chromatin. Chromatin is a higher order nucleoprotein complex with the nucleosome as its basic unit. The electron microscopic examination of chromatin, at low salt concentration, shows "beads on a string" structure. The string is free DNA called "linker-DNA" connecting nucleosomes that appear as beads. Linker histones bind to the nucleosomes and fold the chromatin structure further into a higher level. The following topics briefly discuss this chromatin organization.

Nucleosomal Core Particle

Nucleosomes are 11 nm in diameter and are composed of DNA and core histone proteins (Lodish, 2004). Each nucleosomal core particle is composed of an octamer of core histones (two each of histones H2A, H2B, H3 and H4), around which 1.65 turns of a left-handed helical DNA (~147 bp) is wrapped (Libertini, 1988; Lodish, 2004) (Fig. 3).

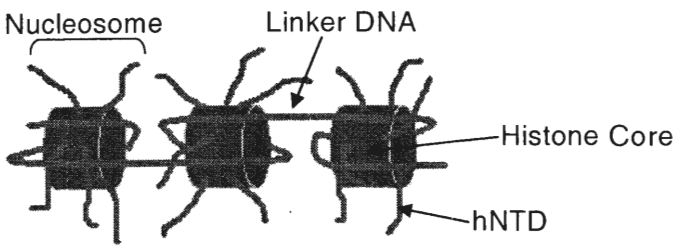

Figure 3: DNA organization in nucleosomal structure.

Core histones are small (11-15 kDa), highly basic proteins which are associated with the DNA . The core histones share a common structural motif, a histone-fold domain, and a unstructured histone N-terminal domain (hNTD) (Luger, 1997). The C-terminal regions of most core histones are tightly folded in the octamer structure while the hNTD is structurally non-conserved and freely extends out (Luger, 1998). The N-terminal tails of the core histones play an important role in the assembly of nucleosomes into the higher order chromatin fiber. Being an excellent substrate for reversible posttranslational modifications, the tails modulate a dynamic interaction between the nucleosomes within the chromatin fibers. On the hNTDs, various lysine residues (K) are the sites for acetylation, lysine and arginine residues are sites for methylation; whereas serine and threonine residues are the sites for phosphorylation. In addition, the tails can serve as recognition sites for transcription remodeling machinery, and can also interact with the other nuclear proteins responsible for chromatin structure modulation (Watson, 2004). The 10 nm diameter nucleosomal structure is further folded into a 30 nm fiber by the binding of the linker histones to increases the degree of chromatin compaction (Libertini, 1988). Further folding of these fibers generates more compacted higher-order chromatin structures as discussed in the next topic.

Higher Order Chromatin Structure

The 30 nm fiber is stabilized by binding of histone H1 and by interactions of the core histone hNTDs. The chromatin is further compacted into a 300 nm

chromosomal scaffold structure by forming loops of 40-90 kb. The chromosomal protein scaffold is the nuclear structure which anchors the loops to form chromatin fibers of 300 nm during interphase, and 700 nm diameter which represents mitotic chromatids. The two sister chromatids make the mitotic chromosome with a diameter of 1400 nm, the most compact form of the chromatin (Fig. 4). Topoisomerase II and structural maintenance of chromosomes (SMC) protein classes are known to contribute to the higher order scaffold structure (Lewin, 2000; Lodish, 2004; Watson, 2004). Such compaction gives a highly protected form of DNA and makes DNA accessibility difficult for the regulatory proteins. These proteins locally regulate chromatin compaction by interacting with histones and therefore control the accessibility of DNA. Till today, the higher order chromatin structures are well studied, yet the progression of chromatin condensation during mitosis remains unclear.

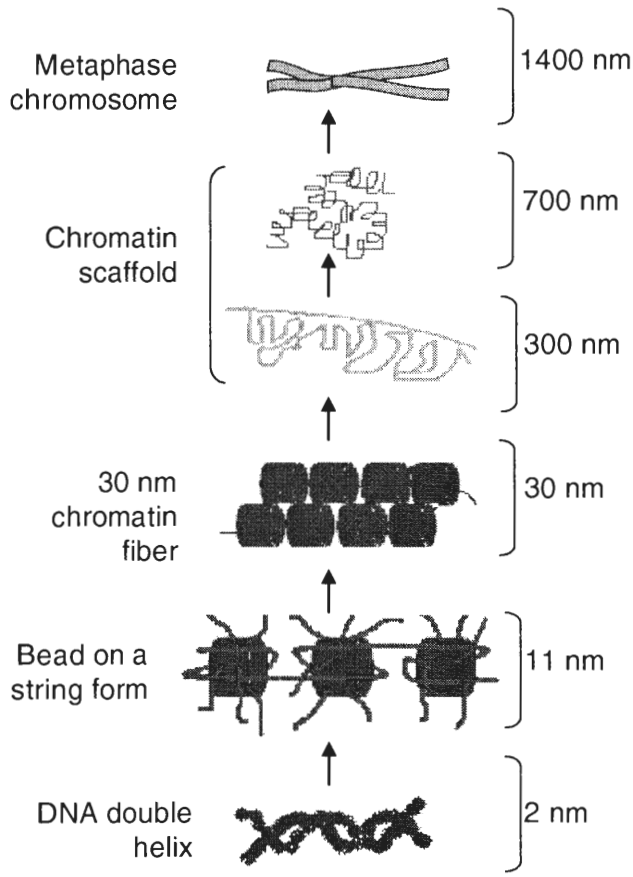

Figure 4: Packaging of dsDNA in to higher order chromatin .

Linker Histone (Histone H1)

The linker histones are composed of three distinct domains—the hNTD, a central globular winged helix domain, and a long (~100 amino acids) highly basic unstructured histone C-terminal domain (hCTD) (Wolffe, 1997). Binding of one molecule of histone H1 to one nucleosomal unit includes an extra of ~20 base pairs (bp) of DNA due to formation of a stem-loop structure in the linker-DNA (Bednar, 1998). Condensation and stabilization of the higher order chromatin

structure is mediated by histone H1 hCTDs (Carruthers, 2000; Lu, 2004). Histone H1 is regarded as a global repressor, acting by compacting the chromatin and blocking nonspecific transcription (Laybourn, 1991).

The number of histone H1 variants and their divergence is much greater than that of core histones. Somatic mammalian cells contain a total of eleven histone H1 variants. The seven major histone H1 variants in somatic cells are—H1.0, H1.1, H1.2, H1.3, H1.4, H1.5, (Albig, 1993) and H1X (Happel, 2005; Yamamoto, 1996). The spermatogenic variants are—H1t (Seyedin, 1980), H1T2 (Martianov, 2005) and HILS1 (Yan, 2003), and the oocytes variant is H1oo (Tanaka, 2003). Histone H1.0 variant is thought to be mainly restricted to non-proliferating and terminally differentiated cells (Zlatanova, 1994). Expression of the histone H1X gene is tissue specific. Linker histone variants like histone H1t (Lennox, 1984; Seyedin, 1981) and H1T2 (Martianov, 2005) are found in testis, H1LS1 (Yan, 2003) is found in spermatids and histone H1oo (Tanaka, 2003) is present in oocytes. Somatic histone H1 variants differ in their expression pattern during development and differentiation (Kochbin, 1994). They also differ in their phosphorylation during the cell cycle (Talasz, 1996).

Histone H1 is shown to play a role in the chromatin condensation during mitosis, and in the gene-specific transcription repression (Bustin, 2005; Herrera, 2000; Sarg, 2006; Vaquero, 2004). Because histone H1 is involved in chromatin folding, it is essential for mitotic condensation (Gurley, 1995). Histone H1 is heavily phosphorylated during mitosis when maximum chromatin compaction is

achieved (Gurley, 1995) and recent findings indicate that the phosphorylated histone H1 are dissociated from mitotic chromosomes (Bhattacharjee, 2006). However the mechanism of histone H1 participation in mitosis is not completely understood. Histone H1 specifically inhibits the core histone acetylation and helps maintain their deacetylated state (Herrera, 2000). Thus, histone H1 is regarded as a global repressor of transcription, acting by compacting the chromatin and blocking nonspecific transcription (Laybourn, 1991). Thus far histone H1 variants were thought to be redundant, but recent research has provided evidence for their specificity which is described in the following topics.

Regulation of Chromatin Structure and Function by Histone H1 Variants

The primary sequences of histone H1 variants are moderately conserved between animal species (Ponte, 1998). While the globular domain shows high sequence conservation, the hCTD shows sequence variation, indicating it is likely that functional heterogeneity of H1 variants is due to hCTD. The number of lysine residues and S/TPXK phosphorylation motifs of the hCTD are highly conserved in each variant (Ponte, 1998). The presence of more S/TPXK sites in the long hCTD of histone H1.4 and H1.5 may be responsible for their higher binding affinity to chromatin (Th'ng, 2005). Histone H1.2 and H1.1 shows the lowest binding affinity to chromatin. Histone H1.1 and H1.2 also show the presence of shorter hCTD as compare to other somatic histone H1 variants, which might contribute to their rapid fluorescence recovery after photobleaching (FRAP)

recovery time (Th'ng, 2005). Histone H1.0 and H1.3 binds to chromatin with the intermediate affinity and have highest lysine content (Th'ng, 2005).

Current FRAP experiments have also shown differences in binding affinities of histone H1 variants to the chromatin (Th'ng, 2005). Their movement and distribution in the chromatin environment could be influenced by post translational modifications such as phosphorylation (Hendzel, 2004; Lever, 2000; Th'ng, 2005), the core histone variant composition of the nucleosome (Ausió, 2001), the transcription activation pathways (Bustin, 2005), and the presence of other chromatin binding proteins such as high mobility group nucleosomal proteins (HMGNs), heterochromatin protein 1 (HP1), methyl CpG binding protein 2 (MeCP2) (Bustin, 2005; Catez, 2002; Luger, 2005). Using immunoflurescence study, Parseghian et al have demonstrated differences in the localization of histone H1 variants in human fibroblast cells (Parseghian, 2000). Histone H1.5 preferentially localizes to the nuclear periphery, histone H1.2 localization changes with the change on DNA content of the chromatin; whereas histone H1.3 and H1.4 demonstrate punctuate staining pattern (Parseghian, 2000). With chromatin immunoprecipitation (ChIP) analysis, it was shown that histone H1.5 is predominant and histone H1.3 and H1.4 are absent from the transcriptionally active chromatin; while inactive chromatin showed presence of all the histone H1 variants (Parseghian, 2001; Parseghian, 2000). Moreover, histone H1.2 is suggested to be responsible for basal level of chromatin compaction as it was seen to reside at a promoter site of transcriptionally induced genes (Parseghian,

2000). Using green fluroscent protein (GFP)-tagged histone H1 variants, Hendzel et al have studied their localization in human neuroblastoma cells, demonstrating that histone H1.0, H1.1, H1.2, and H1.3 are localized to the euchromatin region (Hendzel, 2004); and histone H1.4 and H1.5 were seen to be in the heterochromatic region (Th'ng, 2005). The immunoflurescence studies by Parseghian et al and GFP-tagged protein studies by Hendzel et al are not completely consistent as there are differences in the cell types used for the study, and the effect of the large GFP tag. Specific histone H1 variants also show distinct functionality, suggesting that the structural variability of histone H1 variant is functionally relevant.

Role of Histone H1 in Gene Expression and Cell Growth

Studies have shown that the loss of histone H1 in unicellular organisms can have severe consequences. In *Saccharomyces cerevisiae*, loss of H1 (Hho1p) can shortens cells life span as a result of defect in recombination (Downs, 2003). In *Tetrahymena thermophila*, loss of histone H1 results in enlarged nuclei and less condensed mitotic chromosomes (Shen, 1996). In mouse, knockout of a single histone H1 variant (H1c/H1.2, H1d/H1.3 or H1e/H1.4) causes no noticeable phenotype, but upregulation of remaining variants compensated the loss of a single variant and maintained a normal histone H1 to nucleosomal ratio (Fan, 2001). However, the triple knockout for mouse H1c, H1d, H1e results in a 50% decrease in the histone H1 to nucleosomal ratio (Fan, 2003), and reduces chromatin compaction, H4K12

acetylation, and H3K27 methylation (Fan, 2005). These studies in higher eukaryotes indicate that minimum levels of histone H1 are required for survival and proper functionality. Using short hairpin RNA (shRNA)–mediated knockdown study, Sancho et al have demonstrated that, histones H1.3, H1.2 and H1.4 are the variants to control gene expression, and they control high number of regulated genes (Sancho, 2008).

Histone H1 variants also act as regulators for specific genes. Overexpression of H1(0) and H1c show increase in transcription under mouse mammary tumor virus (MMTV) promoter (Gunjan, 1999), which suggests that a specific chromatin structure influenced by specific variants of histone H1 presence is required for binding of transcription factors. Histone H1b/H1.5 is linked to gene silencing (Kaludov, 1997). Gene specific effects of histone H1 are due to its interaction with DNA regulatory factors. Histone H1.1 associates with DNA binding protein barrier to autointegration factor (BAF) (Montes de Oca, 2005). Histone H1.5 association with transcription factor MSX1 is required for inhibition of specific target promoter (Lee, 2004b). Histone H1.4 associates with SirT1 and allows recruitment of HP1 causing heterochromatinization (Vaquero, 2004). Isolated histone H1.2 complex has recently been shown to acts as a repressor of p53 mediated transcription (Kim, 2008). In addition, histone H1.2 was shown to be involved in apoptosis induced by DNA double strand breaks (Konishi, 2003). Thus, histone H1 variants interaction with transcription factors

seems to be common mechanism for transcription regulation, and yet many histone variants remain to be studied for such a molecular mechanism.

Histone H1 and Cell Cycle

To meet the increased need of histone H1 during DNA replication, the histone H1 synthesis dramatically increases during S phase (Plumb, 1984). The rise in histone production is governed both by the cell cycle control system and by regulatory mechanisms that couple histone production to DNA synthesis. Except for histone H1.1-H1.5, other histone variants are expressed in a replication-independent manner during the cell cycle (Khochbin, 2001).

Studies have shown that the change in the expression of histone H1 variants can have effects on the cell cycle progression. Delay in cell cycle progression is seen due to overexpression of H1(0) in mouse 3T3 cells (Gunjan, 1999). Using inducible shRNA expression system, Sancho et al have showed that the depletion of histone H1.4 leads to cell death in human breast cancer cell line T47D and inhibition of histone H1.2 causes a G_1 arrest, defects in chromatin structure, and changes in expression of genes linked to cell cycle (Sancho, 2008). More studies need to be conducted to learn specific effects of histone H1 variants on cell cycle. Histone H1 has been viewed as a chromatin structural protein. However, recent studies have shed light on the involvement of histone H1 in the non-chromatin functions.

Non-Chromatin Functions of Histone H1

Recent studies in plant cells have helped to broaden perspective about histone H1, as it was found to participate as a structural component of the cellular microtubules. In the attempt to isolate the microtubule nuclei from *Tobacco* BY-2 cells, Hotta et al had identified histone H1 as a component of the microtubule organizing center (MTOC) (Hotta, 2007; Nakayama, 2008). Histone H1 forms a complex with α- and β-tubulin, and organizes the microtubules in asters. This finding suggests the ability of histone H1 to form a complex with tubulin and act as microtubule organizer (Hotta, 2007). The ability of tubulin and histone H1 to form complex *in vitro* has revealed that the tubulin dimer binds to histone H1 in 1:1 ratio (Nakayama, 2008). Furthermore, the immunoflurescence analysis in BY-2 cells has demonstrated localization of histone H1 on the nuclear surface, in contrast to the known localization of histone H1 in chromatin (Hotta, 2007). Further investigation of such non-chromatin function of histone H1 will help us to understand its wider role in cellular architecture.

Histone Deacetylases

The core histone deacetylation mechanism involves removal of acetyl groups from acetylated lysine residues of histones. Mammalian HDACs have been classified into four classes based on their homology to three distinct HDACs isolated from *Saccharomyces cerevisiae*. Class I HDACs (HDAC1, -2, -3, and -8) are closely related to Rpd3p transcription repressor of *Saccharomyces cerevisiae*. Class II HDACs (HDAC4, -5, -6, -7, -9, and -10) are homologous to

Hda1p (De Ruijter, 2003). Based on the similar domain organization of protein sequences class II HDACs are further sub-classified into class IIa (HDAC4, -5, -7, and -9) and class IIb (HDAC6 and -10) (Gregoretti, 2004). The most recently identified HDAC is HDAC11, which is classified as a class IV HDAC (Gregoretti, 2004). Class III HDACs (SirT1-7) are homologous to Sir2p and form structurally distinct class of NAD^+ dependent enzymes and they are located in the nucleus and the cytoplasm (Gray, 2001). The most of the HDACs require association with other proteins and/ or complexes in order to be enzymatically active. Following is a brief summary of various HDAC complexes.

HDAC Complexes

Recombinant HDAC1 and HDAC2 are inactive for deacetylation *in vitro*, suggesting their dependence on other cofactors or complexes (De Ruijter, 2003). *In vivo,* HDAC1 and HDAC2 are found in three protein complexes: Sin3, NuRD (Heinzel, 1997), and Co-REST (De Ruijter, 2003). HDAC1 and HDAC2 activity is regulated by their post-translational modification and interaction with co-repressors. Interestingly, hyper-phosphorylation of HDACs increases their deacetylation ability, but reduces their complex formation ability; whereas hypo-phosphorylation increases complex formation ability but decreases deacetylation activity (Galasinski, 2002). HDAC3 displays some distinct characteristics compared to other members of class I HDACs, requiring hCTD for its activity. In addition to an nuclear localization signal (NLS), it harbors an nuclear export signal (NES) as well, and is localized in both nucleus and cytoplasm.

Endogenous HDAC3 has been reported to associate with itself to form a homodimer (Yang, 2002). HDAC3 is found in complex with silencing mediator for retinoic acid and thyroid hormone receptor (SMRT) and nuclear receptor corepressor (N-CoR) and this association is necessary for its deacetylation activity (Li, 2000b). Little is known about HDAC8 complexes. Unlike other HDAC class I proteins, the recombinant HDAC8 peptide is active for deacetylation without association with other proteins (Hu, 2000) and HDAC8 phosphorylation by protein kinase A leads to its inactivation (Lee, 2004a). Recent experiments have shown HDAC8 to associate with α-actin and is essential for the muscle contractility (Waltregny, 2005).

Class II HDAC proteins have catalytic domains located near the hCTD and NLSs situated close to hNTDs. Their cytoplasmic localization is the result of their phosphorylation and post-phosphorylation interaction with 14.3.3 protein (De Ruijter, 2003). SirT1, a class III HDAC protein, deacetylates H4K16 preferentially and is found in association with linker histone H1 (Vaquero, 2004). SirT2 also has been reported to preferentially deacetylate histone H4 (Inoue, 2007).

HDAC3 complexes. Thus far, HDAC3 has been shown to have association with many proteins: Aurora B kinase (Li, 2006), SMRT (Li, 2000b), N-CoR (Li, 2000b; Wen, 2000), TBL1 (Li, 2000b; Li, 2006; Yoon, 2003), TBLR1 (Yoon, 2003), GPS2 (Li, 2006; Zhang, 2002b), AKAP95 (Li, 2006), YY1 (Thomas, 1999), HA95 (Li, 2006), CORO2A (Yoon, 2003), HDAC10 (Tong, 2002), HDAC7 (Fischle, 2001) HDAC9 (Zhou, 2000), Runx2 (Schroeder, 2004),

DAXX (Li, 2000a), BCoR (Huynh, 2000), SRY (Thevenet, 2004), GLIS2 (Kim, 2005), CBFA2T3 (Amann, 2001), NRIP1 (Wei, 2000), DACH1 (Wu, 2003), JMJD2A (Gray, 2005), CBP (Cowger, 2006), GATA-2 (Ozawa, 2001), MEF2 (Grégoire, 2007), TFII-I family proteins (Wen, 2003), GCMa (Chuang, 2006), and protein phosphatase 4 (PP4) (Zhang, 2005). HDAC3 functions in multiprotein complexes. The most studied HDAC3 complexes contain members of the nuclear receptor co-repressor family N-CoR/ SMRT (Guenther, 2001). Binding of HDAC3 with the membrane associated tyrosine kinase—Src, suggests its role in signal transduction (Longworth, 2006). HDAC3 is also known to play role in cell proliferation by causing inhibition of p15 and p21 (Huang, 2006). Many transcription factors interact with HDAC3 and target it to a specific DNA sequence. HDAC3 also associates with p300 and PCAF to repress p300/PCAF mediated transcription (Blanco-García, 2009). HDAC3 is regulated by phosphorylation, by casein kinase II (CK2) and PP4 (Zhang, 2005). During caspase dependent apoptosis the hCTD of HDAC3 is removed and the resultant cleaved protein accumulates in the cytoplasm (Escaffit, 2007).

Regulation of Chromatin Functions by HDACs

Acetylation of core histone tails, depending on acetylation extent and other associated marks, recruits either co-repressor or coactivator complexes; allowing further changes that can lead to transcription activation or repression (Ogryzko, 2001). Deacetylation of H3K9, H3K14, H4K8, H4K16 sites in the chromatin of the promoter regions and the 5`-terminal region of active genes leads to transcription

repression (Agalioti, 2002; Alberts, 2002). The fact that some acetyl marks on core histones are retained through the mitosis have led to the model that HATs and HDACs remain bounded to chromosomes through mitosis and provide epigenetic imprinting to post-mitotic chromosomes for gene reactivation. However, immunoflurescence study *in situ* have failed to support this hypothesis (Kruhlak, 2001). So even though regulation of chromatin function by HDACs is mainly related to histone deacetylation, HDACs also have many non-histone targets.

Non-Histone Targets of HDACs

Even though HDACs were identified as histone deacetylating enzymes, there are many studies that indicate that HDACs have several substrates which are non-histone proteins. Some of these non-histone targets include transcription factors like p53, Yin-Yang 1 (YY1), GATA factors, and STAT3. The tumor suppressor and DNA binding transcription factor, p53, is acetylated at multiple lysine residues on the hCTD (Gu, 1997). HDAC1 as well as SirT1 can deacetylate p53, and decrease its activity (Luo, 2000; Vaziri, 2001). Sequence specific DNA binding protein, YY1 interacts with HDAC1, HDAC2 and HDAC3 (Yang, 1996), which affects its DNA binding and transcriptional activity (Yao, 2001). Transcription inhibition of a cytoplasmic transcription factor, STAT3, targeted genes can be a result of deacetylation of STAT3, which is deacetylated by HDAC3 (Yuan, 2005). Nuclear receptors like androgen receptor and estrogen receptor α are also targeted by HDACs. HDAC1 can deacetylate androgen

receptor and represses its activation function (Fu, 2002). Another nuclear receptor, an estrogen receptor α is acetylated by p300 (Cui, 2004), while its deacetylation by HDAC1 results in increased cell proliferation (Kawai, 2003). Acetylation of GATA1 transcription factor increases its DNA binding ability. GATA1 interacts with HDAC3, -4, and HDAC5 with its hNTD resulting in its deacetylation (Watamoto, 2003). Acetylation of GATA2 increases its DNA binding and transcriptional activation (Hayakawa, 2004), whereas its deacetylation by HDAC3 represses this ability (Ozawa, 2001).

Tubulin is also targeted by HDACs. Stable and dynamic microtubules include deacetylated α-tubulin, while non-dynamic microtubules include acetylated α-tubulin. HDAC6 and SirT2 are known to deacetylate α-tubulin (Hubbert, 2002; Matsuyama, 2002; North, 2003). Even though not much is known about non-histone deacetylation, it is clear that many HDACs target proteins other than histones and affect various functions in the cell.

HDAC3 and Mitosis

Recent studies have revealed an essential role of HDAC3 in mitosis. Ishii et al have studied the localization of HDAC3 during mitosis in HeLa cells. Using immunoflurescence, HDAC3 core complex, including N-CoR, TBL1, and TBLR1, were shown to localize on mitotic spindles. Ishii et al have also provided evidence for the involvement of HDAC3 in the formation and regulation of functional mitotic spindles, and in the proper assembly of kinetochore-microtubule during metaphase (Ishii, 2008b). A study by Li et al group has also

showed the transcription-independent involvement of HDAC3 in mitosis progression (Li, 2006). Depletion of HDAC3 in HeLa cells leads to G_2/M arrest and chromosomal defects during mitosis (Li, 2006). HDAC3 has to deacetylate the hNTD of core histone H3 and H4, as a primary requirement for phosphorylation of H3S10 during mitosis progression (Li, 2006). Another study by Eot-Houllier et al have described the role of HDAC3 in sister-chromatin cohesion and deacetylation of H3K4 at centromere during mitosis (Eot-Houllier, 2008). Thus far, HDAC3 was thought to be involved only in transcriptional repression of gene expression. However, these new evidences indicate that HDAC3 may also have a non-classical role that is a transcription-independent function in mitosis, which still remains to be studied.

Association Between Linker Histones and HDACs—

Functional Significance

Since both HDAC3 and histone H1 play a role in chromatin compaction mechanisms and in mitosis progression, this dissertation hypothesizes that HDAC3 and histone H1 are associated with each other. Only two reports in the literature have shown association of histone H1 and a HDAC enzyme (Vaquero, 2004). The first report showed *in vivo* association of linker histone H1.4 (H1b) with SirT1 (HDAC class III protein) for formation of heterochromatin. Studies *in vitro*, demonstrated a role of SirT1 in deacetylation of H1K26 (Vaquero, 2004). However, since linker histone is very insignificantly acetylated *in vivo,* this study carried out *in vitro* acetylation of H1 by p300 for further deacetylation studies *in*

vitro. Conversely, other H1 variants also showed similar results to histone H1.4 i.e. SirT1 deacetylates histone H1 variants in the deacetylation assay *in vitro*. Therefore, further studies *in vivo* are required to clarify histone H1 deacetylation by HDAC proteins. The second report of histone H1 and HDAC interaction comes from study in *C. elegance* by Jedrusik et al. In this report, histone H1.1 was shown to participate with Sir-2.1 in repeat-dependent silencing of transgenes in *C. elegance* (Jedrusik, 2003).

Linker histone deacetylation by an associated HDAC enzyme can lead to similar effects on the chromatin structure as a core histone deacetylation. Thus, the deacetylated form of histone H1 can bind to nucleosome with higher affinity and induce compaction. A SirT1 targeted gene repression study showed recruitment of histone H1.4 along with SirT1 to the chromatin region. This finding supports the model that SirT1 and histone H1 interaction is functionally active for chromatin compaction (Vaquero, 2004).

Most HDACs, including SirT1 are part of large complexes which include also histone methyltransferases. Thus, the deacetylated lysine/ arginine residues on the core histones can be readily methylated, which mostly leads to gene repression (Vaquero, 2004). Consequently, in most cases, linker histone binding with core histone deacetylation and followed by core histone hNTD methylation could be facilitating chromatin compaction. HDACs like SirT2 and HDAC6 are known to deacetylate tubulins (Hubbert, 2002; North, 2003). Currently, many HDAC inhibitors (HDIs) are known to cause hyperacetylation of tubulins and are

more potent to kill malignant cells (Blagosklonny, 2002a). This sensitivity indicates the importance of non-chromatin targets of HDACs for cell cycle progression and cell growth.

This dissertation hypothesizes that there are two proteins playing key role in chromatin compaction mechanisms and in mitosis progression i.e. HDACs and linker histone H1 are associated with each other. This hypothesis is derived from the fact that in spite of H1 being very efficiently acetylated by histone deacetylase (HATs) *in vitro*, H1 has very low levels of acetylation *in vivo* (Dr. Michael Bergel, personal communication). This suggests that histone H1 is possibly interacting with HDAC proteins that constitutively deacetylates it. Earlier reports showed that HDAC3 mediated gene repression is due to deacetylation on core histones around the targeted genes (Li, 2002). Here, results indicate that association of HDAC3 with histone H1 plays a role in the chromatin compaction during mitosis or in the other mitosis related activities such as microtubule maintenance.

CHAPTER II

MATERIALS AND METHODS

Cell Culturing and Extraction

HeLa and HeLaS3 cells were maintained in Dulbecco's Modified Eagle's Medium (Gibco/ BRL, #10566), supplemented with 10% fetal bovine serum (Benchmark/ Gemini, #100-106) and 1% penicillin and streptomycin (Gibco/ BRL, #15140-122). Cells were grown in an incubator in presence of 5% atmospheric CO_2 and 100% humidity at 37°C. HeLaS3 cells were grown in spinner flasks and maintained in logarithmic phase. Logarithmically growing HeLaS3 cells were harvested and washed with cold 1X phosphate buffer saline (PBS) (Cellgro, #21-040-CV) and lysed in radio-immunoprecipitation assay (RIPA) buffer [1X PBS with 0.5% Nonidet P40, 0.8% 0.5 M NaF, 2% 100 mM sodium orthovanadate, mini complete protease inhibitor tablet (Roche Diagnostic, cat #1186153001)]. After 30 minutes of incubation at 4°C, cell lysates were passed through 20 gauge needles and centrifuged for 20 minutes at 10,000 X g, 4°C. The supernatant was collected and used for immunoprecipitation assays and Western blot experiments. Protein estimation of the RIPA extracts was done using micro BCA protein assay kit (Pierce Biotechnology, #23235). HeLa cells were maintained routinely in either 75 cm^2 or 185 cm^2 flasks. For immunostaining, logarithmically

growing HeLa cells were seeded at a concentration of 20,000 cells in a 0.8 cm^2 chamber on the chamber slides (LabTek/ Fisher, #12-565-22).

Co-Immunoprecipitation Assay

The RIPA extract of HeLaS3 cell samples were adjusted to 500-2000 µg/ml total protein using RIPA buffer with protease inhibitor (mini complete tablet). The extracts were pre-cleared for 1 hour at 4°C with 0.25 µg of non-immune (control) IgG (Santa Cruz Biotechnology, #2027, #2025) or IgM (Chemicon, #PP50) and with 20 µl of protein-A/G agarose (Santa Cruz Biotechnology, #2003) or protein-L agarose beads (Santa Cruz Biotechnology, #2336), respectively. Immunoprecipitations were performed with 1-2 µg/ml of the following antibodies: goat anti-HDAC1 (Santa Cruz Biotechnology, #6299), goat anti-HDAC2 (Santa Cruz Biotechnology, #6296), mouse anti-HDAC3 (Santa Cruz Biotechnology, #17795), mouse anti-HDAC4 (Abcam, #12171), goat anti-HDAC5 (Santa Cruz Biotechnology, #5252), goat anti-HDAC6 (Santa Cruz Biotechnology, #5258), goat anti-HDAC7 (Santa Cruz Biotechnology, #11489), rabbit anti-HDAC8 (Santa Cruz Biotechnology, #11405), goat anti-HDAC9 (Santa Cruz Biotechnology, #19870), goat anti-HDAC10 (Santa Cruz Biotechnology, #54215), mouse anti-HDAC11 (Abcam, #13694), mouse anti-Histone H1 (Santa Cruz Biotechnology, #8030), or mouse anti-phospho H1 (Millipore, #05-805) (table 1). Immunoprecipitate with 2 µg/ml non-immune IgG or non-immune IgM was used as a negative control for all the experiments. After an overnight incubation at 4°C, immunocomplexes and protein beads were collected by

centrifugation at 1000 X g, 4°C for 5 minutes. The immunocomplexes were washed three times with RIPA buffer. According to the experimental needs, the immunocomplex was either resuspended in 30 µl of 1X Laemmli buffer and denatured by heating at 95°C for 5 minutes for Western blotting or used to perform HDAC assays as described later. Input into immunoprecipitations was assayed from Western blots of 1.5% of the total protein in all experiments. Immunoprecipitations were performed with 2 mg protein from the cell extracts, unless differently specified. Since HeLa and HeLaS3 cells are of human origin, all the antibodies used were against human proteins.

Western Blots

The protein extracts in 1X Laemmli buffer were resolved by sodium dodecyl sulfate polyacrylamide gel electrophoresis (SDS-PAGE) (8% for HDAC3, SMRT and N-CoR; 12% for histone H1; 10% for HDAC8 and actin; 15% for histone H3 and histone H4). Proteins were transferred from the gel to 8.2 cm X 5.6 cm polyvinylidene fluoride (PVDF) membranes (Millipore, #IPVH20200) by using semi-dry blotter (Bio-Rad) operated at 28 mA for 2 hours. The membranes were blocked in 1X PBS containing 5% skim milk (Nestle-Carnation) (mPBS) and 0.1% Tween 20 (Fisher, #BP337) (mPBST) for 45 minutes at room temperature on shaker. The membranes were then incubated overnight at 4°C on a shaker with appropriate primary antibodies: mouse anti-HDAC3 (2 µg/ml in 2.5% mPBS; Santa Cruz Biotechnology, #17795), rabbit anti-HDAC3 (0.2 µg/ml in 2.5% mPBS; Bio-vision, #3603), mouse anti-histone H1 (0.4 µg/ml in 2.5% mPBS;

Santa Cruz Biotechnology, #8030), rabbit anti-histone H1 (0.042 µg/ml in 2.5% mPBS; Dr. M. Bustin, NIH), rabbit anti-HDAC8 (0.1 µg/ml in 2.5% mPBS; Santa Cruz Biotechnology, #11405), mouse anti-actin (1:2000 in 5% mPBS; Sigma, #A4700), rabbit anti-phospho-H3S10 (0.2 µg/ml in 5% mPBS; Upstate, #06-570), rabbit anti-phospho-H1 (0.7 µg/ml in 2.5% mPBS; Upstate, #06-597), rabbit anti-histone H1.1 (1 µg/ml in 2.5% mPBS; Abcam, #17584), rabbit anti-histone H1.2 (1:500 in 2.5% mPBS; Abcam, #4086), rabbit anti-histone H1.3 (0.5 µg/ml in 2.5% mPBS; Abcam, #24174), rabbit anti-histone H1.5 (1:1600 in 2.5% mPBS; Abcam, #18208), goat anti-SMRT (1 µg/ml in 0.5% mPBS; Santa Cruz Biotechnology, #1610), rabbit anti-N-CoR (0.4 µg/ml in 2.5% mPBS; Santa Cruz Biotechnology, #8994), rabbit anti-acetyl-H3K9 (1 µg/ml in 3% mPBS; Millipore, #06-942), rabbit anti-acetyl-H4K5 (0.04 µg/ml in 5% mPBS; Santa Cruz Biotechnology, #8659R), rabbit anti-trimethyl-H3K9 (1:5000 in 3% mPBS; Millipore, #07-523), rabbit anti-phospho-serine (1 µg/ml in 3% BSA; Invitrogen-Zymed laboratories, #61-8100), or rabbit anti-HDAC3-P-S424 (1 µg/ml in 2.5% mPBS; Abcam, #61056). Membranes were rinsed with 1X PBS and then washed once with 1X PBST for 10 minutes, and twice with 1X PBST for 5 minutes. After a quick rinse with 1X PBS, the membranes were incubated with horseradish peroxidase-conjugated secondary antibodies: goat anti-rabbit (0.1 µg/ml in 0.5% mPBS; Pierce Biotechnology, #31460), rabbit anti-mouse (0.1 µg/ml in 2.5% mPBS; Pierce Biotechnology, #31450), or rabbit anti-goat (0.05 µg/ml in 2.5% mPBS; Pierce Biotechnology, #31402) for 1 hour at room temperature. Following

the incubation, membranes were rinsed three times with 1X PBS then washed with 1X PBST as above. The immunoreactive proteins were then visualized by incubating with enhanced chemi-luminescence reagent for 5 minutes according to the ECL Plus kit (Amersham Biosciences/ GE healthcare, #RPN2132), then exposed to X-ray hyperfilm (Amersham Biosciences/ GE healthcare, #28906835) and developed (Kodak; developer #1249259, fixer #8868804). The films were scanned for densitometric analysis, using spot analysis method, with the Fluorchem HD2 Imaging System (Alpha Innotech, San Leandro, CA). For the spot analysis method, the protein bands were selected to obtain integrated density value (IDV). An equal area without bands was selected from the same lane to obtain the background IDV, which was subtracted from the protein band IDV to get the density value of the protein band. Further biostatistical analysis was performed with α=0.05 significance level.

Immunoflurescence Microscopic Analysis

HeLa cells were grown on chamber slides (LabTek/ Fisher, #12-565-22) to 80% confluency, washed with 1X PBS and fixed with 4% para-formaldehyde (Fisher, #T353) for 10 minutes at room temperature. The cells were washed three times with 1X PBS for 7 minutes each time and then treated with 0.1% Triton X-100, 1% FBS, 0.1% NaN_3 in 1X PBS (TNBS buffer) for 20 minutes for permeabilization and blocking. The cells were then incubated overnight at 4°C with a desired primary antibody: mouse anti-HDAC3 (0.004 µg/µl; SantaCruz, #17795), rabbit anti-histone H1.3 (0.02 µg/µl; Abcam, #24174) or goat anti-Eg5

(0.003 µg/µl; Santa Cruz, #31644). Negative control for all the experiments were performed using non-immune IgG (control-IgG) as a primary antibody. Following five washes with 1X PBS for 5 minutes each, cells were incubated with appropriate secondary antibodies: goat/donkey anti-mouse-fluorescein isothiocyanate (FITC) (Santa Cruz Biotechnology, #2010, #2099), goat/donkey anti-rabbit-Texas red (TR) (Santa Cruz Biotechnology, #2780, #2784), donkey anti-goat-FITC (Santa Cruz Biotechnology, #2024) or donkey anti-goat-TR (Santa Cruz Biotechnology, #2783) (0.002 µg/µl) for 1 hour 15 minutes at room temperature in dark. After the 1X PBS washes, DNA and nuclei were stained with Hoechst (2.5 µg/ml; Invitrogen, #H3570) for 5 minutes in dark. The cells were washed with 1X PBS and then prolong antifade mounting medium (5-10 µl per chamber; Invitrogen, #P7481) was added to each chamber of the slide. The slide was then covered with coverslip and sealed using clear nail-paint (Sally-Hansen). The used fluorophores Hoechst (blue), FITC (green) and TR (red) were excited with 405, 488 and 568 nm, respectively, using Zeiss Axiovert 200M optical microscope with confocal attachment. The images were collected with a Hamamatsu camera set for a 64 gain for the blue channel and a 128 gain in the green and red channels. The control samples images were collected at the maximum exposure times used (blue 6 s, green 7 s, red 7 s) for collecting stained images. The emission light was collected using 1000X total magnification (oil emersion objective). The cell images were captured at a single section at the

center of the cell. The digital images were visualized and selected for presentation using ImageJ software.

Cell Synchronization

Exponentially growing HeLaS3 cells were treated twice with 2 mM thymidine (Sigma, #T1895) for 18 hours each time, with 11 hours release between two treatments to block the cells in S phase. Before and after each treatment cells were washed with 1X PBS. Early-G_2 cells were collected 3 hours after the release from S phase block; while late-G_2 cells were collected 6 hours after the release. S phase cells after 3 hours of release were further treated with 100 nM nocodazole (Sigma, #M1404) to arrest the cells in mitosis. After two washes with 1X PBS, the synchronized cell populations (3 X 10^6 cells) were fixed with 4% para-formaldehyde for 15 minutes at room temperature, for analysis with flow cytometry (BD FACSCalibur system). From each synchronized cell population, the cells were washed twice with 1X PBS and the whole cell extracts (20 X 10^6 cells/ 1 ml RIPA buffer) were prepared in RIPA buffer for co-immunoprecipitation assays as described earlier.

Flow-Cytometric Analysis

The formaldehyde fixed cells were washed twice with 1X PBS and permeabilized with 0.25% Triton X-100 (Fisher, #BP151) for 10 minutes at room temperature. The cells were then blocked for non-specific antibody binding using 1% BSA (Sigma, #B4287) for 30 minutes at room temperature. To separate mitotic cells from G_2 phase cells, staining with the mitosis specific marker

antibody phospho-H3S10 conjugated with FITC (1.5 µg in 500 µl of 1% BSA; Millipore, #16-222) at room temperature for 45 minutes in the dark. A negative control staining with control antibody IgG-FITC (1.5 µg in 500 µl of 1%BSA; Millipore, #12-487) was performed to confirm absence of background staining. After washing the cells twice with 1% BSA, the cells were counterstained using propidium iodide (PI) with RNase (BD Biosciences, #550825) for DNA analysis of cell cycle (3 X 10^6 cells/ 1 ml PI). The staining was for 15 minutes at room temperature in the dark. The stained samples were passed through a 37 micron mesh and analyzed by BD FACSCalibur at 585/42 nm for detection of PI and at 530/30 nm for detection of phospho-H3S10-FITC. The Density plots (dot-plots/ histograms) of stained cells were plotted to see different populations of interest.

Hyperacetylated Core Histones Isolation

HeLaS3 cells were logarithmically grown and treated with 2 µM tricostatin A (TSA) (Millipore, #19-138) for 20 hours. Cells were collected by centrifugation and were washed twice with ice cold 1X PBS. Cells were lysed with lysis buffer-A (10 mM Tris-HCl pH 7.4, 10 mM NaCl, 3 mM $MgCl_2$, 0.5% NP-40, 1 mM PMSF) and lysis buffer-B (10 mM Tris-HCl pH 7.4, 3 mM $CaCl_2$, 2 mM $MgCl_2$, 1% NP-40, 1 mM PMSF) (1 ml buffer A and 1 ml buffer B for 50 X 10^6 cells). Cells were broken to isolate nuclei using a Dounce homogenizer (pestle-B, 10 strokes). The nuclei were isolated by centrifugation at 500 X g for 8 minutes at 4°C and were resuspended in glycerol storage buffer (50 mM Tris-HCl pH 8.3, 40% glycerol, 5 mM $MgCl_2$, 0.1 mM EDTA pH 8) to store at -80°C until used. The isolated nuclei

were centrifuged at 500 X g for 15 minutes at 4°C, resuspended and washed in sucrose gradient buffer (10 mM Tris-HCl pH 7.4, 1 mM EDTA, 10 mM NaCl). The nuclei were resuspended in 0.25 M H_2SO_4, passed through a Dounce homogenizer (pestle-A) and then incubated on ice for 15 minutes. The acid extract was centrifuged at 4,000 X g for 10 minutes at 4°C. The supernatant was added to six volumes of ice-cold 100% acetone, incubated at -20°C for 3 hours and then centrifuged at 4,000 X g for 10 minutes at 4°C. The obtained core histone pellet was washed twice with 95% acetone, dried overnight, and reconstituted in sterile de-ionized distilled water to store at -80°C. The obtained core histones were assessed by resolving then on 15% SDS-PAGE to visualize the presence of equimolar quantities of core histones and proteins integrity. A control Western blot analysis was also performed with acetylated H3K9 antibody to assess acetylation of this core histone residue. Only after performing these controls, resulting hyperacetylated core histones were used for HDAC assays.

Hyperacetylated Mononucleosomes Isolation

HeLaS3 cells were treated with 2 µM tricostatin A for 20 hours. The cell nuclei were isolated as described in core histone isolation method. The isolated nuclei were washed and resuspended in mononuclease digestion buffer (85 mM KCl, 1 mM $CaCl_2$, 5 mM PIPES pH 7.5, 5% sucrose). The nuclei were then subjected to micrococcal nuclease digestion (300 units/ 500 µg DNA) at 4°C on a shaker for 1 hour. The digestion reaction was stopped by adding 0.5 M EDTA. Histone H1 was removed from nucleosomes by three sequential 2 hours

incubations with Sephadex beads (Sigma, #C-25120) in wash buffer (0.5 M NaCl, 0.1 mM EDTA, 10 mM Tris-HCl pH 7.5) at 4°C on a rocker. The resulting nucleosomes were dialyzed in Slide-A-Lyzer cassette (10,000 MWCO) (Pierce Biotechnology, #66453) against sucrose dilution buffer (dialysis buffer) (25 mM NaCl, 10 mM Tris-HCl pH 7.5, 0.1 mM EDTA) for overnight at 4°C with constant stirring. After the dialysis the sample was loaded on a 12-50% sucrose gradient. The gradient was ultra-centrifuged at 100,000 X g for 24 hours at 4°C. Fractions were collected from the gradient and analyzed on 2% agarose gel to detect fractions containing mononucleosomes. Fractions containing mononucleosomes were combined and stored in sucrose buffer at 4°C. The isolated mononucleosomes were resolved on 15% SDS-PAGE and stained with Coomassie blue to assess relative equimolar concentrations of core histones. Western blot analysis (12% SDS-PAGE) on mononucleosomes sample was done with anti-histone H1 antibody to confirm stripping of histone H1. Acetylation of core histone residues H3K9 and H4K5 was also checked by performing Western blot (15% SDS-PAGE) using anti-acetylated H3K9 and anti-acetylated H4K5 antibodies. Only after ensuring with control blots, the resulting mononucleosomes were used for HDAC assays.

Histone Deacetylase Assay

HeLaS3 cell extracts from late-G_2 phase and mitosis phase were immunoprecipitated as described earlier using antibodies anti-HDAC3 (Santa Cruz Biotechnology, #17795), anti-histone H1 (Santa Cruz Biotechnology,

#8030), anti-phospho-histone H1 (Upstate, #05-805) or non-immune IgG (Santa Cruz Biotechnology, #2025) mixed with A/G agarose beads (Santa Cruz Biotechnology, #2003). Obtained immunocomplexes were washed twice with RIPA buffer and the last wash was done with deacetylation buffer (10 mM Tris-HCl pH 8.0, 10 mM NaCl, 10% glycerol, and mini complete protease inhibitor). The washed immunocomplexes were incubated with hyperacetylated mononucleosomes or hyperacetylated core histones in HDAC buffer at 37°C for 40 minutes. After the incubation 1X Laemmli buffer was added to the reaction mixture, and proteins were resolved by SDS-PAGE. Western blot analysis was performed using either anti-acetyl-H3K9 or anti-acetyl-H4K5 antibody. The HDAC assay reaction with recombinant HDAC3/N-CoR2 (HDAC3/SMRT) complex (Cell Sciences, #CRH010) served as a positive control; while the reaction with non-immune IgG served as a negative control.

Giemsa Staining

Exponentially growing HeLaS3 cells were treated with 100 nM nocodazole (Sigma, #M1404) for 20 hours to arrest the cells in metaphase. Cells treated with DMSO (vehicle control) were used as a vehicle control for nocodazole treatment. After the treatment, cells were collected by centrifugation and washed twice with 1X PBS. Ice-cold hypotonic solution (0.7% KCl) was added to the cells in drop-wise manner for 5 minutes. The cells were collected by centrifugation, resuspended in 10 ml of methanol:acetic acid (3:1) fixative solution and fixed for 45 minutes at room temperature. The cells were collected by centrifugation,

washed with fixative, and resuspended in fixative (0.5 ml fixative for 10^6 cells). The cell sample was dropped on the ice-cold slides to achieve a metaphase spread. Slides were heated on hot-plate at 70°C and then placed in the Giemsa stain (Gibco, #10092-013) for 4 minutes. The slides were washed in Gurr buffer (pH 6.8) (Gibco, #10582-013) to remove extra stain. After washing the slides twice with deionized distilled water, the metaphase spreads were observed under a light compound microscope (400X total magnification) and cells from 200 microscopic fields are counted per treatment to find the mitotic index. Microscopic fields were scanned from left to right and then down, right to left, in zigzag fashion to ensure each microscopic field was free of overlap from previously counted fields. The mitotic index was calculated using the number of metaphase spreads observed divided by total number of cells counted in the 200 fields for both the treatments independently.

Histone H1 Isolation (5% Perchloric Acid Extraction)

Logarithmically growing HeLaS3 cells were collected by centrifugation and washed twice with 1X PBS. The cells were lysed using lysis buffer (140 mM NaCl, 1.5 mM $MgCl_2$, 10 mM Tris-HCl pH 8.6, 0.5% NP-40, and mini complete protease inhibitor tablet) and Dounce homogenizer (pestle A, 10 strokes). The resulting cell extract was added to 5% perchloric acid and incubated at room temperature for one hour with constant stirring. The mixture was then centrifuged at 13,000 X g for 10 minutes to collect the supernatant of the perchloric acid extract. Ice-cold 100% acetone (six volumes) was added to the perchloric acid

extract and stored at -20°C for 3 hours for precipitating the proteins. The resulting white floating protein precipitates were collected by centrifugation at 13,000 X g for 15 minutes. The protein pellet was washed twice with ice-cold acetone (95% and 80%). The pellet was dried overnight, resuspended in sterile deionized distilled water and stored at -80°C until used. Protein estimation of the extract was done using micro BCA protein assay kit (Pierce Biotechnology, #23235). Proteins obtained were tested by performing Coomassie blue staining on 12% SDS-PAGE to visualize purity and presence of histone H1 bands. Extracts were also analyzed by Western blot with anti-histone H1 antibody to confirm presence of all histone H1 variants before using for pull down assays.

Pull-Down Assays

Recombinant human-HDAC3 (1.05 µg) (Biomol, #SE-507) was incubated with equimolar quantity of 5% perchloric acid extracted histone H1 (1.76 µg). The reaction was incubated at 4°C, overnight with either 2 µg of anti-histone H1 antibody or with non-immune IgG (negative control) and 20 µl of protein A/G-agarose beads. After the incubation, the reaction was subjected to centrifugation at 1000 X g for 5 minutes at 4°C. The complex attached to the beads was washed three times with RIPA buffer to remove nonspecific binding. The complexes were dissociated from the beads by adding 1X Laemmli buffer and then were resolved on 12% SDS-PAGE. The gel was stained with Coomassie blue RX-250 (Bio-Rad, #161-0400) to visualize the protein bands. The stained protein bands were analyzed by densitometry using the Fluorchem HD2 system.

The densitometric values were corrected for the molecular weight of the protein bands of interest to obtain the ratio of HDAC3 to histone H1.3 in the complex. Statistical analysis to compare the ratios was done by using Chi square goodness of fit test at a significance level of 0.05.

Phosphorylation of HDAC3-H1.3 Complex

HDAC3-H1.3 immunocomplexes were isolated from late-G_2 cell extract as described above. The HDAC3-H1.3 was subjected to phosphorylation with CK2 ((New England Biolabs, #P6010S) or cyclinB-cdc2 (New England Biolabs, #P6020S). The reaction included 200 mM ATP with γ-^{32}P-ATP (Perkin Elmer, # BLU002250UC) at a specific activity 500 µCi/mmol. The reaction was performed at 30°C for 30 minutes. To confirm phosphorylation, the proteins from the reaction were dissociated by adding 1X Laemmli buffer, and then the extracts were heated at 95°C for 5 minutes. The resulting extracts were resolved by SDS-PAGE (8% and 12%). The gel was dried and then put in the cassette for exposing to phosphor-imager (Kodak) screen for 48 hours. The image was captured by exposing the screen to Molecular imager FX (Bio-Rad) and using Quantity-One software to visualize phosphorylation of HDAC3 and histone H1.3. Phosphorylated immunocomplexes were used for further HDAC assays as described earlier.

Isolation and Identification of Cellular HDAC3-H1.3 Complex

Immunocomplexes from late-G_2 and mitosis cell extracts were obtained as described earlier with anti-histone H1 antibodies (Santa Cruz Biotechnology, #8030) and with anti-HDAC3 antibodies (Santa Cruz Biotechnology, #17795). Immunoprecipitation with non-immune IgG (Santa Cruz Biotechnology, #2025) was used as a negative control. Immunocomplexes were resolved on SDS-PAGE (8% and 12%) and the gel was stained using silver stain kit (Pierce Biotechnology, #24600). Bands of interest were excised and destained following the procedure from the kit to confirm protein identity using Western blot analysis as described earlier. Excised bands of unidentified proteins were analyzed by mass spectrometry (LC-ESI-MS/MS) at UT Southwestern core facility.

Table 1
Summary of Antibodies Used for Immunoprecipitation Assays and Western Blotting

	ANTIBODY	SPECIES (poly/mono-clonal)	COMPANY	CATALOGUE #
1	Acetylated H3K14	Rabbit (poly)	Upstate	06-911
2	Acetylated H3K9	Rabbit (poly)	Upstate	06-942
3	Acetylated H4K5	Rabbit (poly)	Santa Cruz Biotechnology	8659r
4	Actin	Mouse (mono)	Sigma Aldrich	A4700
5	Control IgG	Mouse	Santa Cruz Biotechnology	2025
6	Control IgG	Rabbit	Santa Cruz Biotechnology	2027
7	Control IgM	Mouse	Chemicon	PP50
8	EG5	Goat (poly)	Santa Cruz Biotechnology	31644
9	HDAC1	Goat (poly)	Santa Cruz Biotechnology	6299
10	HDAC2	Goat (poly)	Santa Cruz Biotechnology	6296

Table 1 continued

11	HDAC3	Mouse (mono)	Santa Cruz Biotechnology	17795
12	HDAC3	Rabbit (poly)	Bio-vision	3603
13	HDAC4	Mouse (mono)	Abcam	12171
14	HDAC5	Goat (poly)	Santa Cruz Biotechnology	5252
15	HDAC6	Goat (poly)	Santa Cruz Biotechnology	5258
16	HDAC7	Goat (poly)	Santa Cruz Biotechnology	11489
17	HDAC8	Goat (poly)	Santa Cruz Biotechnology	11544
18	HDAC8	Mouse (poly)	Santa Cruz Biotechnology	17778
19	HDAC8	Rabbit (poly)	Santa Cruz Biotechnology	11405
20	HDAC9	Goat (poly)	Santa Cruz Biotechnology	19870
21	HDAC10	Goat (poly)	Santa Cruz Biotechnology	54215
22	HDAC11	Goat (poly)	Abcam	13694

Table 1 continued

23	Histone H1	Mouse (mono)	Santa Cruz Biotechnology	8030
24	Histone H1	Rabbit (poly)	Dr. Bustin	--
25	Histone H1.1	Rabbit (poly)	Abcam	17584
26	Histone H1.2	Rabbit (poly)	Abcam	4086
27	Histone H1.3	Rabbit (poly)	Abcam	24174
28	Histone H1.5	Rabbit (poly)	Abcam	18208
29	IgG	Goat Anti-Rabbit	Pierce Biotechnology	31460
30	IgG	Rabbit Anti-Goat	Pierce Biotechnology	31402
31	IgG	Rabbit Anti-Mouse	Pierce Biotechnology	31450
32	IgG-FITC	Donkey Anti-Goat	Santa Cruz Biotechnology	2024
33	IgG-FITC	Donkey Anti-Mouse	Santa Cruz Biotechnology	2099
34	IgG-FITC	Goat Anti-Mouse	Santa Cruz Biotechnology	2010
35	IgG-FITC	Mouse	Upstate	12-487

Table 1 continued

36	IgG-TR	Donkey Anti-Goat	Santa Cruz Biotechnology	2783
37	IgG-TR	Donkey Anti-Rabbit	Santa Cruz Biotechnology	2784
38	IgG-TR	Goat Anti-Rabbit	Santa Cruz Biotechnology	2780
39	N-CoR	Rabbit (poly)	Santa Cruz Biotechnology	8994
40	Phospho H3S10	Rabbit (poly)	Upstate	06-570
41	Phospho HDAC3S424	Rabbit (poly)	Abcam	61056
42	Phospho serine	Rabbit (poly)	Invitrogen-Zymed Lab	61-8100
43	Phospho-H3S10-FITC	Mouse	Upstate	16-222
44	Phospho-histone H1	Mouse (mono)	Upstate	05-805
45	Phospho-histone H1	Rabbit (poly)	Upstate	06-597
46	SMRT	Goat (poly)	Santa Cruz Biotechnology	1610
47	Trimethylated H3K9	Rabbit (poly)	Upstate	07-523

CHAPTER III

RESULTS

HDAC3 is Stably and Directly Associated With Histone H1.3

Histone deacetylases and histone H1 are both known to cause chromatin compaction and are important in the progression through mitotic phase of the cell cycle (Kruhlak, 2001; Li, 2006; Stevens, 2008; Th'ng, 2005). This dissertation hypothesizes that HDACs and histone H1 might associate, and that their interaction might correlate with mitotic events. Experiment explored a possible interaction of HDACs and histone H1 in human cells, with a series of co-immunoprecipitation assays. HeLaS3 cell extracts were made using RIPA buffer and co-immunoprecipitation assays were carried out against class I, II and IV HDACs. Class III HDACs (SirT1-7) were not investigated in this study for association with histone H1 as these are NAD^+ dependent HDACs. Western blot analysis for histone H1 revealed the stable co-immunoprecipitated complex of histone H1 and HDAC3 (Fig. 5A). The reciprocal immunoprecipitation using anti-histone H1 antibody was assayed to detect HDAC3 by Western blotting, which confirmed HDAC3 association with histone H1 (Fig. 5B). This attempt to investigate if histone H1 also interacts with other HDACs showed no association of histone H1 with HDAC1, 2, 4, 5, 6, 7, 9, 10 or HDAC11 (Fig. 6A, 6B) based on

co-immunoprecipitation assays. Co-immunoprcipitation assays also detected association of HDAC8 and histone H1 but only when using anti-HDAC8 for immunoprecipitation (Fig. 6C) and not when using anti-histone H1 antibody (data not shown). Therefore, further experiments tested to see if HDAC3 and HDAC8 are part of the same complex with histone H1. The immunoprecipitate with anti-HDAC3 was analyzed for presence of HDAC8 and vice versa, which indicated no association between HDAC3 and HDAC8 (Fig. 6D, E); suggesting that these two HDACs might form two different complexes with histone H1.

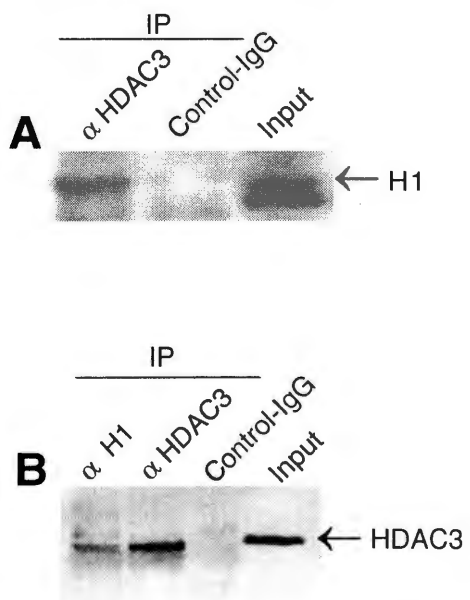

Figure 5: HDAC3 interacts with histone H1.
(A) Representative blot of HeLaS3 whole cell extracts, co-immunoprecipitated with anti-HDAC3, non-immune IgG (negative control) and Western blotted (12% SDS-PAGE) for the presence of histone H1 (n=5). (B) Representative blot of HeLaS3 whole cell extracts, co-immunoprecipitated with anti-histone H1, anti-HDAC3 (positive control), and non-immune IgG (negative control), and analyzed by Western blotting (8% SDS-PAGE) for the presence of HDAC3 (n=5). All input lanes represent 1.5% of the total protein used for immunoprecipitation in this and all other figures.

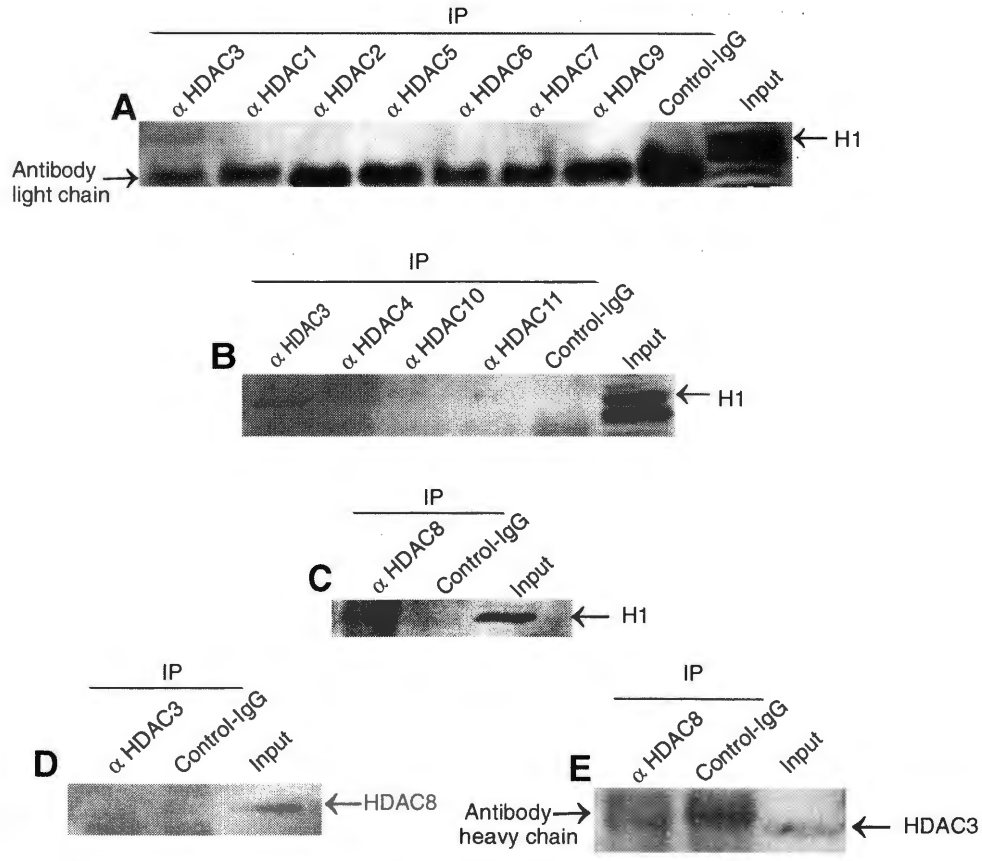

Figure 6: HDAC3 and HDAC8, but no other class I, II and IV HDAC proteins, associate with histone H1.
(A) Western blot for detecting histone H1 (12% SDS-PAGE) in immunoprecipitates of anti-HDAC1, 2, 3, 5, 6, 7 and HDAC9 from HeLaS3 cell extracts. (B) Western blot for detecting histone H1. Immunoprecipitate with anti-HDAC3, 4, 10 and HDAC11 were tested for the presence of histone H1 by Western blotting. (C) Western blot to detect histone H1 in anti-HDAC8 (1 µg antibody) immunoprecipitate (with 1 mg protein extract) from HeLaS3 cell extracts. (D) Western blot (10% SDS-PAGE) to detect presence of HDAC8 in anti-HDAC3 immunoprecipitate from HeLaS3 cell extracts. (E) Western blot (8% SDS-PAGE) to test presence of HDAC3 in anti-HDAC8 immunoprecipitate. Immunoprecipitate with non-immune IgG served as a negative control in all the experiments. All the experiments were performed in triplicate with similar results.

There are five major histone H1 variants (histone H1.1, H1.2, H1.3, H1.4, H1.5) in human somatic cells. To find out which specific histone H1 variant is associated with HDAC3, co-immunoprecipitation assays were carried out using antibody against HDAC3. The following Western blot analysis was performed using antibodies for histone H1.1, H1.2, H1.3 and H1.5. A specific association between HDAC3 and histone H1.3 was observed by virtue of the interaction with anti-histone H1.3 antibody on the Western blot analysis and by using the molecular weight of histone H1.3, in input, as a marker (Fig. 7B). Experiments could not detect association of HDAC3 with histone H1.5 (Fig. 7A), H1.2 (Fig. 7C), or H1.1 (Fig. 7D) based on co-immunoprecipitation assays.

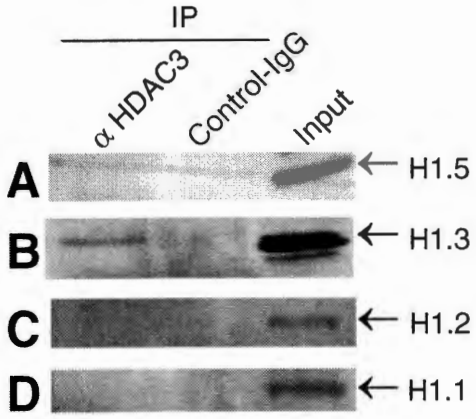

Figure 7: HDAC3 interacts specifically with histone variant H1.3.
(A-D) Western blot analysis (12% SDS-PAGE) for detecting (A) H1.5, (B) H1.3, (C) H1.2 and (D) H1.1 in immunoprecipitates with anti-HDAC3. Immunoprecipitation with non-immune IgG was used as a negative control. All experiments were performed three times with similar results.

To confirm direct interaction between HDAC3 and histone H1.3 and to determine their stoichiometric ratio in the complex, pull-down assays *in vitro* were performed using recombinant human HDAC3 (hHDAC3) protein and histone H1 isolated from HeLaS3 cells by 5% perchloric acid extraction. Pull-down was carried out using histone H1 antibody. The pulled-down complex was resolved on SDS-PAGE and Coomassie staining was performed to visualize the protein bands. The results demonstrate that HDAC3 binds directly to histone H1.3 (Fig. 8), which was consistent with the co-immunoprecipitation assays. The density values of histone H1.3 and HDAC3 were obtained using spot analysis method. To compare the density values of histone H1.3 and HDAC3, the density of the proteins was corrected to represent their molecular weight (HDAC3=49; H1.3=28) (Table 2). Chi square analysis with pairwise comparison of three independent experiments supports a stoichiometric ratio of 2:1 between HDAC3 and H1.3 in the complex (Chi square goodness of fit test, α=0.05, χ^2=0.76, p=0.38, df=1). Thus, these results support the association of a HDAC3 dimer with a single histone H1 molecule in the complex.

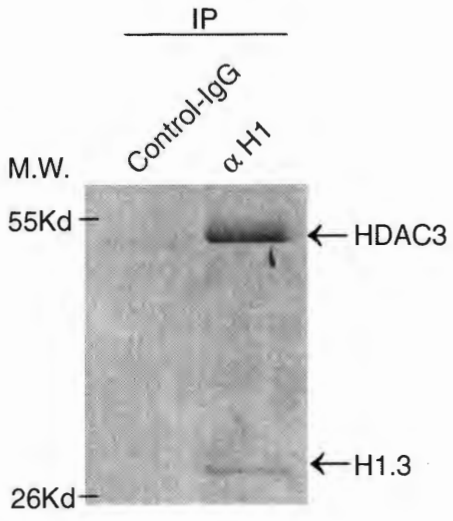

Figure 8: HDAC3 interacts directly with histone H1 in 2:1 molar ratio. Representative Coomassie blue stained SDS-PAGE gel for pull down assays (n=3). Recombinant hHDAC3 and histone H1 (extracted with 5% perchloric acid) were mixed in equimolar concentrations and subjected to pull-down with anti-histone H1. The precipitate was resolved on 12% SDS-PAGE followed by Coomassie blue staining. Pull-down with non-immune IgG served as a negative control.

Table 2
Integrated Density Values (IDV) for HDAC3 and H1.3 in Pull-Down Assays. The Average Corrected IDV and SD Were Calculated After Correcting IDV for Molecular Weight of The Proteins. (n=3)

	set 1	set 2	set 3	average corrected IDV ± SD	HDAC3: H1.3 ratio (a / b)
IDV (HDAC3)	6929	5840	8649		
Corrected IDV= IDV (HDAC3) / MW (HDAC3) (a)	141.41	119.18	176.51	145.70 ± 28.90	1.86
IDV (histone H1.3)	1632	1575	3361		
Corrected IDV= IDV (H1.3) / MW (H1.3) (b)	58.29	56.25	120.04	78.19 ± 36.25	

SD=standard deviation; MW=molecular weight

During mitosis, chromatin is in its most condensed form (Lewin, 2000; Lodish, 2004). Since the experiments have shown that HDAC3 associates with histone H1 and we know that both of these proteins participate in compaction of chromatin (Eot-Houllier, 2008; Herrera, 2000; Li, 2000b; Li, 2002; Maresca, 2005a; Th'ng, 2005; Vaquero, 2004), the question was whether this complex has a role in mitosis. Since earlier studies demonstrated higher phosphorylation levels on histone H1 during mitosis (Halmer, 1996 ; Sarg, 2006), experiments examined whether HDAC3 can interact with a phosphorylated form of histone

H1. To this end, co-immunoprecipitation assays were carried out using antibodies against HDAC3 and Western blot analysis with antibodies against phosphorylated histone H1. The resulting immunoblot, demonstrated an association of HDAC3 and phosphorylated histone H1 (Fig. 9). Based on the molecular weight of the immunoprecipitated band, it is assumed that HDAC3 interacts with phosphorylated H1.3 but not with other phosphorylated histone variants.

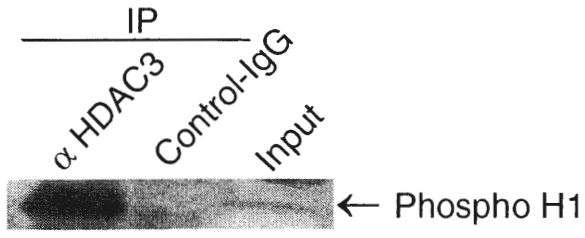

Figure 9: HDAC3 associates with phosphorylated histone H1.
Representative blot of, HeLaS3 whole cell extracts, co-immunoprecipitated with anti-HDAC3 and non-immune IgG (negative control) then resolved on 12% SDS-PAGE and tested by Western blotting for the presence of phosphorylated histone H1 (n=3).

To determine if HDAC3 is preferentially binding phosphorylated histone H1.3 over the non-phosphorylated histone H1.3, immunoprecipitation against HDAC3 was performed on unsynchronized HeLaS3 cells extracts. The immunoprecipitated extract was divided into halves and each half was analyzed by immunoblotting against either phospho-histone H1 antibody or histone H1.3 antibody. The experiment was performed three times and densitometric analysis was carried out on the immunoblots to analyze the amount of proteins present. The resulting band was normalized against the input band to standardize for the effect of band intensity due to antibody specificity (Fig. 10). The resultant densitometric value was used to evaluate the relative binding of HDAC3 to histone H1.3 in logarithmically growing cells. The obtained ratio was 2.05:1 for phospho-histone H1.3:H1.3 (Table 3). Therefore, HDAC3 shows a twice more binding to phosphorylated histone H1.3 (see Fig. 9) as compare to non-phosphorylated histone H1.3 (see Fig. 7B) (Chi square goodness of fit test, α=0.05, χ^2=3.94x10^{-6}, p=0.99, df=1, n=3). Thus, HDAC3 binds twice more to phosphorylated histone H1.3 than non-phosphorylated histone H1.3 in logarithmically growing HeLaS3 cells.

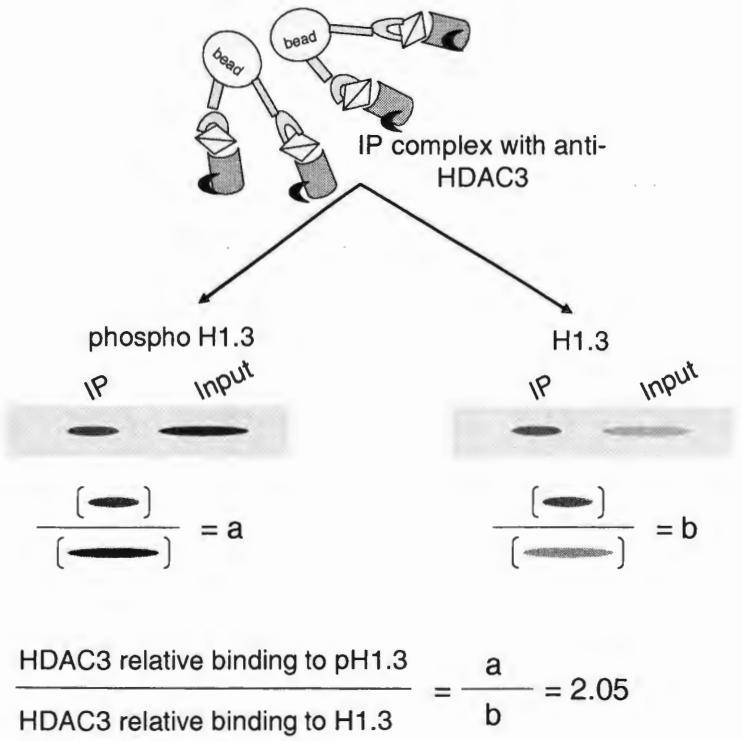

Figure 10: Schematic to calculate relative binding of HDAC3 to phosphorylated and unphosphorylated H1.3 in an unsynchronized HeLaS3 cell extracts.

Table 3
Integrated Density Values (IDV) for Calculation of Relative HDAC3 Binding With Phospho H1.3 and Histone H1.3. (n=3)

	set 1	set 2	set 3	average relative binding ± SD	average relative binding ratio (a / b)
IDV (IP: pH1.3)	4193664	3448313	44837010		
IDV (Input pH1.3)	1137925	588565	12941643		
HDAC3 relative binding to phospho H1 (a)	3.69	5.86	3.46	4.33 ± 1.32	
IDV (IP: histone H1.3)	11834483	10823795	29644040		2.05
IDV (Input H1.3)	5938326	3547854	20245971		
HDAC3 relative binding to histone H1.3 (b)	1.99	3.05	1.46	2.11 ± 0.81	

IP=immunoprecipitated band; SD=standard deviation

The Interaction of HDAC3 With Histone H1.3 Increases During Late-G_2 and Mitosis

Both HDAC3 and histone H1 were independently known to be involved in mitosis regulation (Eot-Houllier, 2008; Ishii, 2008b; Izzo, 2008; Li, 2006; Magnaghi-Jaulin, 2007; Maresca, 2005a; Ohsumi, 1993; Stevens, 2008; Thoma, 1979). Therefore, after demonstrating HDAC3 interaction with phosphorylated histone H1.3, the correlation of this complex with mitosis was studied using the hypothesis that if this complex is involved in mitosis regulation, its level will increase during mitosis. HeLaS3 cells were treated with nocodazole to obtain a higher proportion of mitotic cells. Then quantified the mitotic index of cells was quantified by Giemsa staining. Metaphase spreads were counted from 200 microscopic fields. Experiments obtained 54% of metaphase cells (Fig. 11) after nocodazole treatment versus 2.28% metaphase cells with DMSO (vehicle control).

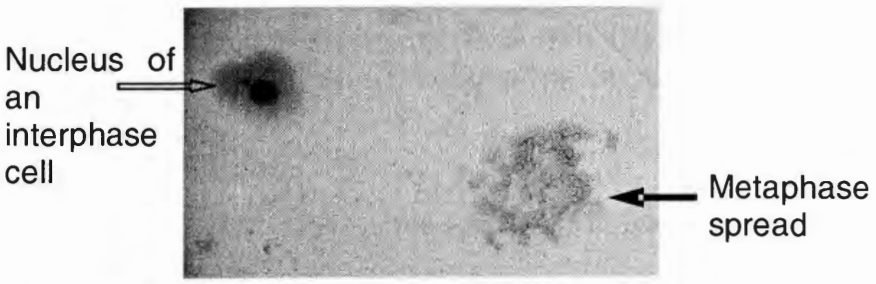

Figure 11: Nocodazole treatment arrested 54% HeLaS3 cells in metaphase. Representative Giemsa staining, of HeLaS3 cells after 100 nM nocodazole treatment for 20 hours, showed metaphase spreads (bold arrow) and interphase cells (open arrow). Observing and counting 200 microscopic fields (total cells=3178) at 400X total magnification, 54% of the cells were arrested in metaphase compared to 2.28% metaphase cells with DMSO (vehicle control) treatment.

Nocodazole and DMSO treated HeLaS3 cell extracts were further analyzed by immunoblotting to confirm high phosphorylation levels of histone H1 (Fig. 12B). The phosphorylation of histone H1 indeed was elevated correlating with the higher levels of mitotic cells. The levels of HDAC3 proteins were also tested by performing Western blot analysis and no observable changes between the nocodazole treated and untreated cells were seen (Fig. 12A).

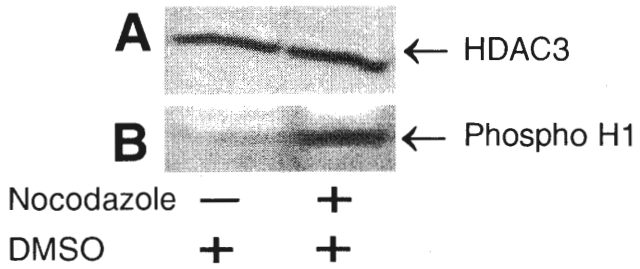

Figure 12: HeLaS3 cell extracts were treated with Nocodazole and analyzed for protein expression by Western blot analysis.
(A, B) Western blot analysis of HeLaS3 cells treated with nocodazole or DMSO (vehicle control) (30 µg protein for each treatment), with: (A) anti-HDAC3 (8% SDS-PAGE) to evaluate protein levels; and with (B) anti-phospho-histone H1 (12% SDS-PAGE) to confirm higher phosphorylation of histone H1 in the mitotic cells.

After confirming the higher phosphorylation levels of histone H1 upon nocodazole treatment, the complex levels were analyzed by immunoprecipitation assays with anti-HDAC3 antibodies followed by a Western blot analysis using antibodies against phosphorylated histone H1 (Fig. 13A). The results demonstrate higher levels of HDAC3 and phospho-histone H1 complex after

nocodazole treatment. To confirm the results, a reciprocal co-immunoprecipitation was done against phosphorylated histone H1 and Western blot analysis was performed to detect HDAC3 levels. The resulting immunoblot supported the earlier findings, i.e. higher levels of HDAC3 and phospho-histone H1 association during mitosis (Fig. 13B).

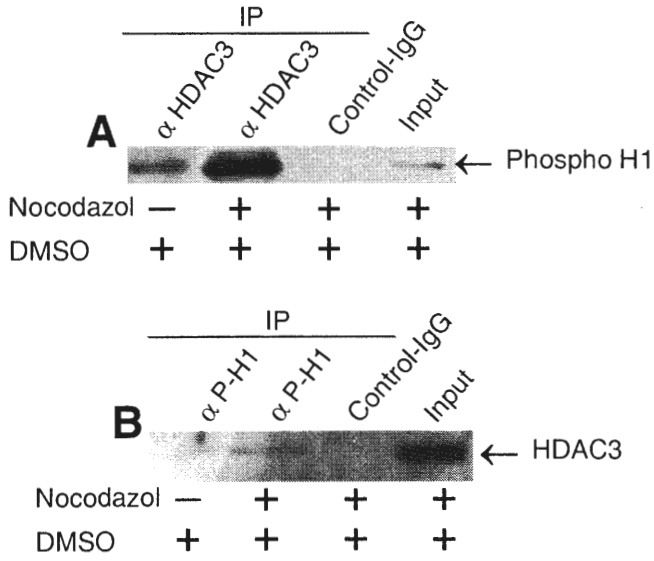

Figure 13: HDAC3 interaction with phospho-H1 is higher after nocodazole treatment.
(A) Western blot (12% SDS-PAGE) to detect phosphorylated histone H1 in anti-HADC3 immunoprecipitate from nocodazole and DMSO treated HeLaS3 cell extracts. (B) Presence of HDAC3 was tested with Western blot (12% SDS-PAGE) in anti-phospho-histone H1 immunoprecipitate from nocodazole and DMSO treated HeLaS3 cell extracts.

Since only 54% metaphase arrest was obtained after nocodazole treatment, the question was what the cell cycle phase of the remaining cells was and if that influenced the higher complex formation upon treatment. This

dissertation hypothesized that if the complex is essential for the onset of mitosis, it must accumulate in higher levels before mitosis. To answer this question, a flow-cytometric cell cycle analysis of nocodazole treated cells was performed. The cells were stained first with PI, which stains DNA, to distinguish among cells in G_o-G_1 phase, S phase, and G_2-M phase (Fig. 14A, C; histograms). Experiments showed higher G_2-M phase cell population (second peak in histograms) after nocodazole treatment as compared to DMSO treatment (Fig. 14A, C). Since PI staining cannot distinguish between G_2 phase cells and mitotic cells, mitosis-specific marker antibodies were used against phosphorylated histone H3 serine 10 (phospho H3S10) conjugated with FITC, along with PI for DNA counterstaining (Fig. 14B, D, E; dot-plots). In this analysis, mitotic cells separated out higher on the Y-axis (dot-plots, upper right quadrants) due to FITC staining and could be distinguished from the G_2 phase cell population (dot-plots, bottom right quadrants). The result from this analysis showed 38.39% G_2 phase cells after nocodazole treatment (Fig. 14D, upper right quadrant) as compared to 22.74% G_2 phase cells with DMSO treatment (Fig. 14B, upper right quadrant), which raised the question, whether the higher levels of HDAC3-H1.3 complex occurred in mitosis or G_2 phase.

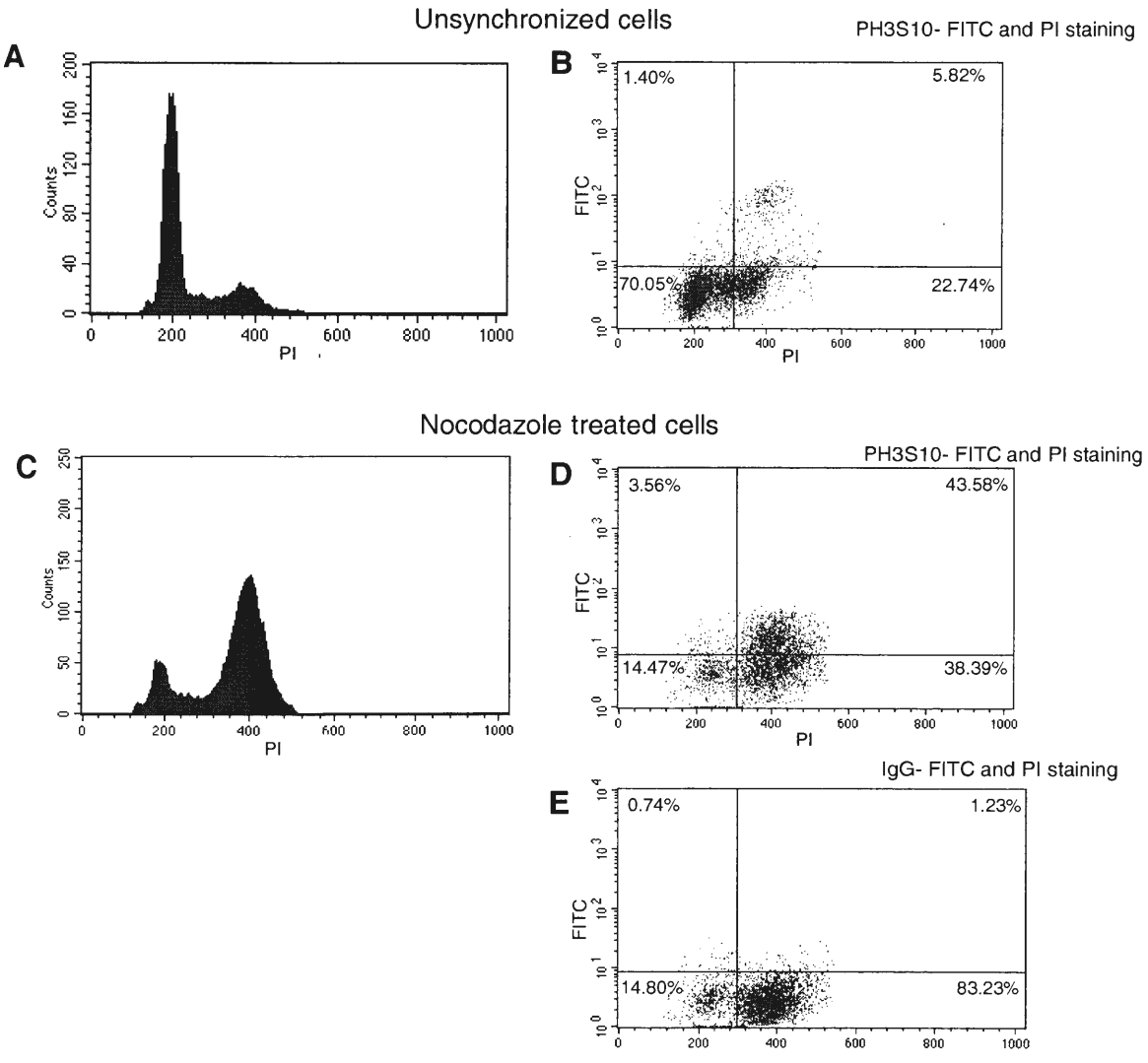

Figure 14: Cell cycle flow-cytometric analysis of nocodazole treated cells. (A) Histogram of DMSO treated cells (unsynchronized) subjected to PI staining showed G_0/G_1 (first peak), G_2/M (second peak), and S phase (cell population in the middle of two peaks). (B) Dot-plot of DMSO treated cells (unsynchronized) stained with phospho-H3S10-FITC and PI that separated 5.82% mitotic cells (upper right quadrant) from 22.74% G_2 phase cells (bottom right quadrant). (C) Histogram of 100 nM nocodazole cells subjected to PI staining showed higher G_2/M cell population (taller second peak). (D) Dot-plot of 100 nM nocodazole treated cells after phospho-H3S10-FITC and PI staining showed 43.58% mitotic cells and 38.39% G_2 phase cells. (E) Dot-plot of 100 nM nocodazole treated cells after IgG-FITC (negative control) and PI staining showed 1.23% mitotic cells.

Histone H1 and HDAC3 were independently implicated in mitosis regulation by earlier studies (Ishii, 2008a; Li, 2006; Maresca, 2005b). The nocodazole treatment studies suggested that HDAC3-H1.3 complex may have a potential role in inducing and/or progressing mitosis. Therefore, the dissertation hypothesized that the complex may be formed in higher amounts just before entering mitosis. To test this hypothesis, the HDAC3-H1.3 complex concentration was examined in a more detailed cell cycle analysis (Fig. 15).

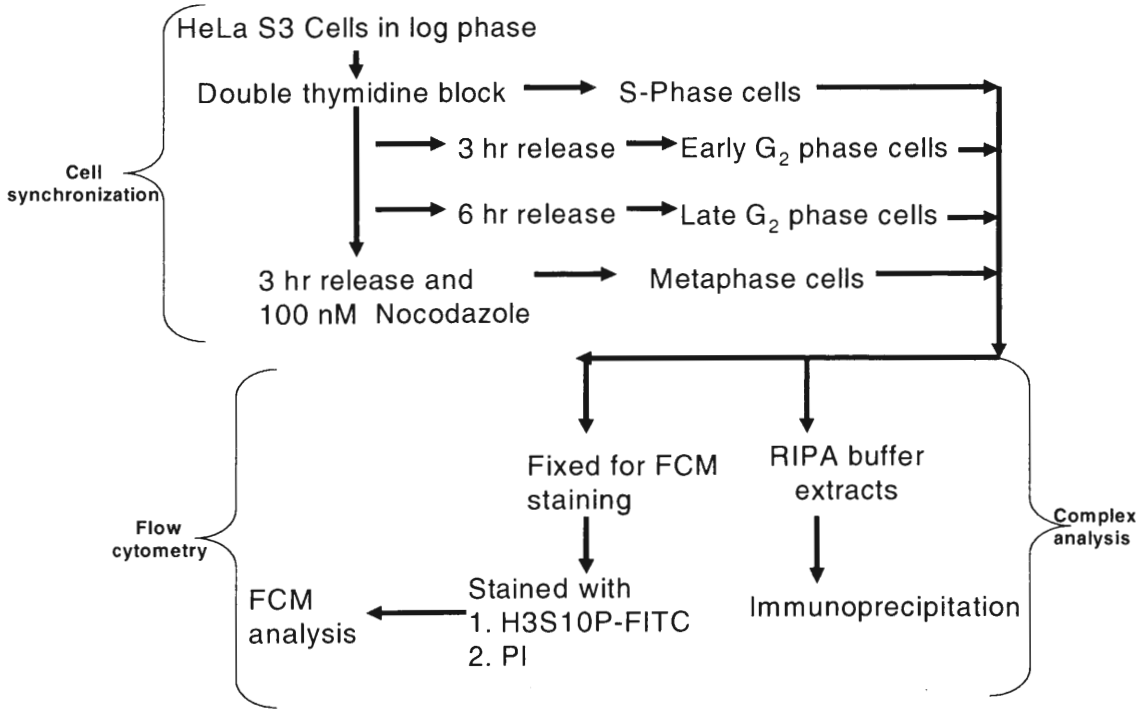

Figure 15: Schematic plan for analysis of HDAC3-H1.3 complex abundance during cell cycle phases. HeLaS3 cells were synchronized in S phase, early-G_2, late-G_2 and mitosis, using double thymidine and nocodazole treatments. Double thymidine block (2 μM) for 18 hours each with 11 hours release between two treatments helped synchronize cells in S phase. A release of 3 hours from S phase yielded early-G_2 cells, while late-G_2 cells were collected after a release of 6 hours. Following a release of 3 hours from double thymidine block, a nocodazole treatment (100 nM) arrested the cells in mitosis.

A flow-cytometric analysis on synchronized cell population was performed using a double staining with PI for DNA quantitation and phospho-H3S10-FITC as a mitotic marker. The staining was used to analyze the synchronization of the cell populations; and with the help of obtained density plots, (dot-plots and histograms) experiments confirmed that the cells are in the desired cell cycle stages (Fig. 16A-F). The percentage of mitotic cells obtained based on the flow-cytometric analysis was 86.42% (Fig. 16E), which was much higher than the range of mitotic cells obtained by synchronizing with nocodazole alone. Mitotic cells in the late-G_2 cell population were detected to be 0.55% (Fig. 16D, dot-plot), which is same as a background staining of mitotic cells performed using IgG-FITC antibody (Fig. 16F), thus the late-G_2 cell population was free of mitotic cell contamination. Further investigations of the levels of phopsho-H3S10 in the various cell cycle stages (Fig. 17) were performed using the synchronized cell extracts to support the flow-cytometric analysis with immunoblotting. Experiments demonstrated with the help of the immunoblot (Fig. 17), that the mitotic cells had higher levels of phosphorylated H3S10 in comparison to all the other stages. The levels of phosphorylation on H3S10 seen in all other synchronized cell cycle stages were the basal level modification on this residue. Thus, the Western blot and flow cytometric analysis support the conclusion that the late-G_2 phase was free of contamination with mitotic cells.

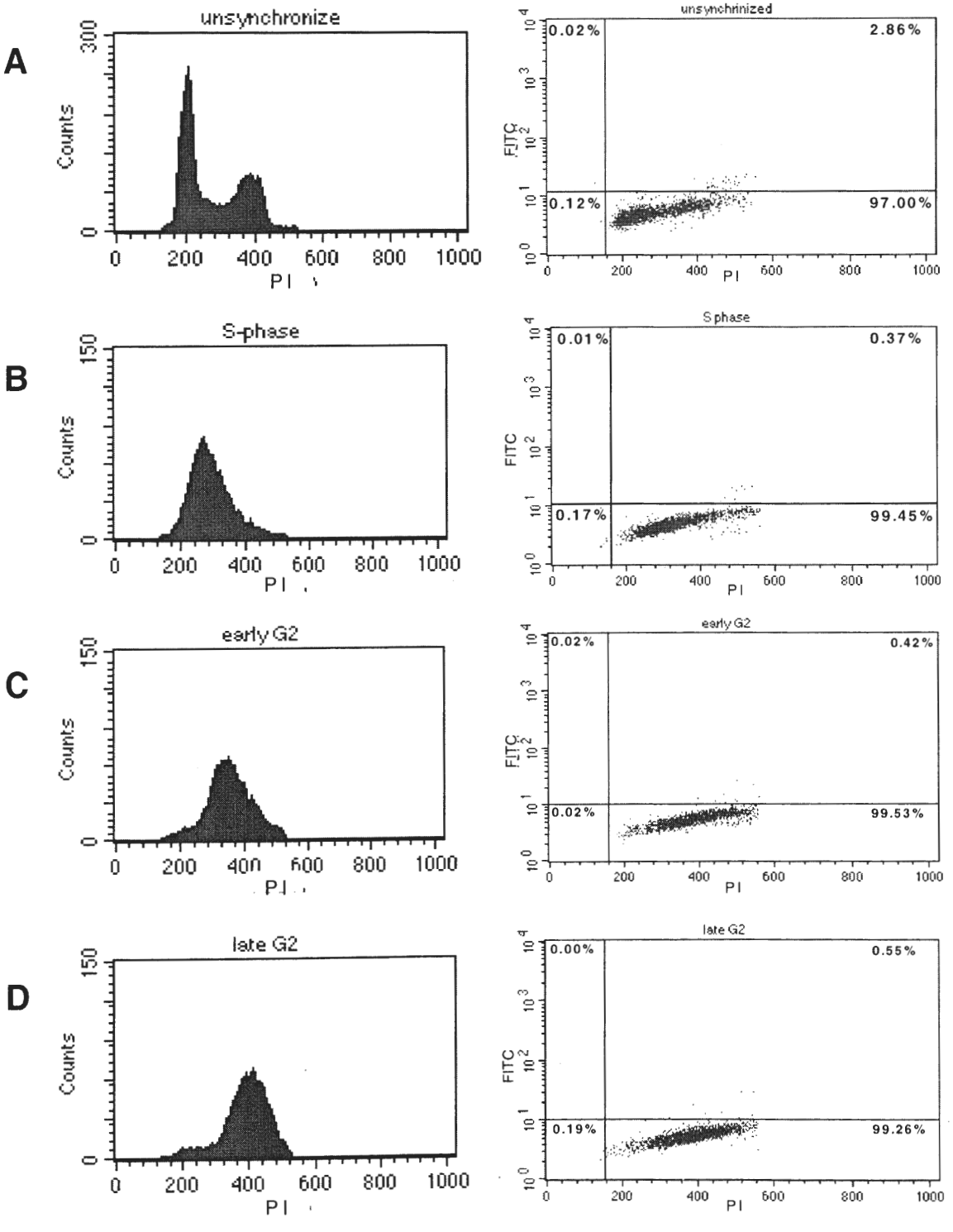

Figure 16 continued

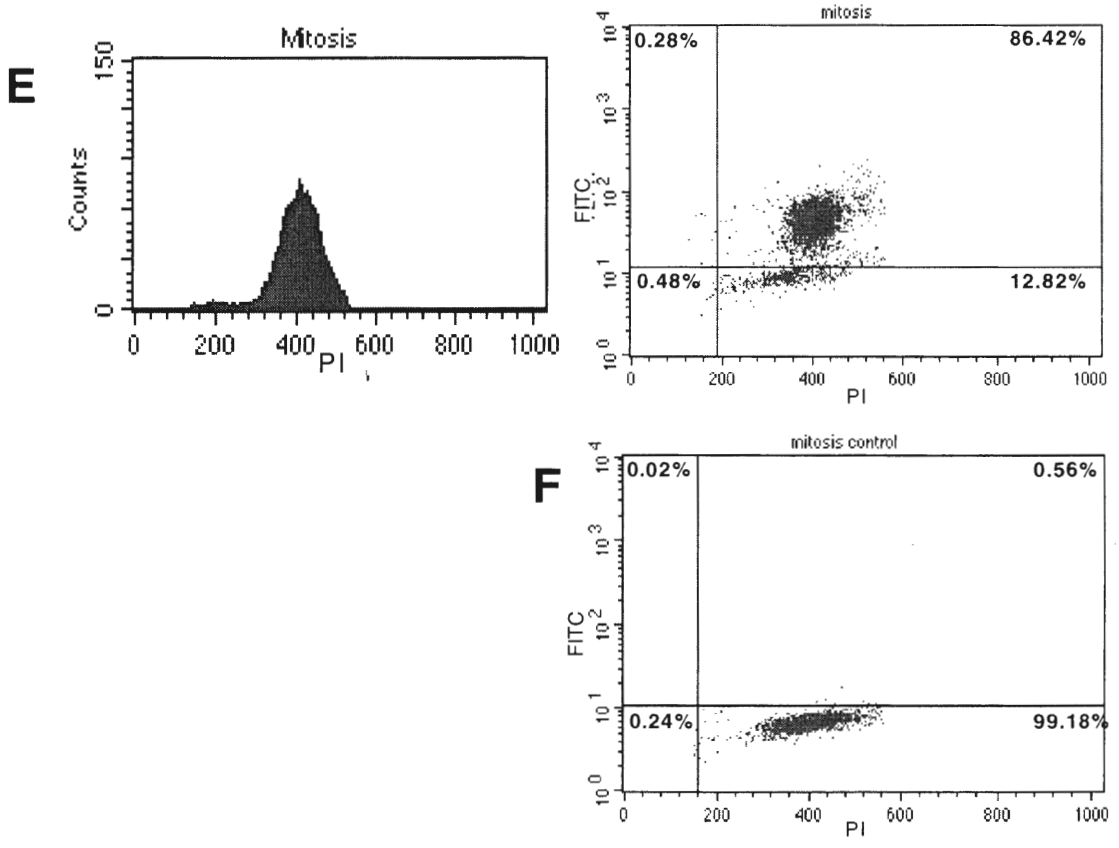

Figure 16: Flow cytometric analysis of synchronized S phase, early-G_2, late-G_2 and mitosis cells.
(A) Histogram (PI staining) and dot-plot (phospho-H3S10-FITC and PI staining) of unsynchronized HeLaS3 cells. Histogram showed G_0/G_1 (first peak), G_2/M (second peak), and S phase (cell population in the middle of two peaks). Dot-plot showed 2.86% mitosis in unsynchronized cells. (B-F) Histogram and dot-plot of HeLaS3 cells synchronized to S phase (B) using double thymidine block (2 μM), early-G_2 (C) after 3 hours of release from double thymidine block, late-G_2 (D) after 6 hours of release from double thymidine block and mitosis (E) after 3 hours of release from double thymidine block followed by nocodazole (100 nM) treatment. (F) Mitosis control dot-plot serves as a negative control staining for mitosis population with IgG-FITC and PI staining.

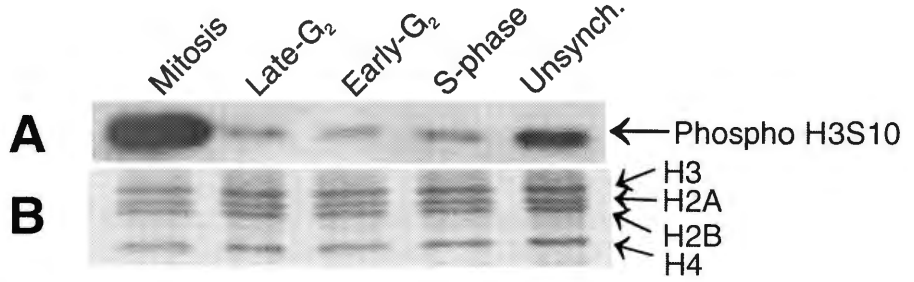

Figure 17: Phosphorylated histone H3 serine-10 levels are elevated during mitosis.
(A) Western blot of synchronized HeLaS3 cell cycle extracts from S phase, early-G_2, late-G_2 and mitosis, resolved on 15% SDS-PAGE and immunoblotted for phospho-H3S10 as a mitosis marker. (B) Coomassie blue staining of the same extracts served as a loading control.

To examine the HDAC3-H1.3 complex levels at different cell cycle stages, co-immunoprecipitation assays were carried out using antibodies against histone H1 (Fig. 18A) or phospho-histone H1 (Fig. 18B) followed with the Western blot analysis for detection of HDAC3 protein. With the results from three independent experiments, the results show a significantly higher association between HDAC3 and histone H1, and also between HDAC3 and phospho-histone H1 at late-G_2 phase as compared to other cell cycle stages; and the complex levels remained high during mitosis [Kruskal-Wallis nonparametric one way analysis of variance with Student-Newman-Keuls (SNK) grouping, $p \leq 0.05$, $n=3$]. To further confirm the results, the reciprocal co-immunoprecipitation assays were performed with anti-HDAC3 and Western blot analysis was carried out for detection of either histone H1.3 (Fig. 18C) or phospho-histone H1 (fig. 18D). The results from this

experiment supported the previous experimental conclusions that HDAC3-H1.3 complex was at higher levels during late-G_2 and remained higher during mitosis (Fig. 19). To test if one of the proteins in the complex was more abundant in late-G_2 or mitosis, the levels of histone H1.3 (Fig. 20A), phospho-histone H1.3 (Fig. 20B), and HDAC3 (Fig. 20C) were examined by Western blot analysis in three independent experiments. Levels of phosphorylated histone H1.3 were detected using a general anti-phospho histone H1 antibody and based on the molecular weight of the histone H1.3. The amount of histone H1.3 seemed to be unaltered during various cell cycle stages (Kruskal-Wallis nonparametric one way analysis of variance with SNK grouping, $p \geq 0.05$). However HDAC3 levels were relatively higher during late-G_2 ($p \leq 0.05$) (Fig. 20E), perhaps explaining the observed higher complex formed during late-G_2. Phosphorylation of histone H1.3 was seen to be higher during mitosis (Fig. 20B); however this could not explain the higher levels of complex during late-G_2. Immunoblot against actin (Fig. 20D) served as a loading control of proteins.

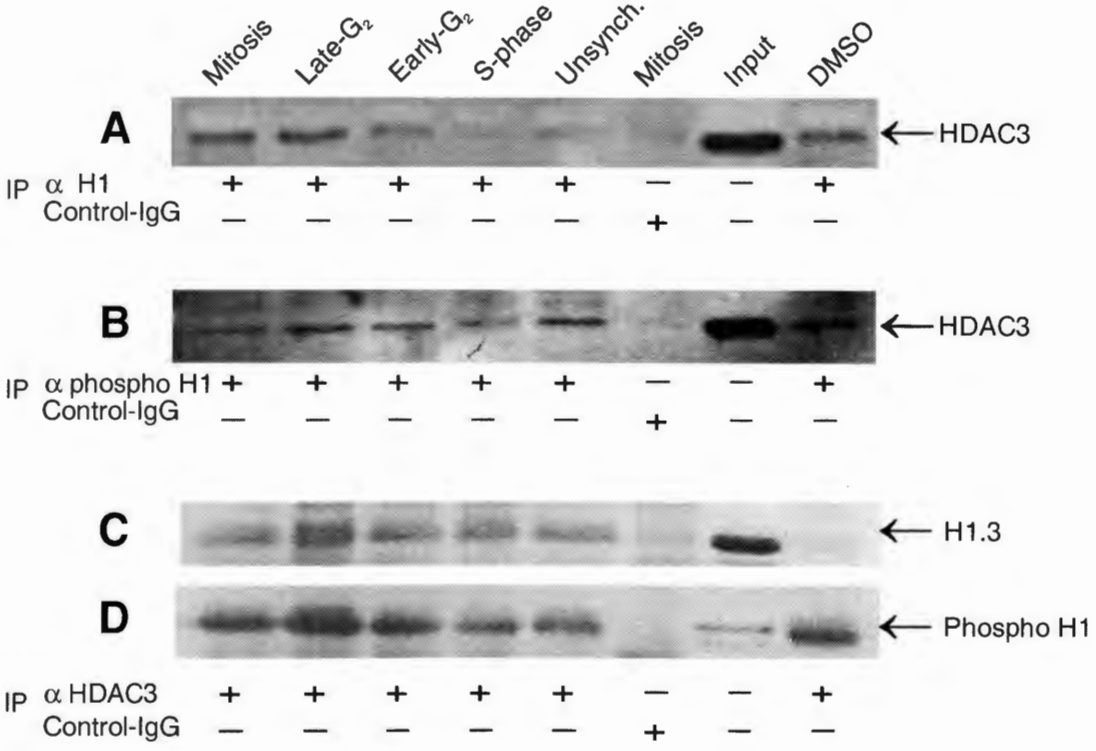

Figure 18: Interaction of HDAC3 with histone H1.3 increases during late-G_2 and mitosis.
(A-D) Representative Western blots (n=3). Synchronized HeLaS3 cell extracts from S phase, early-G_2, late-G_2 and mitosis were co-immunoprecipitated with antibodies: (A) anti-histone H1, (B) anti-phospho-H1 and (C, D) anti-HDAC3. This followed by Western blot analysis to detect (A and B) HDAC3 (8% SDS-PAGE), (C) histone H1.3 (12% SDS-PAGE) and (D) phospho-H1 (12% SDS-PAGE). Immunoprecipitation with non-immune IgG on mitotic cell extracts served as a negative control. Immunoprecipitation on DMSO treated cell extracts served as a vehicle control.

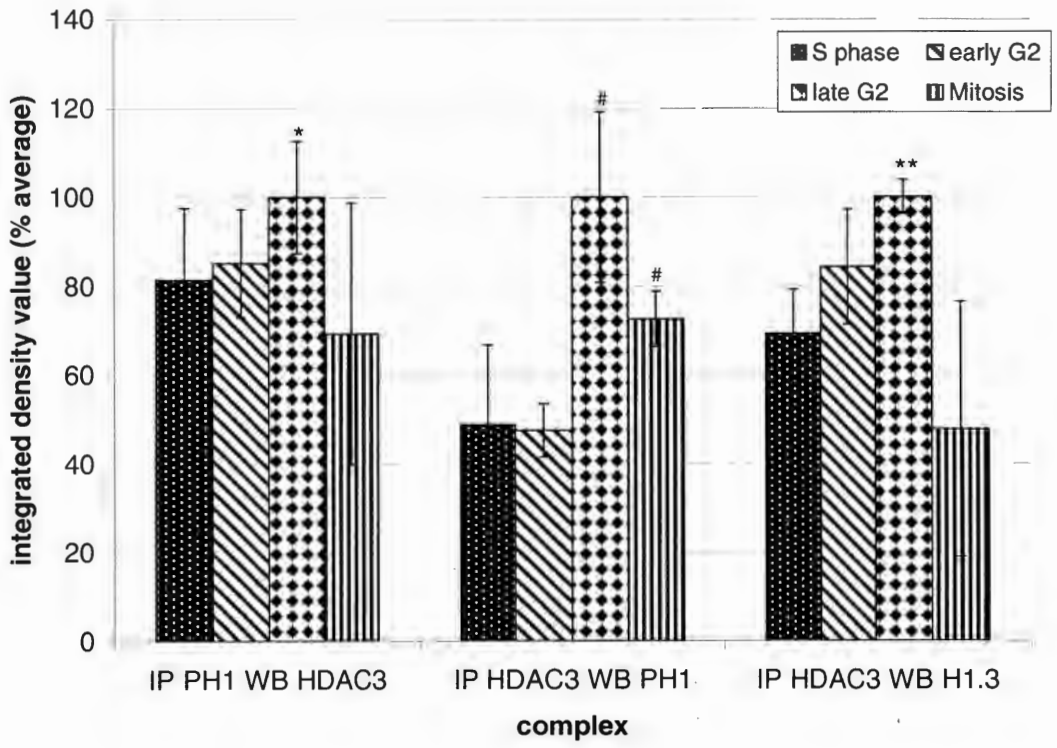

Figure 19: HDAC3-H1.3 complex is higher during late-G_2. The graph illustrates average % $\pm$ SD integrated density values of HDAC3-H1.3 complex levels in S phase, early-G_2, late-G_2 and mitosis (n=3); *, #, and ** indicates significant difference in the complex levels from other cell cycle phase, $p \leq 0.05$ (Kruskal-Wallis nonparametric one way analysis of variance with SNK grouping).

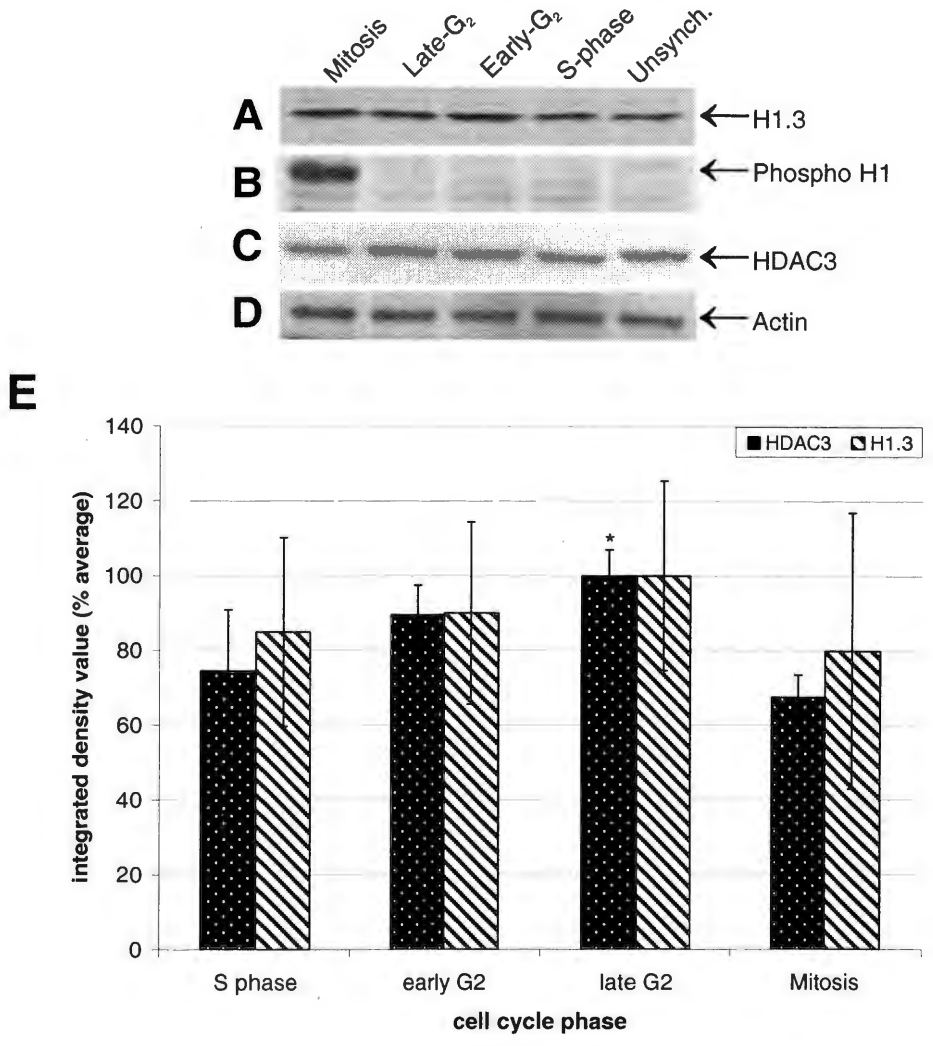

Figure 20: Histone H1.3, phospho histone H1 and HDAC3 levels in S, early-G_2, late-G_2, and mitosis phase of synchronized HeLa cells.
(A-D) Western blots of, HeLaS3 cells synchronized for S phase, early-G_2, late-G_2 and mitosis, analyzed to detect protein levels of (A) histone H1.3 (12% SDS-PAGE), (B) phospho-histone H1 (12% SDS-PAGE), (C) HDAC3 (8% SDS-PAGE) and (D) actin (10% SDS-PAGE) as a loading control. (E) The graph illustrates average % $\pm$ SD integrated density value of HDAC3 and histone H1.3 protein levels in S phase, early-G_2, late-G_2 and mitosis (n=3); * indicates significant difference in HDAC3 protein level from other cell cycle phases, $p \leq 0.05$ (Kruskal-Wallis nonparametric one way analysis of variance with SNK grouping).

HDAC3 Associated With Histone H1.3 in a Complex is Functionally Active as Deacetylase When Isolated From Mitotic but not From Late-G_2 Cells

Class I HDACs are known to be regulated by their association with protein complexes (De Ruijter, 2003; Guenther, 2001; Heinzel, 1997). To characterize the activity of HDAC3 associated with histone H1.3, experiments were performed to investigate ability of HDAC3 to deacetylate acetylated histone H3 lysine 9 (H3K9) and histone H4 lysine 5 (H4K5). These lysine residues were previously described as specific substrates for HDAC3 (Eot-Houllier, 2008; Fu, 2005). As a substrate for deacetylation assay, hyper-acetylated mononucleosomes from HeLaS3 cell nuclei were isolated by sedimentation on sucrose gradient and by stripping the nucleosomes of histone H1. Results confirmed absence of histone H1 from the nucleosomes by immunoblotting nucleosomes against histone H1 antibody (Fig. 21A). Experiments were done to test the nucleosomes for integrity of all the core histones by Coomassie staining (Fig. 21B) and for presence of linker DNA region by agarose gel electrophoresis (Fig. 21C). Only after all these control-tests were successful, the nucleosomes were used as substrates for the HDAC assays.

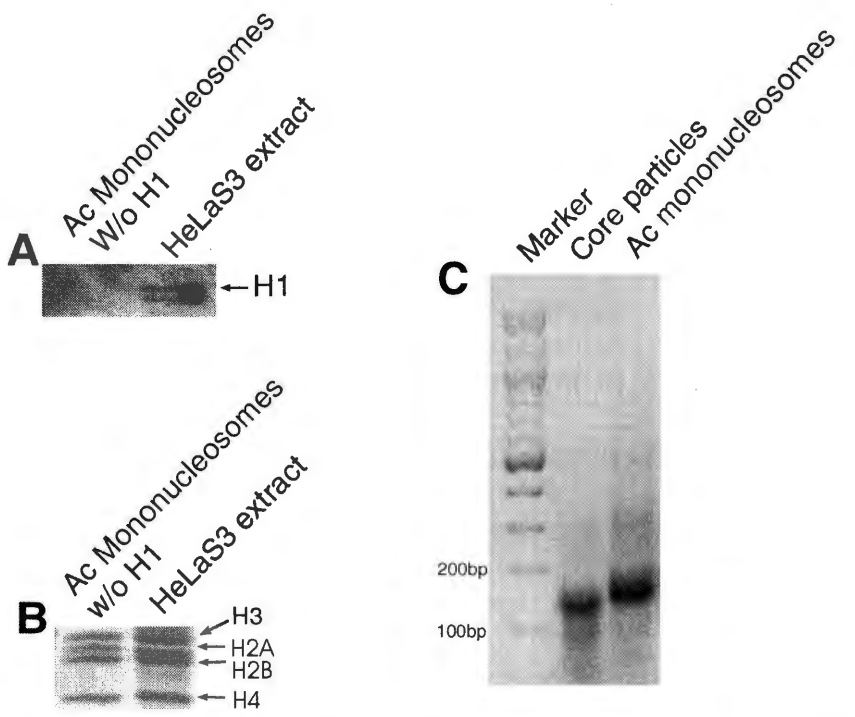

Figure 21: Controls—Isolated mononucleosomes are depleted of histone H1, have core histones in equimolar proportions and contain linker DNA.
(A) The Western blot analysis with anti-histone H1 antibody verified stripping of histone H1 from hyperacetylated mononucleosomes. Hyperacetylated mononucleosomes were isolated from HeLaS3 cells treated with TSA (2 µM) and then subjected to 12% SDS-PAGE. (B) Coomassie staining (15% SDS-PAGE) of acetylated mononucleosomes showed the presence of core histones in equimolar proportions suggesting the lack of degradation. (C) Agarose gel electrophoresis (2%) of hyperacetylated mononucleosomes to verify the presence of linker DNA. Loading of core particles served as a negative control (absence of linker DNA).

HDAC3-H1.3 complexes were isolated by co-immunoprecipitation with antibodies against histone H1, HDAC3 or phospho-histone H1. The last wash during the co-immunoprecipitation was with deacetylation buffer. These complexes were then tested by immunoblotting against HDAC3 (Fig. 22A), to show the presence of HDAC3 in each complex and also to allow the quantification of the amount of HDAC3 present in each immunoprecipitated complex. These immunocomplexes were subjected to HDAC assay by incubating them with acetylated mononucleosomes in deacetylation buffer at 37°C for 40 minutes. The reaction was stopped by adding 1X Laemmli buffer and by boiling the samples at 95°C for 3 minutes. The resulting deacetylation was detected by Western blotting using antibodies against acetylated H3K9 and against acetylated H4K5. The immunoblots show deacetylation of acetylated H3K9 (Fig. 22B, top panel; lane 1, 2, and 3), but not H4K5 (Fig. 22B, bottom panel; lane 1, 2, and 3), in the anti-histone H1 precipitates, and anti-phospho-histone H1 precipitates for a less extent when complexes were isolated from mitotic extracts (Fig. 22B) (Table 4). Interestingly, when the same complexes were isolated from late-G_2 cell extract, the HDAC3 from the complex did not deacetylate the same substrates (Fig. 22C). Control IgG (negative control) did not immunoprecipitate any HDAC activity (Fig. 22B, C; lane 4). Incubation of acetylated mononucleosomes with anti-HDAC3 immunoprecipitates and with recombinant HDAC3/N-CoR2 (HDAC3/SMRT) complex was used as a positive control for HDAC assay (Fig. 22B, C; lane 5).

In order to rule out the possibility of intrinsic HDACs in the fraction of mononucleosomes, the levels of deacetylation of acetylated nucleosomes incubated for 40 minutes at 37°C (Fig. 22B, C; lane 6) were compared to the same nucleosomes incubated at 4°C (Fig. 22B, C; lane 7). No difference was observed indicating that there is little intrinsic HDAC contamination in the nucleosomes preparation. The levels of the acetylation in negative controls using IgG immunoprecipitation were also comparable, indicating that there is no detectable non-specific absorbance of HDACs to the beads.

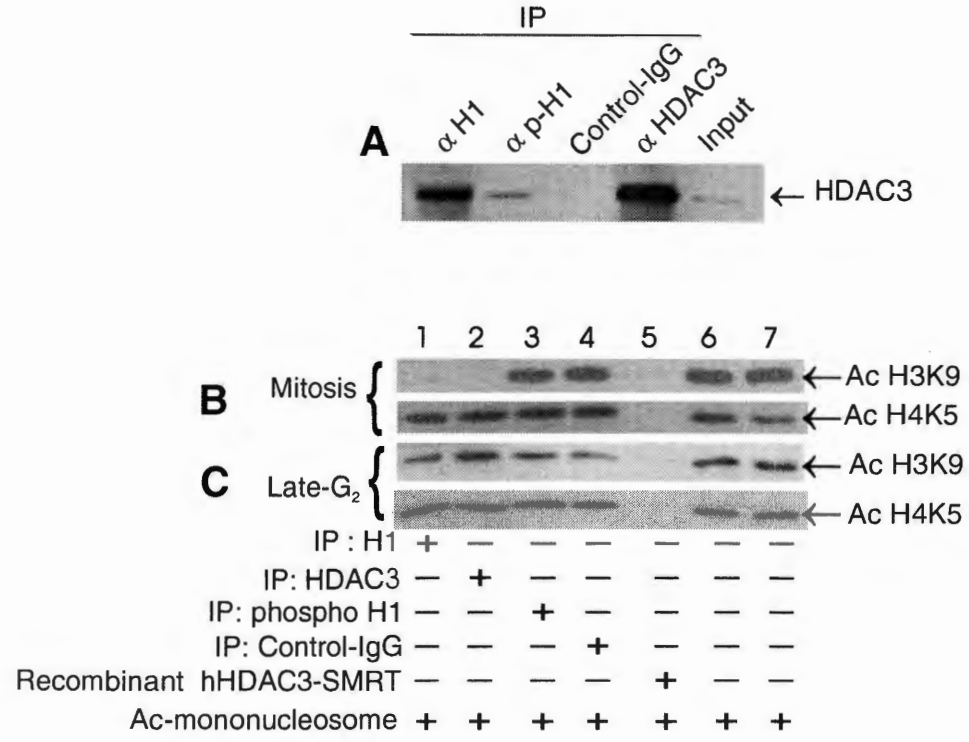

Figure 22: Deacetylation activity of HDAC3 is associated with histone H1.3 during late-G_2 and mitosis.
(A) control—HDAC3 input for HDAC assay determined by Western blot analysis using HDAC3 antibody on immunoprecipitated HeLaS3 cell extracts (mitosis) with anti-histone H1, anti-phospho-histone H1, non-immune IgG (negative control) and anti-HDAC3 (positive control). (B, C) Deacetylation activity of HDAC3-H1.3 complex was assayed upon immunoprecipitation with anti-histone H1, anti-HDAC3, and anti-phospho H1 in HeLaS3 cell extracts from (B) mitosis and (C) late-G_2. Deacetylation of acetylated H3K9 and acetylated H4K5 in hyperacetylated mononucleosomes is assessed by Western blot analysis (15% SDS-PAGE) after deacetylation assay. Deacetylation with recombinant hHDAC3-SMRT complex and anti-HDAC3 immunoprecipitate served as a positive control; while non-immune IgG immunoprecipitate served as a negative control.

Table 4
Integrated Density Values for H3K9 Acetylation (Fig. 22B, Top Panel) and HDAC3 Input (Fig. 22A) for Calculation of Relative Deacetylation in HDAC Assay.

IP	H1	Pospho-H1	HDAC3	IgG
IDV (acetylation signal) (from Fig. 18B, top panel)	44000	519000	43000	552000
IDV (IgG) - IDV (IP) (a)	508000	33000	509000	-
HDAC input (from Fig 18.A) (b)	7022	1014	9643	130
Relative deacetylation (a/b)	72.34	32.54	52.78	-

IDV= integrated density value

Since the HDAC3-H1.3 complex deacetylates H3K9 but not H4K5 *in vitro*, it was examined whether histone H3K9 and H4K5 are deacetylated *in vivo* (HeLaS3 cells) during mitosis. The levels of acetylation on H3K9 and H4K5 were determined by Western blot analysis, in the synchronized cell extracts, using antibodies for acetylated H3K9 and for acetylated H4K5. With help of immunoblots, results demonstrated a significant reduction in acetylation of H3K9 and H4K5 during mitosis (Fig. 23A, B). The results support the postulated that the novel complex of HDAC3 associated with histone H1.3 may be involved in deacetylation of acetylated H3K9 during mitosis. The mechanism for deacetylation of H4K5 remains undetermined.

Acetylation-deacetylation and methylation of core histone residues can be coordinately regulated (Berger, 2002). Since acetylation of H3K9 and methylation of H3K9 is on the same histone residue, it can be mutually exclusive. Experiments were done to determine if deacetylation of H3K9 during mitosis contributes to its trimethylation, which is a well known marker for heterochromatinization (Bernstein, 2005; Rougeulle, 2004; Schotta, 2004). When synchronized cell extracts were analyzed for the levels of methylation on H3K9, the immunoblot indicated no correlation between the H3K9 tri-methylation and H3K9 deacetylation (Fig. 23C). Coomassie staining of the cell cycle extracts indicated no observable differences in protein loading (Fig. 23D) for all the Western blot analysis.

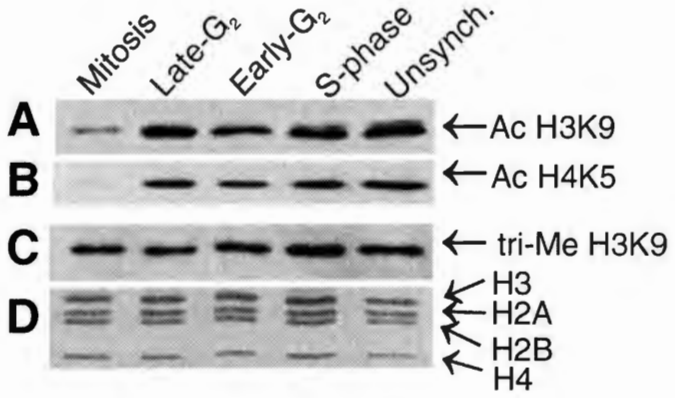

Figure 23: Acetylation levels of histone H3K9, H4K5 and methylation of histone H3K9 during S phase, early-G_2, late-G_2 and mitosis.
(A, B) Western blots of, HeLaS3 cells synchronized for S phase, early-G_2, late-G_2 and mitosis. The cell extracts were resolved on 15% SDS-PAGE, and then analyzed by Western blotting to detect acetylation levels of (A) H3K9 and (B) H4K5. (C) Western blot analysis for detection of trimethylation levels on H3K9 during various cell cycle stages. (D) Coomassie staining served as a loading control.

The HDAC3-H1.3 Complex Includes SMRT but not N-CoR

Since the HDAC3 within HDAC3-H1.3 complex was active in mitotic cells but not in late-G_2, it was desirable to find out the mechanism that activates HDAC3 upon the entry of the cells to mitosis. Activation of HDAC3 by its association with SMRT or with N-CoR was previously documented (Guenther, 2001; Li, 2000b). Therefore, it was desirable to examine if SMRT or N-CoR are associated with the isolated complex and if their presence is altered between late-G_2 and mitosis. To this end, co-immunoprecipitation with antibodies against histone H1 and HDAC3 on mitotic (Fig. 24A) and late-G_2 (Fig. 24B) cell extracts were performed and tested by Western blot analysis for the presence of SMRT and N-CoR. Using the resulting immunoblots, experiments demonstrate that SMRT but not N-CoR was associated with the isolated complex. Since the presence of the SMRT was detected in mitosis as well as in late-G_2, it cannot explain the activation of the HDAC3-H1.3 complex during mitosis.

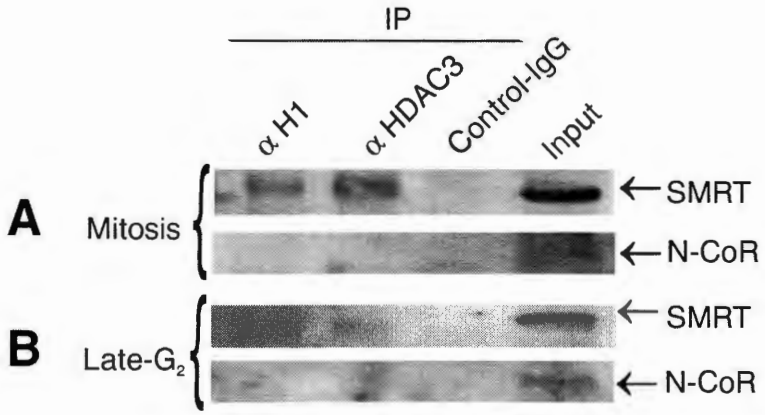

Figure 24: SMRT but not N-CoR associates with HDAC3-H1.3 complex.
(A, B) Representative Western blot of, HeLaS3 whole cell extracts of (A) mitosis and (B) late-G_2 phase, immunoprecipitated with anti-histone H1, anti-HDAC3, and non-immune IgG (negative control). The immunoprecipitates were resolved on 8% SDS-PAGE and tested by Western blotting for the presence of SMRT (A and B, top panels) and N-CoR (A and B, bottom panels). (n=3)

Phosphorylation of HDAC3 by CK2 Upregulates its Deacetylation Activity in the HDAC3-H1.3 Complex

The previous experiments showed that the HDAC3-H1.3 complex was active during mitosis but not during late-G_2 (Fig 22B, C). A recent study by Zhang et al. (Zhang, 2005) showed that HDAC3 can be activated by phosphorylation of Ser-424 by CK2; however, this activation has not previously been associated with mitosis. Experiments were done to explore the possibility that phosphorylation of HDAC3 by CK2 can contribute to its activation in the transition from late-G_2 to mitosis. The first goal was to investigate if HDAC3 is phosphorylated during mitosis. For this purpose, HDAC3 was immunoprecipitated from synchronized cell cycle extracts using anti-HDAC3 antibody. The immunoblot with phospho-serine antibody on the immunoprecipitates showed higher levels of serine residue phosphorylation in HDAC3 during mitosis and for some extent during S phase (Fig. 25). Further, to confirm if Ser-424 is being phosphorylated at a higher level during mitosis as compare to late-G_2, histone H1 was immunoprecipitated from late-G_2 and mitosis cell extracts and carried out Western blot analysis with anti-phospho-HDAC3-Ser-424. The resultant immunoblot demonstrates higher phosphorylation of Ser-424 residue in HDAC3 during mitosis as compared to late-G_2 (Fig. 26).

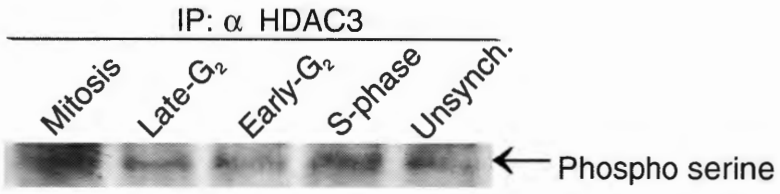

Figure 25: Phosphorylation of serine residues on HDAC3 is higher during mitosis and S phases of cell cycle.
Western blot of, HeLaS3 cell extracts from synchronized S phase, early-G_2, late-G_2 and mitosis, immunoprecipitated with anti-HDAC3 antibody then resolved on 8% SDS-PAGE to analyzed the levels of phosphorylated serine residues in HDAC3 protein.

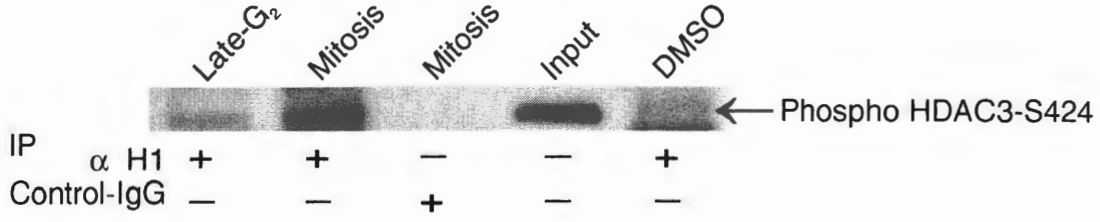

Figure 26: HDAC3 is highly phosphorylated at serine-424 residue in mitosis as compare to late-G_2 cell cycle phase.
Western blot of histone H1 immunoprecipitates from late-G_2 and mitosis cell cycle extracts immunoprecipitated with anti-histone H1. The immunoprecipitates were subjected to 8% SDS-PAGE, and then analyzed for levels of phospho-HDAC3-Ser424 on immunoblot. Immunoprecipitation with non-immune IgG served as a negative control. DMSO treated cell extract was used as a vehicle control for nocodazole treated cells.

Since CK2 has been previously found to phosphorylate HDAC3 on Ser-424 (Zhang, 2005), it was next investigated if CK2 can phosphorylate HDAC3 *in vitro,* in the HDAC3-H1.3 complex obtained from late-G_2 cell extracts. Late-G_2 extracts were immunoprecipitated using anti-histone H1 antibody. The precipitate was then incubated with CK2 in the presence of ATP (200 mM) and γ-^{32}P-ATP (500 µCi/mmol) (specific activity of γ-^{32}P-ATP was calculated independently for each experiment). Non-immune IgG immunoprecipitate (negative control) was used to confirm specific phosphorylation by CK2 (Fig. 27; lane 2). Immunoprecipitate obtained by using histone H1 antibody, incubated without CK2 enzyme showed no intrinsic kinase activity of the complex (Fig. 27; lane 3). However, when HDAC3-H1.3 complex was incubated with CK2, HDAC3 was phosphorylated (Fig. 27, top panel; lane 1). Thus, the resultant phosphorimage data demonstrate that CK2 can specifically phosphorylate HDAC3 from HDAC3-H1.3 complex obtained from late-G_2 cell extracts. To check the possibility of mitotic kinase being involved in phosphorylation of HDAC3, Cdc2-cyclin B was incubated with HDAC3-H1.3 complex. From the resultant phosphorimage (Fig. 27, top panel; lane 5) HDAC3 phosphorylation with Cdc2-cyclin B kinase could not be detected. Experiments were performed to also test whether CK2 or cdc2-cyclin B can phosphorylate histone H1.3 in the complex and no band was detected on the phosphorimage (Fig. 27, bottom panel; lane 1, 5).

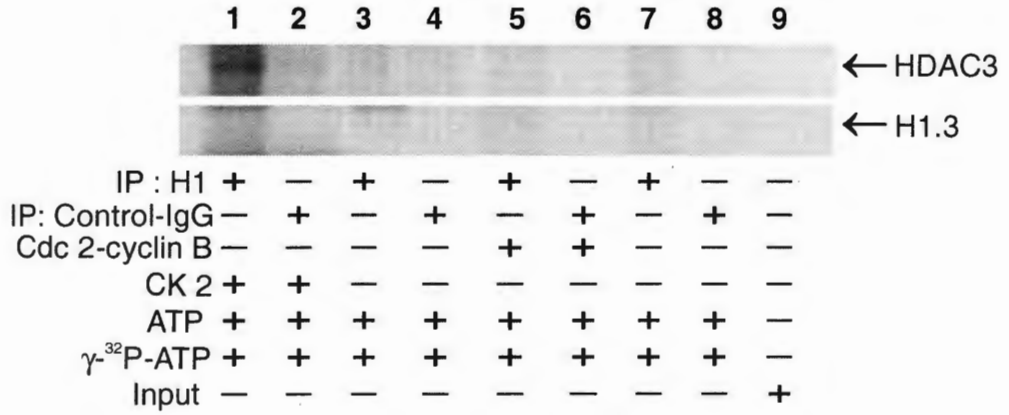

Figure 27: HDAC3 in the HDAC3-H1.3 complex isolated from late-G_2 can be phosphorylated *in vitro* by CK2.
Phosphorimage detection of *in vitro* phosphorylation of HDAC3-H1.3 complex. HDAC3-H1.3 complexes were isolated from late-G_2 cell extract and phosphorylated using CK2 enzyme or cdc2-cyclinB and γ-^{32}P-ATP in the reaction mixture. The results were examined using phosphorimage for detecting phosphorylation of HDAC3 (8% SDS-PAGE) (top panel) and histone H1.3 (12% SDS-PAGE) (bottom panel).

To address the original question about the activation of HDAC3 within the HDAC3-H1.3 complex upon its phosphorylation, experiments needed to confirm that HDAC3 remained bound to the complex and was not dissociated. Earlier studies have indicated that higher levels of phosphorylation on HDAC3 may dissociate it from its complex (Zhang, 2005). Therefore, experiments explored whether HDAC3 dissociates from the HDAC3-H1.3 complex after phosphorylation *in vitro* with CK2. The phosphorylation was carried out on the immunoprecipitated complex attached to the agarose beads using γ-^{32}P-ATP. The resultant proteins attached to the beads (in the pellet) and the proteins from the reaction mixture (supernatant) were loaded on the SDS-PAGE to analyze the

amount of HDAC3 dissociated from the complex. The resulting phosphorimage demonstrates that major of HDAC3 remained associated with the complex after phosphorylation *in vitro* (Fig. 28). The small amount of dissociated HDAC3 in the supernatant did not change the capacity to test whether the phosphorylated HDAC3 within the complex can be activated.

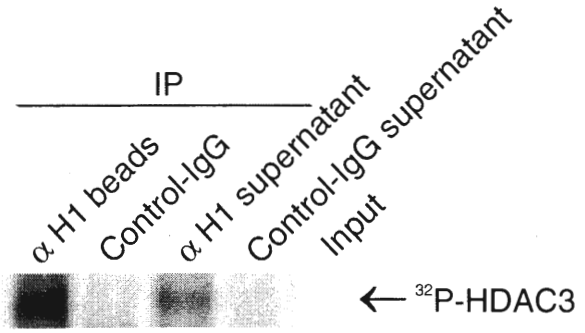

Figure 28: HDAC3 remains associated with H1.3 and bound to the beads after phosphorylation *in vitro* by CK2 enzyme.
Phosphorimage detection of phosphorylated HDAC3 complex. HDAC3-H1.3 complex was phosphorylated using CK2 enzyme and γ-^{32}P-ATP (500 µCi/mmol). The dissociation ability of HDAC3 from HDAC3-H1.3 complex, upon phosphorylation of HDAC3 by CK2, is assessed by assaying the complex remained bound to the beads and in the supernatant of the reaction after spinning the beads down. The resulting extracts were resolved on 8% SDS-PAGE and phosphorimage was used for the detection of the levels of ^{32}P-HDAC3.

Since, HDAC3 can be phosphorylated by CK2 and that phosphorylated HDAC3 remains part of the complex, HDAC assays were carried out to test the hypothesis that phosphorylation of HDAC3 induces its activation during the transition from late-G_2 to mitosis. Acetylated core histones were prepared by acid extraction upon incubation of HeLaS3 cells with the HDAC inhibitor TSA for 24

hours. The HDAC3-H1.3 complex was immunoprecipitated from late-G_2 cell extracts. Half of the immunoprecipitate was phosphorylated with CK2 while the other half was left unphosphorylated. These two immunoprecipitated samples were incubated with acetylated core histones (Fig. 29). The deacetylation capacity of the immunoprecipitated complex was visualized by immunoblotting against acetylated H3K9 antibody, which has been shown to be a substrate for this complex earlier (see Fig. 22B, top panel). Immunoprecipitated complex taken from mitosis was used for comparing the percent deacetylation recovered upon phosphorylation of HDAC3 from the late-G_2 complex. Three independent experiments were carried out and suggest that immunoprecipitated complex from late-G_2 does not deacetylate acetylated H3K9; however, after phosphorylation of HDAC3 in the complex, by CK2 enzyme, 70% of the mitotic complex deacetylation activity was observed (Fig. 30). Immunoprecipitation using control non-immune IgG and recombinant HDAC3-N-CoR2 complex were used as negative and positive controls respectively (data not shown). Statistical testing by Friedman nonparametric analysis ($p=0.04$) indicated a significant difference between the groups tested. Further, pairwise comparison indicates statistical significance between HDAC3-H1.3 & P-HDAC3-H1.3 complex from late-G_2 ($p=0.006$), and between HDAC3-H1.3 complex from late-G_2 and the complex from mitosis ($p=0.0108$). These results support the conclusion that phosphorylation of HDAC3, and specifically phosphorylation of Ser-424 by CK2, is a trigger for activation of HDAC3 in HDAC3-H1.3 complex as it enters mitosis.

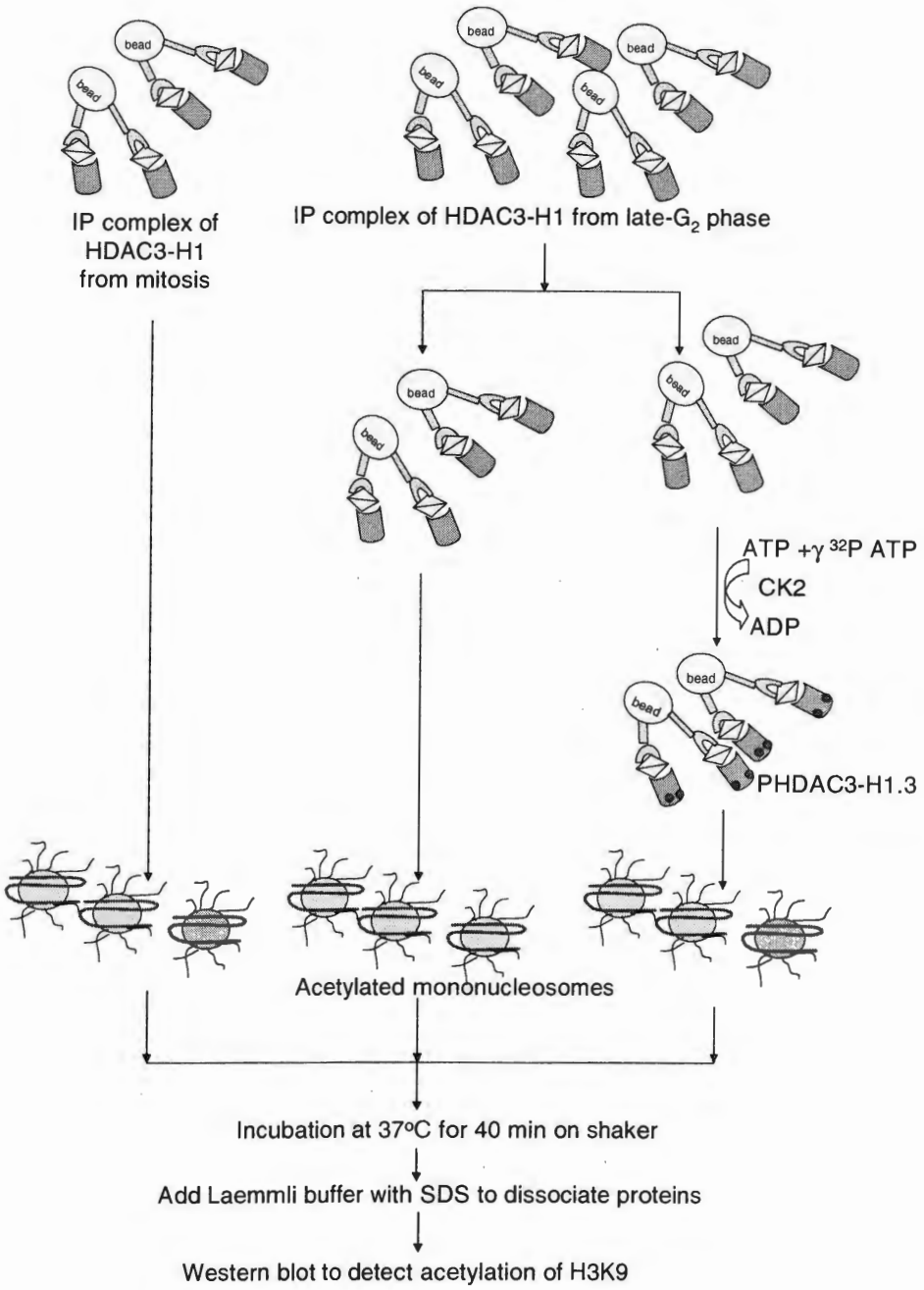

Figure 29: Schematic plan for phosphorylating HDAC3 in HDAC3-H1.3 complex and performing HDAC assay on the phospho-HDAC3-H1.3 complex.

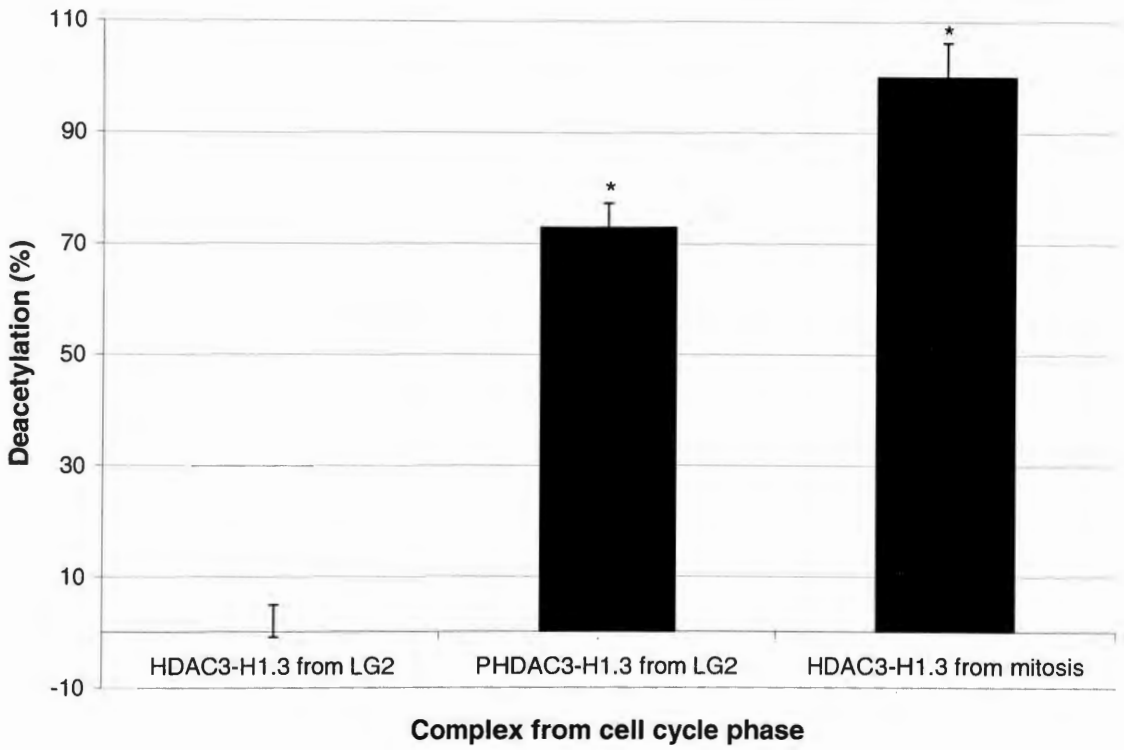

Figure 30: Triggering HDAC3 deacetylation activity in HDAC3-H1.3 complex by HDAC3 phosphorylation.
The graph illustrates a deacetylation activity assay of HDAC3-H1.3 complex from late-G_2 without and with phosphorylation by CK2 and the activity of a complex from mitotic cell extracts. Deacetylation of acetylated H3K9 residue is examined by Western blot analysis. Graph represents % deacetylation median and range (n=3); * indicates significant difference from deacetylation activity of late-G_2 complex, $p \leq 0.05$ (Friedman nonparametric analysis, followed by pairwise comparison).

HDAC3-H1.3 Complex is Co-localized on the Polar Microtubules During Mitosis

In order to explore the cellular localization of the HDAC3-H1.3 complex and to support the association between HDAC3 and histone H1.3 *in situ*, immunostaining experiments were carried out followed by confocal microscopy analysis. Unsynchronized HeLa cells were used for the co-localization studies. Cells were stained using primary antibodies against HDAC3 and histone H1.3. The secondary antibody used to visualize HDAC3 was conjugated with FITC whereas the secondary antibody used to visualize histone H1.3 was conjugated to TR. Consistent with the co-immunoprecipitation experiment results, partial but very distinct, co-localization of HDAC3 and histone H1.3 proteins in all mitotic stages (Fig. 31A-E), as well as in the nucleus of the interphase cell (Fig. 31F) was detected. Histone H1.3 seen as red spots was localized mainly around the condensed chromosomes and to some degree, on the chromosomes. HDAC3 was seen specifically around the condensed chromosomes. In all mitotic stages chromosomes were depleted of HDAC3 staining, seen as green spots localized around the chromosomes. Many of the regions around the chromosome showed a yellow staining in the merged images, indicating the co-localization of histone H1.3 and HDAC3. All negative controls (Fig. 31G) were performed using control IgG and the secondary antibodies used for the immunostaining of the specific primary antibodies. These results suggest that the HDAC3-H1.3 complex is localized outside the condensed chromosomes, possibly attached to mitotic

structures such as microtubules. Also, experiments provided further support for the existence of *in situ* association of histone H1.3 with HDAC3.

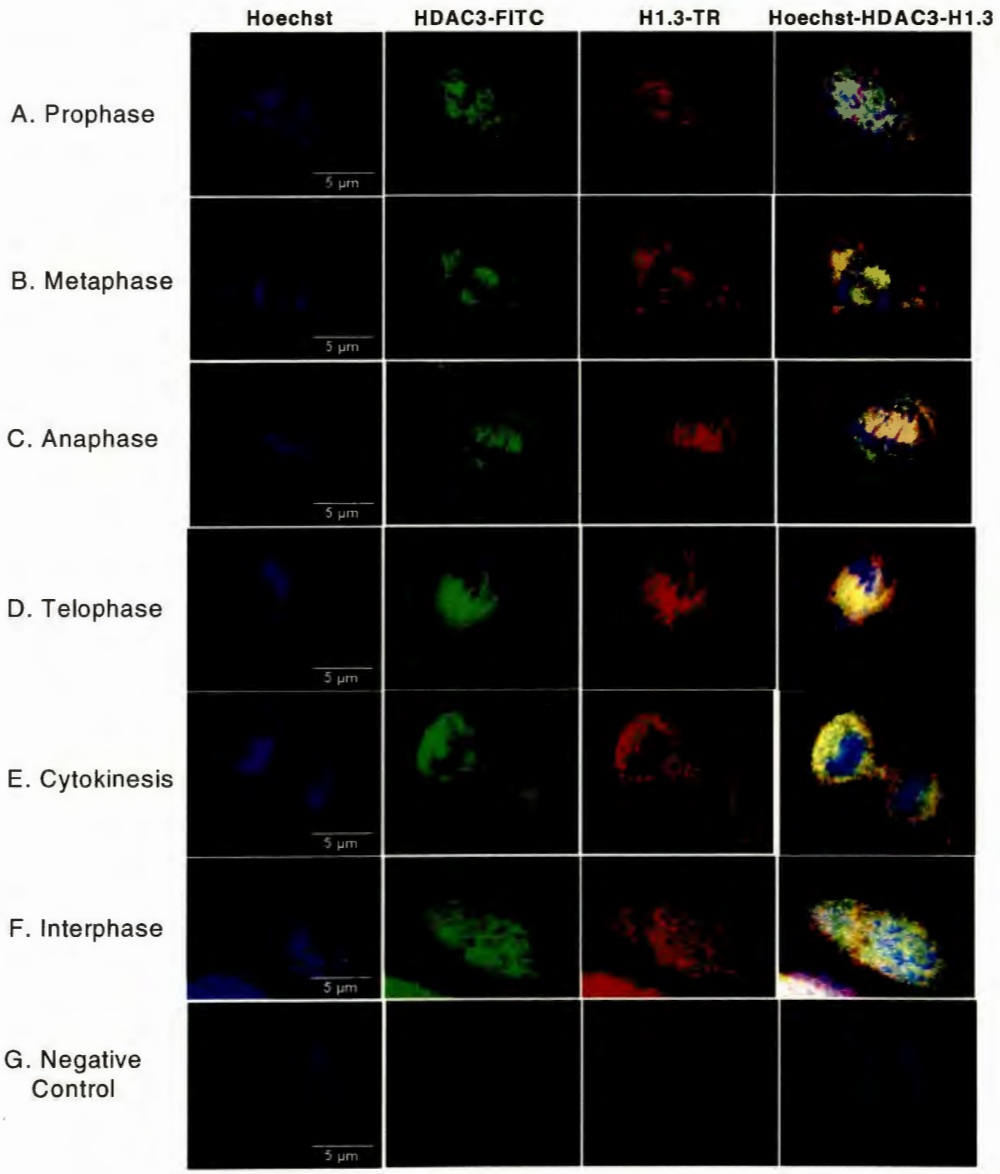

Figure 31: HDAC3 and H1.3 were partially colocalized during all mitotic stages. (A-F) Representative confocal imaging of immunoflurescence staining (1000X total magnification) of HeLa cells from mitotic stages—prophase (A), metaphase (B), anaphase (C), telophase (D), cytokinesis (E) and interphase nucleus (F), stained with anti-HDAC3 (green), anti-histone H1.3 (red) and DNA counterstaining with Hoechst (blue). (G) A negative control using non-immune IgG with the corresponding FITC and TR conjugated secondary antibodies.

Recently Ishii et al has shown that HDAC3 core complex is associated on microtubules and is required for kinetochore-microtubule attachment (Ishii, 2008b). In the immunostaining of anaphase identified that HDAC3-H1.3 complexes were specifically localized between the separating sister-chromatids at the center of the anaphase cell (see Fig. 31C). This implies that HDAC3-H1.3 complex may be associated with the polar microtubules. Polar microtubules are one of the three forms of mitotic microtubules which build the spindle; they are not attached to chromosomes but rather help in stabilizing the two centrosomes by overlapping with each other at the center of the cell (Valentine, 2006). To further investigate if the HDAC3-H1.3 complex is associated with polar microtubules, immunostaining was performed with Eg5, a member of mitotic kinesin family associated with the assembly and maintenance of the mitotic spindle. Eg5 is involved in cross linking and anti-parallel sliding of polar microtubules (Goldstein, 1999); and therefore it could serve as a specific marker for the polar spindle fibers. When chromosomes separate during the anaphase stage, polar microtubules can be viewed between the separating sister-chromatids stained with Eg5 immunostaining (for example see Fig. 32C). In addition, Eg5 can be seen to localized throughout the spindle and enriched at the poles as compared to microtubules (Sawin, 1995b), even though Eg5 is a plus end directed motor protein (Sawin, 1992). To test the hypothesis that HDAC3 and H1.3 complex could be localized on polar microtubules, immunostaining of Eg5 was performed concomitantly with the immunostaining of either HDAC3 or

histone H1.3. With the resultant confocal images, the results clearly show the co-localization of H1.3, HDAC3 and Eg5 to the polar microtubules (Fig. 32C), during anaphase. Thus, the newly identified HDAC3-H1.3 complex is localized to the polar microtubules, a unique site for HDAC3.

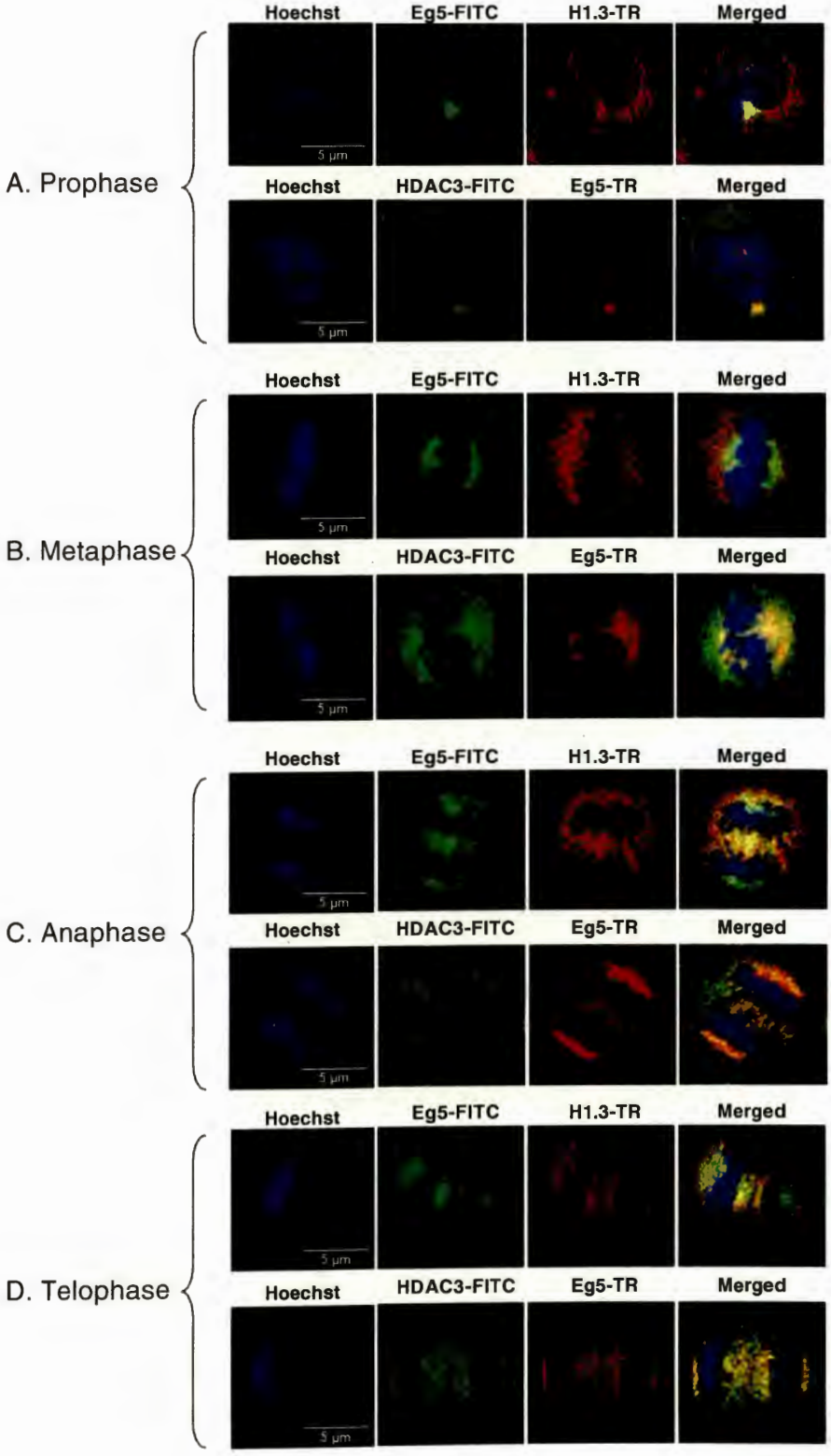

Figure 32 continue

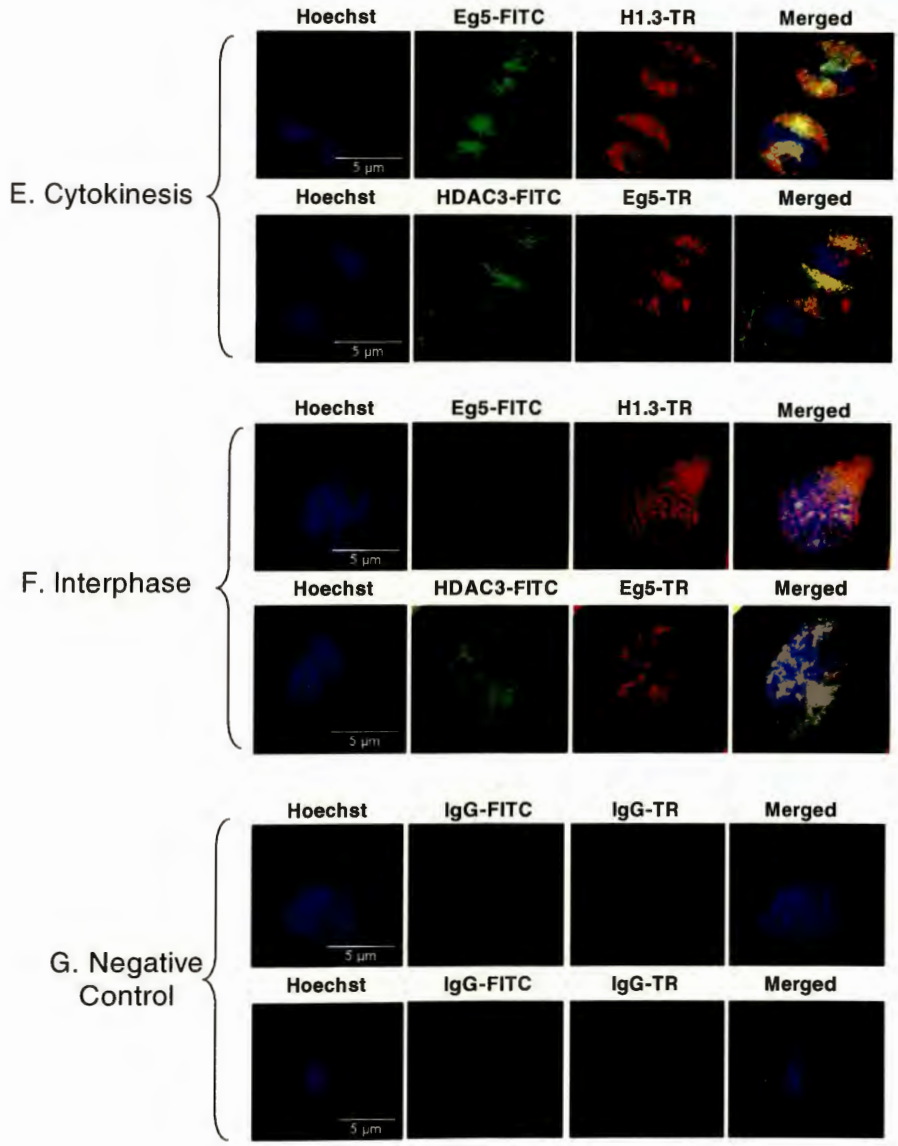

Figure 32: HDAC3 and H1.3 were colocalized on polar microtubules.
(A-F) Representative confocal imaging of immunoflurescence staining (1000X total magnification) of HeLa cells from mitotic stages—prophase (A), metaphase (B), anaphase (C), telophase (D), cytokinesis (E) and interphase nucleus (F), stained with either anti-histone H1.3 (red) and Eg5 (green) (top panels) or with anti-HDAC3 (green) and anti-Eg5 (red) (bottom panels). Hoechst (blue) counterstaining was used for staining DNA. (G) A negative control using non-immune IgG with the corresponding FITC and TR conjugated secondary antibodies.

The Isolated HDAC3-H1.3 Complex Contains at Least Eight Proteins Including GAPDH and Annexin I

None of the three proteins in the HDAC3-H1.3-SMRT complex possess a known microtubule binding characteristic; therefore it was desirable to determine if there are additional proteins in the HDAC3-H1.3 complex which can explain the localization of complex to polar microtubules. To this end the HDAC3-H1.3 complex was immunoprecipitated using either antibody against HDAC3 or against histone H1 and a control of non-immune IgG antibody. The isolated immunocomplexes were resolved on SDS-PAGE and the protein bands were visualized by using silver staining (Fig. 33A, B). Common bands obtained from the immunoprecipitated complex using HDAC3 and histone H1 antibodies, which were excluded from non-immune IgG control, were potential components of HDAC3-H1.3 complex. Overall, eight such protein bands were possible candidates for members of the isolate complex. Of these eight, bands representing HDAC3, H1.3 and SMRT proteins were verified by destaining the silver stained bands and analyzing them by immunoblotting. Performing mass spectrometric analysis (LC-ESI-MS/MS) of two of the additional bands, experiments identified glyceraldehyde-3-phosphate dehydrogenase (GAPDH) (molecular weight 36 KDa) and annexin I (molecular weight 38.7 KDa) as members of the complex. Furthermore, the silver staining pattern of the isolated complex looked different than the pattern of the complex reported by Yun Li and colleagues (Li, 2006), which suggests the identification of a novel complex which

might perform distinct functions. To answer the question if there are different proteins associated with this complex during mitosis and late-G_2, silver staining analysis of complexes from late-G_2 (Fig. 33A) and mitosis (Fig. 33B) was performed. To great surprise the staining pattern between both the stages was identical, which suggested that exchange of the complex components may not be contributing to the activation of the complex.

Earlier studies have shown that GAPDH and annexin I can bind to tubulin (Kumagai, 1983; Traverso, 1998). This provides a possible explanation for the mechanism by which HDAC3-H1.3 complex might be tethered to microtubules. A recent study by Nakayama et al has shown that histone H1 binds to tubulin in tobacco BY-2 cells (Nakayama, 2008); however, the literature search uncovered no reports linking histone H1 to microtubules in an animal kingdom.

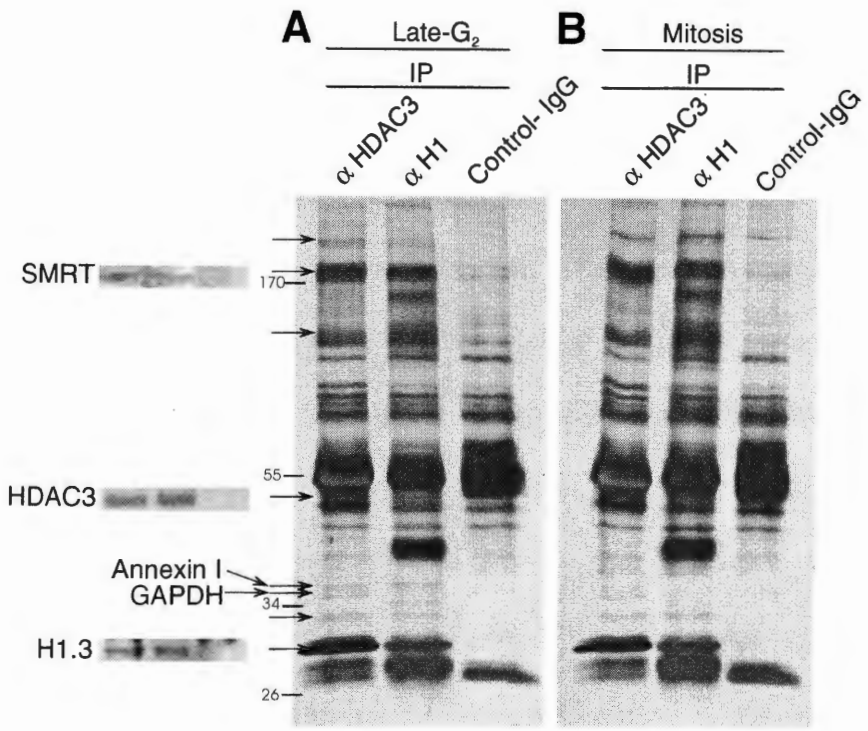

Figure 33: Isolation and identification of HDAC3-H1.3 complex shows the presence of eight proteins including SMRT, GAPDH and annexin I.
(A, B) Silver staining of proteins associated with anti-HDAC3, anti-histone H1 and non-immune IgG, immunoprecipitated from HeLaS3 cell extracts from (A) late-G_2 phase and (B) mitosis. Proteins in HDAC3-H1.3 complex were identified based on their common presence in the histone H1 and HDAC3 immunoprecipitates and lack of their presence in the non-immune IgG immunoprecipitate (labeled by small arrows). Protein bands were excised and further identified by either mass spectrometric analysis (LC-ESI-MS/MS) (labeled by large arrows) or verified by immunoblotting if the protein was recognized by its molecular weight.

CHAPTER IV

DISCUSSION

In this work, it was hypothesized that histone H1 and HDAC proteins may interact with each other and that their interaction correlates with mitotic events. The hypothesis was suggested by two observations. Both histone H1 and HDAC3 protein are involved in chromatin compaction and in mitosis. The dissertation describes the isolation of a novel complex containing HDAC3 and histone H1.3 proteins by co-immunoprecipitation. In spite of histone H1 being very efficiently acetylated by p300 *in vitro* it has very low levels of acetylation *in vivo* (Dr. Michael Bergel, personal communication), which suggests the possibility of its interaction with HDAC proteins. The pull-down study *in vitro* indicated the direct binding of HDAC3 dimer to histone H1.3. By silver staining and mass spectrometric analysis experiments also identified three other components of the complex—SMRT, GAPDH, and annexin I. By synchronizing the cells growth followed by co-immunoprecipitation assays experiments demonstrate that the complex levels in late-G_2 phase and mitosis are higher. The results have also demonstrated that HDAC3-H1.3 complex is active in deacetylation during mitosis, but not during late-G_2 and it shows target specificity. Through studies *in vitro* experiments further determined that the complex was being activated as a result of HDAC3 phosphorylation of Ser-424 by CK2. Using

immunocytochemistry the co-localization of HDAC3 and histone H1.3 on the mitotic polar microtubules was also demonstrated.

The HDAC3-H1.3 Complex

Two previous studies have shown an interaction of linker histones with HDAC proteins. SirT1 interaction with histone variant H1.4 was demonstrated in 293 cells (human embryonic kidney cells) (Vaquero, 2004), and in *C. elegance* histone H1.1 was shown to participate with Sir-2.1 in repeat-dependent silencing transgenes (Jedrusik, 2003). In these previous studies class III HDACs were reported to interact with histone H1. On the contrary, this study shows the first evidence for the formation of complex between a HDAC class I protein, HDAC3, and a linker histone. Although many complexes described in the literature contain HDAC3 and its coactivator proteins, none of the studies have investigated activation of the HDAC3 in the complex in relation to cell cycle. Also, according to a literature search, histone H1 has not been shown to bind to cytoskeletal structures such as microtubules in vertebrate cells. This study suggests for the first time that one of the histone H1 variant is associated with microtubules in vertebrate cells. Also, unlike linker histone variant H1.1, H1.2 and H1.4, histone H1.3 has never been described in association with any other protein.

Since HDAC3 interacted specifically with H1.3 variant and not with other histone H1 variants, the question was what protein domains in histone H1.3 enables this specific association. Comparing the amino-acid sequences of the human histone H1 variants, the core domain is highly conserved; while the N-

and C-terminal tails show diversity (Izzo, 2008). Protein sequence alignment of histone H1.3 with other histone variants indicates their heterogeneity [H1.1 (67.7%), H1.2 (81.1%), H1.4 (86.0%), and H1.5 (77.6%)]. This heterogeneity is observed mainly in hCTD of histone variants. Till recently, histone variants were thought to be redundant in their functions; however recent studies have shown that the various H1 variants may vary in function. Orrego et al have recently shown the difference in the binding affinities of histone variant to the chromatin (Orrego, 2007). Also, the residence time of different histone H1 variants seems to vary according to the length of their C-terminal domain and the content of positive residues (Th'ng, 2005). Immunostaining of histone H1 variants in human fibroblast cells showed varying localization: histone H1.5 was localized to nuclear periphery, histone H1.2 was stained according to the DNA concentration, whereas histone H1.3 and H1.4 showed punctuate staining pattern (Parseghian, 2000). These significant differences of histone variant characteristics suggest that they have different functions and provide clues to understand why HDAC3 associates specifically with histone variant H1.3. This dissertation suggest that HDAC3-H1.3 complex has several roles during mitosis such as stabilizing mitotic spindles or global chromatin condensation. During interphase, it may help in the chromatin compaction based on the recruitment by histone H1.3. Moreover, these results have demonstrated higher binding of HDAC3 with phosphorylated histone H1 as compare to unphosphorylated histone H1, which suggests there

could be an additional role of HDAC3-H1 complex during mitosis, which is to keep H1 out of chromatin environment when H1 is phosphorylated.

Cell Cycle Dependent Association of HDAC3-H1.3 Complex

Previous studies have described the importance of HDAC3 in mitosis progression. RNAi mediated HDAC3 knockdown of HeLa cells has shown to cause cell arrest in G_2/M phase (Li, 2006; Wilson, 2006), loss of H3S10 phosphorylation (mitosis marker) as well as impaired mitotic progression such as incomplete chromosomal condensation and "lagging" chromosomes (Li, 2006). HDAC3 knockdown in HeLa cells using siRNA showed smaller, collapsed mitotic spindles and excluded chromosomes from mitotic bipolar spindles (Ishii, 2008b). Ishii et al have also shown the necessity of active HDAC3 enzyme in spindle formation and chromosomal alignment at mitosis (Ishii, 2008b). SiRNA transfection of HDAC3 in HeLaS3 cells cause cells to arrest in mitosis, and showe premature sister chromatid separation (Eot-Houllier, 2008). On the other side, previous studies have also discussed the importance of histone H1 for chromatin condensation during mitosis (Gurley, 1995; Maresca, 2005a), and in gene-specific transcription repression (Bustin, 2005; Herrera, 2000; Sarg, 2006; Vaquero, 2004). Because histone H1 is involved in chromatin folding, it is considered to be vital for mitotic condensation. Histone H1 is heavily phosphorylated during mitosis when maximum chromatin compaction is achieved (Gurley, 1995), though recent studies indicated that phosphorylated H1 dissociates from mitotic chromosomes (Bhattacharjee, 2001; Halmer, 1996 ;

Orrego, 2007; Talasz, 1996). Thus, HDAC3 and histone H1 both are known to contribute independently to mitosis. This work tested the hypothesis that HDAC3-H1.3 complex may also have role to play in mitosis progression by performing sequential cell synchronization. This analysis, using co-immunoprecipitation assay on synchronized cell extracts, demonstrated higher levels of complex formation during late-G_2 phase and mitosis. Having a higher complex at late-G_2 may indicate that the complex has a role at the beginning of mitosis for the onset of chromatin compaction and/or cell division process during mitosis, and it supports this hypothesis. In the Western blot analysis of extracts from the various cell cycle stages, both H3K9 and H4K5 residues had low levels of acetylation during mitosis compared to other cell cycle stages (Fig. 23), indicating deacetylation of both the residues during mitosis. Thesefore, it was desirable to test the HDAC activity of the immunoprecipitated complex by analyzing the deacetylation of Ac-H3K9 and Ac-H4K5 on mono-nucleosomes, as these two residues have been shown to be the specific target of HDAC3 (Eot-Houllier, 2008; Fu, 2005). The HDAC assays, indicated that HDAC3-H1.3 complex could deacetylate Ac-H3K9, but not Ac-H4K5, in mitotic precipitates; which demonstrates a target specificity of the complex. HDAC assay studies with HDAC3-H1.3 complex isolated from late-G_2 showed lack of HDAC activity, suggesting that even if the complex levels are higher during late-G_2, the HDAC activity of the complex is triggered during mitosis. This situation is reminiscent to the cyclin-CDK complex accumulation before the onset of the corresponding cell

cycle stage, and the rapid activation of the complex that occurs upon the need of the cell cycle progression (Lodish, 2004).

Cell Cycle Dependent Activation of HDAC3-H1.3 Complex

The question was what is the molecular event that activates the HDAC3-H1.3 complex. It was possible that the association of HDAC3 with SMRT could activate its HDAC activity. However, since the SMRT is a member of this complex in late-G_2 as well as in mitosis, this possibility was eliminated. Alternatively, HDAC3 phosphorylation was checked for the activation of the HDAC activity in the HDAC3-H1.3 complex. Recently, Zhang et al have demonstrated that HDAC3 is activated upon its phosphorylation by CK2 *in vitro* (Zhang, 2005). However, this activation was not related to any cell cycle stage. Experiments therefore investigated the possibility of activating HDAC3-H1.3 complex isolated from late-G_2 by phosphorylating HDAC3 in the complex. There is increasing body of evidence that a tetrameric protein—CK2 (CK2α, CK2α`, CK2β, CK2β) is involved in controlling cell cycle progression. Studies in *Saccharomyces cerevisiae* have indicated requirement of CK2 during G_2/M phase transition (Hanna, 1995). CK2 is also reported to interact and modulate the activity of condensin I via phosphorylation to influence chromatin organization during mitosis (Takemoto, 2006). CK2β, a regulatory subunit of tetrameric CK2 protein, is also shown to regulate cell cycle progression at the beginning of mitosis phase (Yde, 2008). There are evidences that CK2β could be regulated

with its phosphorylation by CDK1 (mitotic kinase) in a cell cycle dependent manner; and CK2β is suggested to be regulating the target specificity of the catalytic subunits CK2α and CK2α` based on its phosphorylation status (Bosc, 1999; Litchfield, 1995; Zhang, 2002a). Recent work also has shown mitotic catastrophe in CK2α and CK2α` knockdown cells (Shimada, 2009; St-Denis, 2009). With this support from literature, it was desirable to analyze if CK2 can phosphorylate HDAC3 in HDAC3-H1.3 complex isolated from late-G_2, and whether the phosphorylation of HDAC3 in the complex will activate it. The phosphorylation assays *in vitro* determined successful phosphorylation of HDAC3 using CK2 enzyme. Results also confirmed that CK2 does not phosphorylate histone H1.3 in the complex (Fig. 27) and that phosphorylated HDAC3 in these assays do not dissociate from the complex (Fig. 28). Comparing the levels of phosphorylated Ser-424 site on HDAC3 in late-G_2 and mitosis extract, experiments showed higher levels of phosphorylated Ser-424 in mitosis extracts. The HDAC assays suggested that phosphorylation of HDAC3 in the complex isolated from late-G_2, by CK2, activated the complex for deacetylation of Ac-H3K9. Thus, we suggest that the HDAC3 activity in the HDAC3-H1.3 complex is cell cycle dependent and the complex is activated upon phosphorylation of HDAC3 by CK2 enzyme in mitosis.

Localization of HDAC3-H1.3 Complex

Knowing that the HDAC3-H1.3 complex is active during mitosis, experiments analyzed the co-localization of HDAC3 and histone H1.3 during

mitosis using immunocytochemistry and confocal microscopy. Both HDAC3 and histone H1.3 were co-localized during all mitotic stages as well as during interphase. However, to great surprise during mitosis the complex was not localized on the chromosomes but around them. Based on the co-localization pattern observed during anaphase stage, the dissertation hypothesized that the complex is localized on polar microtubules. A recent study by Ishii et al has indicated that HDAC3 is localized on microtubules (Ishii, 2008b). However, other results by Bhaskara et al showed that HDAC3 was associated with chromatin in the interphase and prophase but not metaphase and anaphase in wild type mouse embryonic fibroblasts (Bhaskara, 2008), this discrepancy could be due to a study conducted on different species. Li et al also showed that HDAC3 is localized to condensed chromosomes in prophase of HeLa cells (Li, 2006). This controversy could be a result of differences in the staining technique and different species under study. Ishii et al observed that in HeLa cells HDAC3 is concentrated on the microtubules near the pole during prophase, during prometaphase and metaphase; while, in anaphase HDAC3 was observed spread over entire spindles and absent from the poles, and during telophase HDAC3 was diffused through out the cytosole (Ishii, 2008b). These results are more consistent with the present results. However, this study has not specifically pointed out the type of microtubules where HDAC3 is localized. Moreover, the complex studied by Ishii et al involved the association with N-CoR which is absent in the HDAC3-H1.3 complex described in the current study. Thus, it was

desirable to test the hypothesis that HDAC3-H1.3 complex is localized to polar microtubules using Eg5 as a marker for polar microtubules.

Eg5 is the motor protein involved in cross linking and anti-parallel sliding of polar microtubules (Goldstein, 1999). In the co-immunostaining, it was observed that in anaphase and telophase cells HDAC3 and histone H1.3 co-localize with Eg5 at a center of the cell while sister chromatids separate. Thus, the data supports that HDAC3-H1.3 complex is localized to polar microtubules and this specific localization has not been previously reported for HDAC3, histone H1.3 or any of the known HDAC3 complexes.

Several reports published recently claim that tubulin acetylation and deacetylation regulates microtubule stability (Matsuyama, 2002; Tran, 2007). Specifically, tubulin deacetylation could contribute to microtubule stabilization and thus the possibility suggests itself that deacetylating tubulin by HDAC3 could be a mechanism that stabilizes polymerization of polar microtubules during mitosis. The Ishii et al study has already reported that HDAC3 does not alter acetylation levels of α-tubulin (Ishii, 2008b). However, this study was done only by microscopic methods and it does not involve any biochemical testing. Furthermore, no study has been done to test if HDAC3 could deacetylate β- or γ-tubulin. Thus, HDAC3 could deacetylate α-, β- or γ-tubulin.

Other Components of the HDAC3-H1.3 Complex: SMRT, GAPDH, Annexin I

In this study, the silver staining pattern of HDAC3-H1.3 immunocomplex indicated that at least eight proteins participated in this immunocomplex. By

immunoblotting on the destained silver-stained bands and their mass spectrometric analysis, experiments have identified the presence of SMRT, GAPDH and annexin I in HDAC3-H1.3 complex. SMRT was previously reported to associate with HDAC3 and to function as an activating cofactor for HDAC3 activity (Guenther, 2001), and is well known to intercede repression of various transcription repressors (Chen, 1995). Deacetylase activating domain of SMRT is shown to physically interacts with HDAC3 and it helps to activate the deacetylase function of inactive HDAC3 enzyme (Guenther, 2001). Presence of SMRT in HDAC3-H1.3 core complex could be an indication of its probable role as a deacetylase in the chromatin environment. However, identification of GAPDH and annexin I as components of the complex has suggested a new insight into the functional role of this complex.

GAPDH is a well known enzyme involved in a glycolysis process, but it has been implicated in multiple non-glycolytic processes such as: DNA repair (Arenaz, 1983), nuclear RNA export (Zang 1998), transcription activation (Zheng, 2003), apoptosis initiation (Hara, 2005; Nakazawa, 1997), membrane transport and in membrane fusion (Morero, 1985; Tisdale, 2004) etc. GAPDH is also known to bind the cytoskeleton. GAPDH binding to actin filament was shown to be associated with neuronal disorders (Wu, 1997). For the first time, in 1983 Kumagai and Sakai identified GAPDH binding ability to tubulin and its involvement in microtubule bundling (Kumagai, 1983); this was further confirmed by Somers et al in 1990 (Somers, 1990). Recently, Cueille et al showed that

GAPDH binds to microtubule-associated protein 1B (MAP1B), which is a major component of cytoskeleton (Cueille, 2007). Considering the characteristics of GAPDH, especially its ability to bind to microtubules, its presence in HDAC3-H1.3 complex suggests that this complex might be involved in a novel function of deacetylating and regulating microtubule stabilization. Microtubules are an important component during mitosis phase of the cell cycle. Many classic HDAC inhibitors have been shown to cause impaired chromosomal separation (Blagosklonny, 2002b; Li, 2006; Magnaghi-Jaulin, 2007; Stevens, 2008); this could be a result of weakened microtubule function as an indirect effect of HDAC inhibition. A recent study by Schemies et al has shown hyperacetylation of α-tubulin by inhibiting HDAC6 and SirT2 enzymes, thus identifying them as deacetylase of α-tubulin (Schemies, 2009). Similar conclusions supporting the role of the HDAC3-H1.3 complex in the microtubule dynamics can be drawn while examining the presence of annexin I in the HDAC3-H1.3 core complex, since a previous study has reported that annexin I colocalizes with tubulin using immunocytochemistry (Traverso, 1998).

A recent study by Nakayama et al has suggested that histone H1 also has the ability to bind to tubulin in tobacco BY-2 cells (Nakayama, 2008); however, until today, animal histone H1 was not identified in association with the microtubule filaments. The current study could lead to the first identification of histone H1 role in microtubule structure and dynamics. Overall, the presence of GAPDH, annexin I and histone H1 in the complex could play a role in tethering

the complex to the polar microtubules. Several multiprotein complexes containing HDAC3 were previously identified and characterize to play a role during mitosis. These complexes have been reported to contain also N-CoR (Ishii, 2008b; Li, 2006). The complex did not include N-CoR, but on the other hand it included histone H1.3, SMRT, annexin I and GAPDH, indicating that this complex is novel and has a distinct function not described earlier.

Further functional analysis of the HDAC3-H1.3 complex may link it also to deacetylation of core histones with the possible synergistic effect by recruitment of SMRT and histone H1.3. Further studies on the potential deacetylation of histone H1.3 in the HDAC3-H1.3 complex can shed light on the possible role of HDAC3 in deacetylating histone H1.3. The possible deacetylation of tubulin by HDAC3 via its recruitment by GAPDH and annexin I may help to explain an important step in the coupling of chromatin condensation at the beginning of mitosis to the coordinated spindle fiber formation and maintenance. Thus the HDAC3-H1.3 complex might be involved in variety of functions during mitosis, such as chromatin compaction, microtubule organization and stability, and capturing and anchoring of phosphorylated histone H1.3 out of the condensed chromosomes. Further studies with knockdown of histone H1.3 and CK2 subunits can help us to understand the possible roles of the HDAC3-H1.3 complex during mitosis. A detailed study of the functionality of this complex may help us to understand the mitotic process and may possibly provide novel targets for cancer therapy.

A great deal of efforts are being devoted today to understand the molecular mechanism behind the cell proliferation in normal and cancer cells, with the hope to identify specific targets for cancer therapy. Understanding functionality of the histone H1.3-HDAC3 complex could be of vital importance, as histone H1.3-HDAC3 complex could play a role in mitosis progression. Identifying the protein complexes responsible for mitosis progression can help find ways to specifically inhibit these proteins interactions to form a complex and thus stop cancer.Malignant cells lack the cell cycle checkpoints and thus are immortalized. Making the histone H1.3-HDAC3 complex nonfunctional in such malignant cells could cause mitotic catastrophe and could trigger apoptosis. Defects in the spindle assembly can also contribute to the generation of post mitotic cells with unbalanced chromosomal content. Characterizing the chromatin region where this complex could be targeted will also help us to understand the chromatin condensation coordinating with microtubule dynamics.

Summary

Thus, this dissertation proposes the following model to summarize these findings (Fig. 34). Histone H1.3 and HDAC3 associate directly in 1:2 molar ratio. The presence of SMRT, GAPDH and annexin I was found in the HDAC3-H1.3 complex. The levels of this complex increases in late-G2 and mitosis. In spite of the higher levels of the complex, HDAC3 in the complex is inactive to perform deacetylation of core histones. There is strong evidence to propose that, during the transition from late-G_2 to mitosis CK2 phosphorylates HDAC3 in HDAC3-H1.3 complex and activates HDAC3 deacetylation activity. The dissertation proposes three hypotheses for the functionality of this active complex during mitosis. First, since experiments show the localization of this complex on microtubules, the dissertation also proposes that this active complex could be participating in microtubule stabilization and assembly. Second, due to the presence of co-repressor SMRT, the dissertation proposes that this complex could be helping chromatin compaction at the beginning of mitosis. Third, since most of the phosphorylated histone H1 resides outside the chromatin, the dissertation proposes that the interaction of histone H1.3 and HDAC3 could be helping the capturing and anchoring of histone H1.3 outside the chromatin.

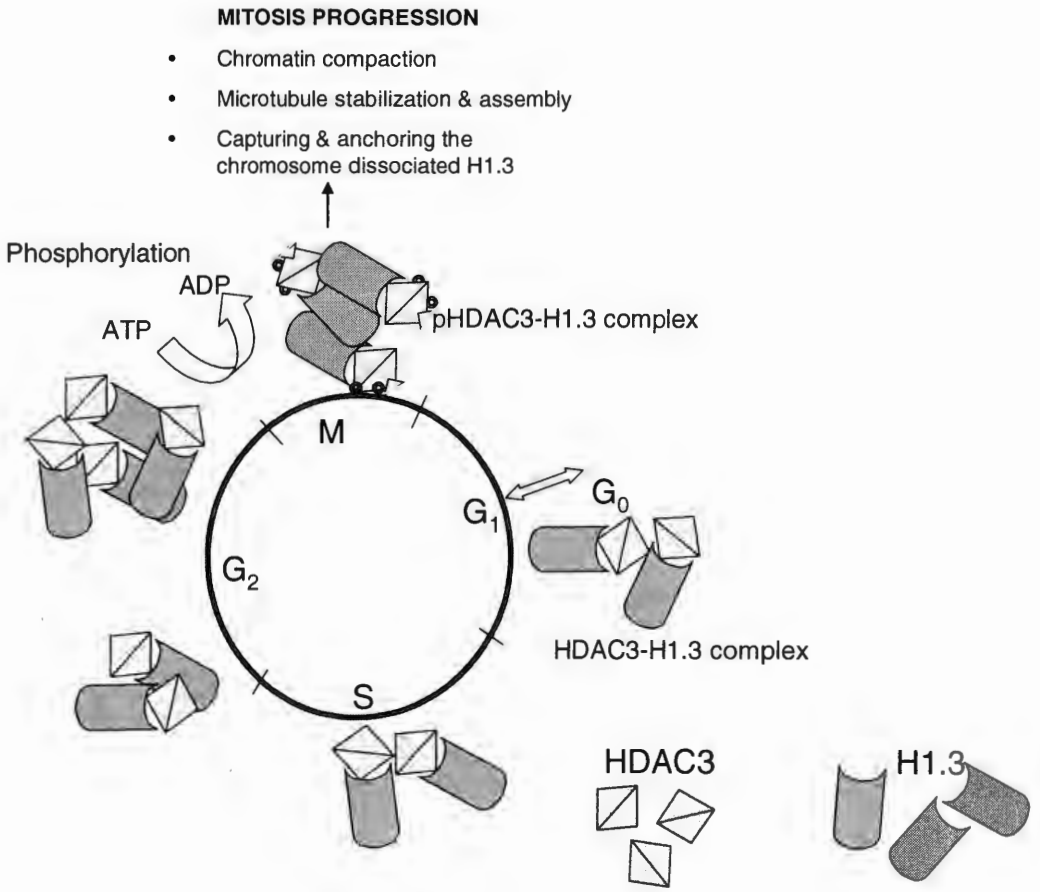

Figure 34: The proposed model for HDAC3-H1.3 complex.

REFERENCES

Agalioti, T., G. Chen, and D. Thanos. (2002) Deciphering the Transcriptional Histone Acetylation Code for a Human Gene. *Cell* **111**, 381–392.

Alberts, B., A. Johnson, J. Lewin, M. Raff, K. Roberts, and P. Walter. (2002) *Molecular Biology of THE CELL*. Garland Science Publishing.

Albig, W., B. Drabent, J. Kunz, M. Kalff-Suske, K. Grzeschik, and D. Doenecke. (1993) All known human H1 histone genes except the H1(0) gene are clustered on chromosome 6. *Genomics*, **16**, 649-654.

Amann, J.M., J. Nip, D. K. Strom, B. Lutterbach, H. Harada, N. Lenny, J. R. Downing, S. Meyers, and S. W. Hiebert. (2001) ETO, a target of t(8;21) in acute leukemia, makes distinct contacts with multiple histone deacetylases and binds mSin3A through its oligomerization domain. *Mol Cell Biol.*, **21**, 6470-6483.

Arenaz, P., and M. A. Sirover. (1983) Isolation and characterization of monoclonal antibodies directed against the DNA repair enzyme uracil DNA glycosylase from human placenta. *Proc Natl Acad Sci U S A.* , **80**, 5822-5826.

Ausió, J., D. W. Abbott, X. Wang, and S. C. Moore. (2001) Histone variants and histone modifications: a structural perspective. *Biochem Cell Biol.*, **79**, 693-708.

Barlow, P.W. (1977) Changes in chromatin structure during the mitotic cycle. *Protoplasma.*, **91**, 207-211.

Bednar, J., R. A. Horowitz, S. A. Grigoryev, L. M. Carruthers,J. C. Hansen, A. J. Koster, and C. L. Woodcock. (1998) Nucleosomes, linker DNA, and linker histone form a unique structural motif that directs the higher-order folding and compaction of chromatin. *Proc Natl Acad Sci U S A*, **95**, 14173-14178.

Berger, S.L. (2002) Histone modifications in transcriptional regulation *Curr. Opin. Genet. Dev.* , **12**, 142-148.

Bernstein, B.E., M. Kamal, K. Lindblad-Toh, S. Bekiranov, D. Bailey, D. Huebert, S. McMahon, E. Karlsson, E. Kulbokas, T. Gingeras, S. Schreiber, and E. Lander. (2005) Genomic maps and comparative analysis of histone modifications in human and mouse. *Cell*, **120**, 169-181.

Bhaskara, S., B. J. Chyla, J. M. Amann, S. K. Knutson, D. Cortez, Z. W. Sun, and S. W. Hiebert. (2008) Deletion of histone deacetylase 3 reveals critical roles in S phase progression and DNA damage control. *Mol Cell.*, **30**, 61-72.

Bhattacharjee, R.N., and T. K. Archer. (2006) Transcriptional silencing of the mouse mammary tumor virus promoter through chromatin remodeling is concomitant with histone H1 phosphorylation and histone H3 hyperphosphorylation at M phase. *Virology*, **346**, 1-6.

Bhattacharjee, R.N., G. Banks, K. Trotter, H. Lee, and T. Archer. (2001) Histone H1 phosphorylation by Cdk2 selectively modulates mouse mammary tumor virus transcription through chromatin remodeling. *Mol Cell Biol.*, **21**, 5417-5425.

Bischoff, J.R., and G. D.Plowman. (1999) The Aurora/Ipl1p kinase family: regulators of chromosome segregation and cytokinesis. *Trends Cell Biol.*, **9**, 454-459.

Blagosklonny, M.V., R. Robey, D. L. Sackett, L. Du, F. Traganos, Z. Darzynkiewicz, T. Fojo, and S. E. Bates. (2002a) Histone deacetylase inhibitors all induce p21 but differentially cause tubulin acetylation, mitotic arrest, and cytotoxicity. *Mol Cancer Ther.* , **1**, 937-941.

Blagosklonny, M.V., R. Robey, D. L. Sackett, L. Du, F. Traganos, Z. Darzynkiewicz, T. Fojo, and S. E. Bates. (2002b) Histone deacetylase inhibitors all induce p21 but differentially cause tubulin acetylation, mitotic arrest, and cytotoxicity. *Mol Cancer Ther.*, **1**, 937-941.

Blanco-García, N., E. Asensio-Juan, X. de la Cruz, and M. A. Martínez-Balbás. (2009) Autoacetylation regulates P/CAF nuclear localization. *J Biol Chem.* , **284**, 1343-1352.

Bosc, D.G., B. Lüscher, and D. W. Litchfield. (1999) Expression and regulation of protein kinase CK2 during the cell cycle. *Mol Cell Biochem.*, **191**, 213-222.

Bustin, M., F. Catez, and J. Lim. (2005) The dynamics of histone H1 function in chromatin. *Mol Cell.*, **17**, 617-620.

Carruthers, L.M., and J.C. Hansen. (2000) The core histone N termini function independently of linker histones during chromatin condensation. *J Biol Chem*, **275**, 37285-37290.

Catez, F., D. T. Brown, T. Misteli, and M. Bustin. (2002) Competition between histone H1 and HMGN proteins for chromatin binding sites. *EMBO Rep.* , **3**, 760-766.

Chen, J.D., and R. M. Evans. (1995) A transcriptional co-repressor that interacts with nuclear hormone receptors. *Nature*, **377**, 454-457.

Chuang, H.C., C. W. Chang, G. D. Chang, T. P. Yao, and H. Chen. (2006) Histone deacetylase 3 binds to and regulates the GCMa transcription factor. *Nucleic Acids Res.*, **34**, 1459-1469.

Colomb, E., and P. M. Martin. (1992) S phase, an evolutionary chromatin condensation state from G1 to G2, in a breast epithelial cell line. *Anal Cell Pathol.*, **4**, 369-379.

Cowger, J.J., and J. Torchia. (2006) Direct association between the CREB-binding protein (CBP) and nuclear receptor corepressor (N-CoR). *Biochemistry* . **45**, 13150-13162.

Cueille, N., C. T. Blanc, I. M. Riederer, and B. M. Riederer. (2007) Microtubule-associated protein 1B binds glyceraldehyde-3-phosphate dehydrogenase. *J Proteome Res.* , **6**, 2640-2647.

Cui, Y., M. Zhang, R. Pestell, E. M. Curran, W. Welshons, and S. A. Fuqua. (2004) Phosphorylation of estrogen receptor alpha blocks its acetylation and regulates estrogen sensitivity. *Cancer Res.*, **64**, 9199-9208.

De Ruijter, A.J., A. van Gennip, H. Caron, S. Kemp, and A. van Kuilenburg,. (2003) Histone deacetylases (HDACs): characterization of the classical HDAC family. *Biochem J.* , **370**, 737-749.

De Souza, C.P., A. H. Osmani, L. Wu, J. Spotts, and S. Osmani. (2000) Mitotic histone H3 phosphorylation by the NIMA kinase in Aspergillus nidulans. *Cell*, **102**, 293–302.

Downs, J.A., E. Kosmidou, A. Morgan, and S. P. Jackson. (2003) Suppression of homologous recombination by the Saccharomyces cerevisiae linker histone. *Mol Cell.* , **11**, 1685-1692.

Eot-Houllier, G., G. Fulcrand, Y. Watanabe, L. Magnaghi-Jaulin, and C. Jaulin. (2008) Histone deacetylase 3 is required for centromeric H3K4 deacetylation and sister chromatid cohesion. *Genes Dev.* , **22**, 2639-2644.

Escaffit, F., O. Vaute, M. Chevillard-Briet, B. Segui, Y. Takami, T. Nakayama, and D. Trouche. (2007) Cleavage and cytoplasmic relocalization of histone deacetylase 3 are important for apoptosis progression. *Mol Cell Biol.* , **27**, 554-567.

Fan, Y., A. Sirotkin, R. Russell, J. Ayala, and A. Skoultchi. (2001) Individual somatic H1 subtypes are dispensable for mouse development even in mice lacking the H1(0) replacement subtype. *Mol Cell Biol.* , **21**, 7933-7943.

Fan, Y., T. Nikitina, E. M. Morin-Kensicki, J. Zhao, T. R. Magnuson, C. L. Woodcock, and A. Skoultchi. (2003) H1 Linker Histones Are Essential for Mouse Development and Affect Nucleosome Spacing In Vivo. *Mol Cell Biol.*, **23**, 4559–4572.

Fan, Y., T. Nikitina, J. Zhao, T. Fleury, R. Bhattacharyya, E. Bouhassira, A. Stein, C. Woodcock, and A. Skoultchi. (2005) Histone H1 depletion in mammals alters global chromatin structure but causes specific changes in gene regulation. *Cell.*, **123**, 1199-1212.

Fischle, W., F. Dequiedt, M. Fillion, M. J. Hendzel, W. Voelter, and E. Verdin. (2001) Human HDAC7 histone deacetylase activity is associated with HDAC3 in vivo. *J Biol Chem.* , **276**, 35826-35835.

Fry, A.M., T. Mayor, P. Meraldi, Y. D. Stierhof, K. Tanaka, and E. A. Nigg. (1998) C-Nap1, a novel centrosomal coiled-coil protein and candidate substrate of the cell cycle-regulated protein kinase Nek2. *J Cell Biol.* , **141**, 1563-1574.

Fu, M., C. Wang, J. Wang, X. Zhang, T. Sakamaki, Y. Yeung, C. Chang, T. Hopp, S. Fuqua, E. Jaffray, R. Hay, J. Palvimo, O. Jänne, and R. Pestell. (2002) Androgen receptor acetylation governs trans activation and MEKK1-induced apoptosis without affecting in vitro sumoylation and trans-repression function. *Mol Cell Biol.* , **22**, 3373-3388.

Fu, M., M. Rao, T. Bouras, C. Wang, K. Wu, X. Zhang, Z. Li, T. P. Yao, and R. G. Pestell. (2005) Cyclin D1 inhibits peroxisome proliferator-activated receptor gamma-mediated adipogenesis through histone deacetylase recruitment. *J Biol Chem.*, **280**, 16934-16941.

Galasinski, S.C., K. A. Resing, J. A. Goodrich, and N. G. Ahn. (2002) Phosphatase inhibition leads to histone deacetylases 1 and 2 phosphorylation and disruption of corepressor interactions. *J Biol Chem.*, **277**, 19618–19626.

Goldstein, L.a.A.V.P. (1999) THE ROAD LESS TRAVELED: Emerging Principles of Kinesin Motor Utilization. *Annual Review of Cell and Developmental Biology*, **15**, 141-183.

Gray, S.G., A. H. Iglesias, F. Lizcano, R. Villanueva, S. Camelo, H. Jingu, B. T. Teh, N. Koibuchi, W. W. Chin, E. Kokkotou, and F. Dangond. (2005) Functional characterization of JMJD2A, a histone deacetylase- and retinoblastoma-binding protein. *J Biol Chem.* , **280**, 28507-28518.

Gray, S.G., and T. J. Ekstrom. (2001) The human histone deacetylase family. *Exp Cell Res.* , **262**, 75-83.

Grégoire, S., L. Xiao, J. Nie, X. Zhang, M. Xu, J. Li, J. Wong, E. Seto, and X. J. Yang. (2007) Histone deacetylase 3 interacts with and deacetylates myocyte enhancer factor 2. *Mol Cell Biol.* , **27**, 1280-1295.

Gregoretti, I.V., Y. M. Lee, and H. V. Goodson. (2004) Molecular evolution of the histone deacetylase family: functional implications of phylogenetic analysis. *J Mol Biol.*, **338**, 17-31.

Gu, W., and R. G. Roeder. (1997) Activation of p53 sequence-specific DNA binding by acetylation of the p53 C-terminal domain. *Cell.* , **90**, 595-606

Guenther, M.G., O. Barak, and M. Lazar. . (2001) The SMRT and N-CoR corepressors are activating cofactors for histone deacetylase 3. *Mol. Cell. Biol.*, **21**, 6091–6101.

Gunjan, A., and D. T. Brown. (1999) Overproduction of histone H1 variants in vivo increases basal and induced activity of the mouse mammary tumor virus promoter. *Nucleic Acids Res.*, **27**, 3355-3363.

Gurley, L.R., J. G. Valdez, and J. S. Buchanan. (1995) Characterization of the mitotic specific phosphorylation site of histone H1. Absence of a consensus sequence for the p34cdc2/cyclin B kinase. *J Biol Chem.* , **271**, 27653-27660.

Halmer, L.a.C.G. (1996) Effects of cell cycle dependent histone H1 phosphorylation on chromatin structure and chromatin replication. *Nucleic Acids Res.*, **24**, 1420-1427.

Hanna, D.E., A. Rethinaswamy, and C. V. Glover. (1995) Casein kinase II is required for cell cycle progression during G1 and G2/M in Saccharomyces cerevisiae. *J Biol Chem.* , **270**, 25905-25914.

Happel, N., E. Schulze, and D. Doenecke. (2005) Characterisation of human histone H1x. . *Biol. Chem.*, **386**, 541-551.

Hara, M.R., N. Agrawal, S. F. Kim, M. B. Cascio, M. Fujimuro, Y. Ozeki, M. Takahashi, J. H. Cheah, S. K. Tankou, L. D. Hester, C. D. Ferris, S. D. Hayward, S. H. Snyder, and A. Sawa. (2005) S-nitrosylated GAPDH initiates apoptotic cell death by nuclear translocation following Siah1 binding. *Nat Cell Biol.*, **7**, 665-674.

Hayakawa, F., M. Towatari, Y. Ozawa, A. Tomita, M. L. Privalsky, and H. Saito. (2004) Functional regulation of GATA-2 by acetylation. *J Leukoc Biol.*, **75**, 529-540.

Heinzel, T., R. M. Lavinsky, T. M. Mullen, M. Soderstrom, C. D. Laherty, J. Torchia, W. Yang, G. Brard, S. D. Ngo, and J. R. Davie. . (1997) A complex containing N-CoR, mSin3 and histone deacetylase mediates transcriptional repression. . *Nature (London)*, **387**, 43-48.

Hendzel, M.J., M. A. Lever, E. Crawford, and J. P. Th'ng. (2004) The C-terminal domain is the primary determinant of histone H1 binding to chromatin in vivo. *J Biol Chem.* , **279**, 20028-20034.

Herrera, J., K. L. West, R. L. Schiltz, Y. Nakatani, and M. Bustin. (2000) Histone H1 Is a Specific Repressor of Core Histone Acetylation in Chromatin. *Molecular and Cellular Biology*, **20**, 523-529.

Hotta, T., T. Haraguchi, and K. Mizuno. (2007) A novel function of plant histone H1: microtubule nucleation and continuous plus end association. *Cell Struct Funct.* , **32**, 79-87.

Hu, E., Z. Chen, T. Fredrickson, Y. Zhu, R. Kirkpatrick, G. Zhang, K. Johanson, C. Sung, R. Liu, and J. Winkler. (2000) Cloning and characterization of a novel human class I histone deacetylase that functions as a transcription repressor. *J Biol Chem.* , **275**, 15254-15264.

Huang, W., D. Tan, X. Wang, S. Han, J. Tan, Y. Zhao, J. Lu, and B. Huang. (2006) Histone deacetylase 3 represses p15(INK4b) and p21(WAF1/cip1) transcription by interacting with Sp1. *Biochem Biophys Res Commun.*, **339**, 165-171.

Hubbert, C., A. Guardiola, R. Shao, Y. Kawaguchi, A. Ito, A. Nixon, M. Yoshida, X. F. Wang, and T. P. Yao. (2002) HDAC6 is a microtubule-associated deacetylase. *Nature.* , **417**, 455-458.

Huynh, K.D., W. Fischle, E. Verdin, and V. J. Bardwell. (2000) BCoR, a novel corepressor involved in BCL-6 repression. *Genes Dev.*, **14**, 1810-1823.

Inoue, T., M. Hiratsuka, M. Osaki, and M. Oshimura. (2007) The Molecular Biology of Mammalian SIRT Proteins: SIRT2 in Cell Cycle Regulation. *Cell Cycle.*, **6**.

Ishii, S., Y. Kurasawa, J. Wong and L. Yu-Lee. (2008a) Histone deacetylase 3 localizes to the mitotic spindle and is required for kinetochore–microtubule attachment. *Proc Natl Acad Sci U S A.* , **105**, 4179-4184.

Ishii, S., Y. Kurasawa, J. Wong, and L. Yu-Lee. (2008b) Histone deacetylase 3 localizes to the mitotic spindle and is required for kinetochore–microtubule attachment. *Proc Natl Acad Sci U S A.*, **105**, 4179-4184.

Izzo, A., K. Kamieniarz, and R. Schneider. (2008) The histone H1 family: specific members, specific functions? *Biol Chem.* , **389**, 333-343.

Jedrusik, M.A., and E. Schulze. (2003) Telomeric position effect variegation in Saccharomyces cerevisiae by Caenorhabditis elegans linker histones suggests a mechanistic connection between germ line and telomeric silencing. *Mol Cell Biol.*, **23**, 3681-3691.

Kaludov, N.K., L. Pabón-Peña, M. Seavy, G. Robinson, and M. M. Hurt. (1997) A mouse histone H1 variant, H1b, binds preferentially to a regulatory sequence within a mouse H3.2 replication-dependent histone gene. *J Biol Chem.* , **272**, 15120-15127.

Karp, G. (2005) *Cell and Molecular Biology*. John Wiley & Sons Inc.

Kawai, H., H. Li, S. Avraham, S. Jiang, and H. K. Avraham. (2003) Overexpression of histone deacetylase HDAC1 modulates breast cancer progression by negative regulation of estrogen receptor alpha. *Int J Cancer.*, **107**, 353-358.

Khochbin, S. (2001) Histone H1 diversity: bridging regulatory signals to linker histone function. *Gene.* , **271**, 1-12.

Kim, K., J. Choi, K. Heo, H. Kim, D. Levens, K. Kohno, E. M. Johnson, H. W. Brock, and W. An. (2008) Isolation and characterization of a novel H1.2 complex that acts as a repressor of p53-mediated transcription. *J Biol Chem.* , **283**, 9113-9126.

Kim, S.C., Y. S. Kim, and A. M. Jetten. (2005) Krüppel-like zinc finger protein Gli-similar 2 (Glis2) represses transcription through interaction with C-terminal binding protein 1 (CtBP1). *Nucleic Acids Res.* , **33**, 6805-6815.

Kimura, K., M. Hirano, R. Kobayashi, and T. Hirano. (1998) Phosphorylation and activation of 13S condensin by Cdc2 in vitro. *Science.* , **282**, 487-490.

Kireeva, N., M. Lakonishok, I. Kireev, T. Hirano, and A. S. Belmont. (2004) Visualization of early chromosome condensation: a hierarchical folding, axial glue model of chromosome structure. *J Cell Biol.* , **166**, 775-785.

Kochbin, S., and A. P. Wolffe. (1994) Developmentally regulated expression of linker histone variants in vertebrates. . *Eur J Biochem*, **225**, 501-510.

Konishi, A., S. Shimizu, J. Hirota, T. Takao, Y. Fan, Y. Matsuoka, L. Zhang, Y. Yoneda, Y. Fujii, A. Skoultchi, and Y. Tsujimoto. (2003) Involvement of histone H1.2 in apoptosis induced by DNA double-strand breaks. *Cell.* , **114**, 673-688.

Kruhlak, M.J., M. Hendzel, W. Fischle, N. Bertos, S. Hameed, X. Yang, E. Verdin, and D. Bazett-Jones. (2001) Regulation of global acetylation in mitosis through loss of histone acetyltransferases and deacetylases from chromatin. *J Biol Chem.* , **276**, 38307-38319.

Kumagai, H., and H. Sakai. (1983) A porcine brain protein (35 K protein) which bundles microtubules and its identification as glyceraldehyde 3-phosphate dehydrogenase. *J Biochem.*, **93**, 1259-1269.

Lane, H.A., and E. A. Nigg. (1996) Antibody microinjection reveals an essential role for human polo-like kinase 1 (Plk1) in the functional maturation of mitotic centrosomes. *J Cell Biol.* , **135**, 1701-1713.

Laybourn, P.J., and, J. T. Kadonaga (1991) Role of nucleosomal cores and histone H1 in regulation of transcription by RNA polymerase II. *Science*, **254**, 238-245.

Lee, H., N. Rezai-Zadeh, and E. Seto. (2004a) Negative regulation of histone deacetylase 8 activity by cyclic AMP-dependent protein kinase A. *Mol Cell Biol.*, **24**, 765-773.

Lee, H., R. Habas, and C. Abate-Shen. (2004b) MSX1 cooperates with histone H1b for inhibition of transcription and myogenesis. *Science.* , **304**, 1675-1678.

Lennox, R.W., and L. H. Cohen. (1984) The alterations in H1 histone complement during mouse spermatogenesis and their significance for H1 subtype function. . *Dev. Biol.*, **103**, 80-84.

Lever, M.A., J. P. Th'ng, X. Sun, and M. J. Hendzel. (2000) Rapid exchange of histone H1.1 on chromatin in living human cells. *Nature.* , **408**, 873-876.

Lewin, B. (2000) *Genes VII.* Oxford university press.

Li, H., L. Christopher, Z. Jiang, W. Xiaoyang, O. Jennifer, P. Eun-Ju, and J. D. Chen. (2000a) Sequestration and Inhibition of Daxx-Mediated Transcriptional Repression by PML *Molecular and Cellular Biology*, **20**, 1784-1796.

Li, H.Y., and Y. Zheng. (2004) Phosphorylation of RCC1 in mitosis is essential for producing a high RanGTP concentration on chromosomes and for spindle assembly in mammalian cells. *Genes Dev.*, **18**, 512-527.

Li, J., J. Wang, J. Wang, Z. Nawaz, J. M. Liu, J. Qin, and J. Wong. (2000b) Both corepressor proteins SMRT and N-CoR exist in large protein complexes containing HDAC3. *EMBO J.* , **19**, 4342–4350.

Li, J., Q. Lin, W. Wang, P. Wade, and J. Wong. . (2002) Specific targeting and constitutive association of histone deacetylase complexes during transcriptional repression. *Genes Dev.*, **16**, 687–692.

Li, Y., G. Kao, B. Garcia, J. Shabanowitz, D. Hunt, J. Qin, C. Phelan, and M. Lazar. (2006) A novel histone deacetylase pathway regulates mitosis by modulating Aurora B kinase activity. *Genes Dev.* , **20**, 2566-2579.

Libertini, L.J., J. Ausió, K. E. van Holde, and E. W. Small. (1988) Histone hyperacetylation. Its effects on nucleosome core particle transitions. *Biophysics J.*, **53**, 477–487.

Litchfield, D.W., D. G.Bosc, and E. Slominski. (1995) The protein kinase from mitotic human cells that phosphorylates Ser-209 on the casein kinase II beta-subunit is p34cdc2. *Biochim Biophys Acta.*, **1269**, 69-78.

Lodish, H., B. Arnold, M. paul, A.K. chris, K. Monty, and P.S. Matthew. (2004) *Molecular Cell Biology.* W. H. freeman and Company.

Longworth, M.S., and L. A. Laimins. (2006) Histone deacetylase 3 localizes to the plasma membrane and is a substrate of Src. *Oncogene.* , **25**, 4495-4500.

Lowe, M., C. Rabouille, N. Nakamura, R. Watson, M. Jackman, E. Jämsä, D. Rahman, D. J. Pappin, and G. Warren. (1998) Cdc2 kinase directly phosphorylates the cis-Golgi matrix protein GM130 and is required for Golgi fragmentation in mitosis. *Cell*, **94**, 783-793.

Lu, X., and J. C. Hansen. (2004) Identification of specific functional subdomains within the linker histone H10 C-terminal domain. *J Biol Chem.*, **279**, 8701-8707.

Luger, K., A. W. Mader, R. K. Richmond , D. F. Sargent, and T. J. Richmond. (1997) Crystal structure of the nucleosome core particle at 2.8 A resolution. *Nature*, **389**, 251-260.

Luger, K., and J. C. Hansen. (2005) Nucleosome and chromatin fiber dynamics. *Curr Opin Struct Biol.* , **15**, 188-196.

Luger, K., and T. J. Richmond. (1998) DNA binding within the nucleosome core. *Current Opinion in Structural Biology*, **8**, 33-40.

Luo, J., F. Su, D. Chen, A. Shiloh, and W. Gu. (2000) Deacetylation of p53 modulates its effect on cell growth and apoptosis. *Nature.* , **408**, 377-381.

Magnaghi-Jaulin, L., G. Eot-Houllier, G. Fulcrand, and C. Jaulin. (2007) Histone deacetylase inhibitors induce premature sister chromatid separation and override the mitotic spindle assembly checkpoint. *Cancer Res.* , **67**, 6360-6367.

Maresca, T.J., B. S. Freedman, and R. Heald (2005a) Histone H1 is essential for mitotic chromosome architecture and segregation in Xenopus laevis egg extracts. *The Journal of Cell Biology* **169**, 859-869.

Maresca, T.J., S. B. Freedman and R. Heald (2005b) Histone H1 is essential for mitotic chromosome architecture and segregation in Xenopus laevis egg extracts. *The Journal of Cell Biology*, **169**, 859-869.

Martianov, I., S. Brancorsini, R. Catena, A. Gansmuller, N. Kotaja, M. Parvinen, P. Sassone-Corsi, and I. Davidson. . (2005) Polar nuclear localization of H1T2, a histone H1 variant, required for spermatid elongation and DNA condensation during spermiogenesis. *Proc Natl Acad Sci.*, **102**, 2808-2813.

Matsuyama, A., T. Shimazu, Y. Sumida, A. Saito, Y. Yoshimatsu, D. Seigneurin-Berny, H. Osada, Y. Komatsu, N. Nishino, S. Khochbin, S. Horinouchi, and M. Yoshida. (2002) In vivo destabilization of dynamic microtubules by HDAC6-mediated deacetylation. *EMBO J.*, **21**, 6820-6831.

Montes de Oca, R., K. K. Lee, and K. L. Wilson. (2005) Binding of barrier to autointegration factor (BAF) to histone H3 and selected linker histones including H1.1. *J Biol Chem.* , **280**, 42252-42262.

Morero, R.D., A. L. Viñals, B. Bloj, and R. N. Farías. (1985) Fusion of phospholipid vesicles induced by muscle glyceraldehyde-3-phosphate dehydrogenase in the absence of calcium. *Biochemistry.*, **24**, 1904-1909.

Nakayama, T., T. Ishii, T. Hotta, and K. Mizuno. (2008) Radial microtubule organization by histone H1 on nuclei of cultured tobacco BY-2 cells. *J Biol Chem.* , **283**, 16632-16640.

Nakazawa, M., T. Uehara, and Y. Nomura. (1997) Koningic acid (a potent glyceraldehyde-3-phosphate dehydrogenase inhibitor)-induced fragmentation and condensation of DNA in NG108-15 cells. *J Neurochem.*, **68**, 2493-2499.

Nigg, E.A. (1995) Cyclin-dependent protein kinases: key regulators of the eukaryotic cell cycle. *Bioessays*, **17**, 471-480.

North, B.J., B. L. Marshall, M. T. Borra, J. M. Denu, and E. Verdin. (2003) The human Sir2 ortholog, SIRT2, is an NAD+-dependent tubulin deacetylase. *Mol Cell.* , **11**, 437-444.

Ogryzko, V.V. (2001) Mammalian histone acetyltransferases and their complexes. *Cell. Mol. Life Sci.*, **58**, 683–692.

Ohsumi, K., C. Katagiri, and T. Kishimoto (1993) Chromosome condensation in Xenopus mitotic extracts without histone H1. *Science*, **262**, 2033-2035.

Orrego, M., I. Ponte, A. Roque, N. Buschati, X. Mora, and P. Suau. (2007) Differential affinity of mammalian histone H1 somatic subtypes for DNA and chromatin. *BMC Biol.* , **5**, 22.

Ozawa, Y., M. Towatari, S. Tsuzuki, F. Hayakawa, T. Maeda, Y. Miyata, M. Tanimoto, and H. Saito. (2001) Histone deacetylase 3 associates with and represses the transcription factor GATA-2. . *Blood*, **98**, 2116–2123.

Parseghian, M.H., R. L. Newcomb, and B. A. Hamkalo. (2001) Distribution of somatic H1 subtypes is non-random on active vs. inactive chromatin II: distribution in human adult fibroblasts. *J Cell Biochem.*, **83**, 643-659.

Parseghian, M.H., R. L. Newcomb, S. T. Winokur, and B. A. Hamkalo. (2000) The distribution of somatic H1 subtypes is non-random on active vs. inactive chromatin: distribution in human fetal fibroblasts. *Chromosome Res.* , **8**, 405-424.

Plumb, M., F. Marashi, L. Green, A. Zimmerman, S. Zimmerman, J. Stein, and G. Stein. (1984) Cell cycle regulation of human histone H1 mRNA. *Proc Natl Acad Sci U S A.* , **81**, 434-438.

Ponte, I., J. M. Vidal-Taboada, and P. Suau. (1998) Evolution of the vertebrate H1 histone class: evidence for the functional differentiation of the subtypes. *Mol Biol Evol.* , **15**, 702-708.

Rougeulle, C., J. Chaumeil, K. Sarma, C. Allis, D. Reinberg, P. Avner, and E. Heard. (2004) Differential Histone H3 Lys-9 and Lys-27 Methylation Profiles on the X Chromosome. *Mol. Cell. Biol.*, **24**, 5475–5484.

Sancho, M., E. Diani, M. Beato, and A. Jordan. (2008) Depletion of human histone H1 variants uncovers specific roles in gene expression and cell growth. *PLoS Genet.*, **4**, e1000227.

Sarg, B., W. Helliger, H. Talasz, B. Forg, H. Lindner. (2006) Histone H1 phosphorylation occurs site-specifically during interphase and mitosis: identification of a novel phosphorylation site on histone H1. *J Biol Chem.*, **281**, 6573-6580.

Sawin, K.E., and T. J. Mitchison. (1995a) Mutations in the kinesin-like protein Eg5 disrupting localization to the mitotic spindle. *Proc Natl Acad Sci U S A.* , **92**, 4289-4293.

Sawin, K.E., K. LeGuellec, M. Philippe and T. J. Mitchison. (1992) Mitotic spindle organization by a plus-end-directed microtubule motor. *Nature*, **359**, 540-543.

Sawin, K.E.a.T.J.M. (1995b) Mutations in the kinesin-like protein Eg5 disrupting localization to the mitotic spindle. *Proc Natl Acad Sci U S A.* , **92**, 4289-4293.

Schemies, J., W. Sippl, and M. Jung. (2009) Histone deacetylase inhibitors that target tubulin. *Cancer Lett.*

Schotta, G., M. Lachner, K. Sarma, A. Ebert, R. Sengupta, G. Reuter, D. Reinberg, and T. Jenuwein. (2004) A silencing pathway to induce H3-K9 and H4-K20 trimethylation at constitutive heterochromatin. *Genes Dev.* , **18**, 1251-1262.

Schroeder, T.M., R. A. Kahler, X. Li, and J. J. Westendorf. (2004) Histone deacetylase 3 interacts with runx2 to repress the osteocalcin promoter and regulate osteoblast differentiation. *J Biol Chem.*, **279**, 41998-42007.

Seyedin, S.M., and W. S. Kistler. (1980) Isolation and characterization of rat testis H1t. An H1 histone variant associated with spermatogenesis. *J Biol Chem.*, **255**, 5949-5954.

Seyedin, S.M., R. D. Cole, and W. S. Kistler. . (1981) H1 histones from mammalian testes. The widespread occurrence of H1t. *Exp. Cell Res*, **136**, 399-405.

Shen, X., and M. A. Gorovsky. (1996) Linker histone H1 regulates specific gene expression but not global transcription in vivo. *Cell.* , **86**, 475-483.

Shimada, M., A. Yamamoto, Y. Murakami-Tonami, M. Nakanishi, T. Yoshida, H. Aiba, and H. Murakami. (2009) Casein kinase II is required for the spindle assembly checkpoint by regulating Mad2p in fission yeast. *Biochem Biophys Res Commun.* , **388**, 529-532.

Sillibourne, J.E., B. Delaval, S. Redick, M. Sinha, and S. J. Doxsey. (2007) Chromatin remodeling proteins interact with pericentrin to regulate centrosome integrity. *Mol Biol Cell.* , **18**, 3667-3680.

Somers, M., Y. Engelborghs, and J. Baert. (1990) Analysis of the binding of glyceraldehyde-3-phosphate dehydrogenase to microtubules, the mechanism of bundle formation and the linkage effect. *Eur J Biochem.*, **19**, 437-444.

St-Denis, N.A., D. R. Derksen, and D. W. Litchfield. (2009) Evidence for regulation of mitotic progression through temporal phosphorylation and dephosphorylation of CK2alpha. *Mol Cell Biol.* , **29**, 2068-2081.

Stevens, F.E., H. Beamish, R. Warrener, and B. Gabrielli. (2008) Histone deacetylase inhibitors induce mitotic slippage. *Oncogene.*, **27**, 1345-1354.

Takemoto, A., K. Kimura, J. Yanagisawa, S. Yokoyama, and F. Hanaoka. (2006) Negative regulation of condensin I by CK2-mediated phosphorylation. *EMBO J.*, **25**, 5339-5348.

Talasz, H., W. Helliger, B. Puschendorf, and H. Lindner. (1996) In vivo phosphorylation of histone H1 variants during the cell cycle. *Biochemistry* . **35**, 1761-1767.

Tanaka, M., M. Kihara, B. Meczekalski, G. King, and E. Adashi. (2003) H1oo: a pre-embryonic H1 linker histone in search of a function. . *Mol. Cell. Endocrinol*, **202**, 5-9.

Th'ng, J.P., R. Sung, M. Ye, and M. J. Hendzel. (2005) H1 family histones in the nucleus. Control of binding and localization by the C-terminal domain. *J Biol Chem.* , **280**, 27809-27814.

Thevenet, L., C. Méjean, B. Moniot, N. Bonneaud, N. Galéotti, G. Aldrian-Herrada, F. Poulat, P. Berta, M. Benkirane, and B. Boizet-Bonhoure. (2004) Regulation of human SRY subcellular distribution by its acetylation/deacetylation. *EMBO J.* , **23**, 3336-3345.

Thoma, F., T. Koller, and A. Klug. (1979) Involvement of histone H1 in the organization of the nucleosome and of the salt dependent superstructures of chromatin. *J. Cell Biol.*, **83**, 403–427.

Thomas, M.J., and E. Seto. (1999) Unlocking the mechanisms of transcription factor YY1: are chromatin modifying enzymes the key? *Gene* **236**, 197-208.

Tisdale, E.J., C. Kelly, and C. R. Artalejo. (2004) Glyceraldehyde-3-phosphate dehydrogenase interacts with Rab2 and plays an essential role in endoplasmic reticulum to Golgi transport exclusive of its glycolytic activity. *J Biol Chem.*, **279**, 54046-54052.

Tong, J.J., J. Liu, N. R. Bertos, and X. J. Yang. (2002) Identification of HDAC10, a novel class II human histone deacetylase containing a leucine-rich domain. *Nucleic Acids Res.* , **30**, 1114-1123.

Tran, A.D., T. P. Marmo, A. Salam, S. Che, E. Finkelstein, R. Kabarriti, H. Xenias, R. Mazitschek, C. Hubbert, Y. Kawaguchi, M. Sheetz, T. Yao, and J. Bulinski. (2007) HDAC6 deacetylation of tubulin modulates dynamics of cellular adhesions. *J Cell Sci.* , **120**, 1469-1479.

Traverso, V., J. F. Morris, R. J. Flower, and J. Buckingham. (1998) Lipocortin 1 (annexin 1) in patches associated with the membrane of a lung adenocarcinoma cell line and in the cell cytoplasm. *J Cell Sci.*, **111**, 1405-1418.

Tumbar, T., G. Sudlow, and A. S. Belmont. (1999) Large-scale chromatin unfolding and remodeling induced by VP16 acidic activation domain. *J Cell Biol.*, **145**, 1341-1354.

Valentine, M.T., P. M. Fordyce, and S. M. Block. (2006) Eg5 steps it up! *Cell Division* **1**, 1028-1031.

Vaquero, A., M. Scher, D. Lee, H. Erdjument-Bromage, P. Tempst, and D. Reinberg. (2004) Human SirT1 interacts with histone H1 and promotes formation of facultative heterochromatin. *Mol Cell.* , **16**, 93-105.

Vaziri, H., S. K. Dessain, E. Ng Eaton, S. Imai, R. Frye, T. Pandita, L. Guarente, and R. Weinberg. (2001) hSIR2(SIRT1) functions as an NAD-dependent p53 deacetylase. *Cell.* , **107**, 149-159.

Waltregny, D., W. Glénisson, S. L. Tran, B. J. North, E. Verdin, A. Colige, and V. Castronovo. (2005) Histone deacetylase HDAC8 associates with smooth muscle alpha-actin and is essential for smooth muscle cell contractility. *FASEB J.* , **19**, 966-968.

Watamoto, K., M. Towatari, Y. Ozawa, Y. Miyata, M. Okamoto, A. Abe, T. Naoe, and H. Saito. (2003) Altered interaction of HDAC5 with GATA-1 during MEL cell differentiation. *Oncogene.*, **22**, 9176-9184.

Watson, J.D., T. Baker, S. Bell, A. Gann, M. Levine, and R. Losick. (2004) *Molecular Biology of the Gene.* Pearson Education Ltd.

Wei, L.N., X. Hu, D. Chandra, E. Seto, and M. Farooqui. (2000) Receptor-interacting protein 140 directly recruits histone deacetylases for gene silencing. *J Biol Chem.* , **275**, 40782-40787.

Wen, Y.D., V. Perissi, L. M. Staszewski, w. M. Yang, A. Krones, C. K. Glass, M. G. Rosenfeld, and E. Seto. (2000) The histone deacetylase-3 complex contains nuclear receptor corepressors. *Proc Natl Acad Sci U S A.*, **97**, 7202-7207.

Wen, Y.D., W. D. Cress, A. L. Roy, and E. Seto. (2003) Histone deacetylase 3 binds to and regulates the multifunctional transcription factor TFII-I. *J Biol Chem.*, **278**, 1841-1847.

Wilson, A.J., D. S. Byun, N. Popova, L. B. Murray, K. L'Italien, Y. Sowa, D. Arango, A. Velcich, L. H. Augenlicht, and J. M. Mariadason. (2006) Histone deacetylase 3 (HDAC3) and other class I HDACs regulate colon cell maturation and p21 expression and are deregulated in human colon cancer. *J Biol Chem.* , **281**, 13548-13558.

Wolffe, A.P. (1997) Histone H1. *The International Journal of Biochemistry & Cell Biology*, **29**, 1463-1466.

Wu, K., C. Aoki, A. Elste, A. A. Rogalski-Wilk, and P. Siekevitz. (1997) The synthesis of ATP by glycolytic enzymes in the postsynaptic density and the effect of endogenously generated nitric oxide. *Proc Natl Acad Sci U S A.* , **94**, 13273-13278.

Wu, K., Y. Yang, C. Wang, M. A. Davoli, M. D'Amico, A. Li, K. Cveklova, Z. Kozmik, M. P. Lisanti, R. G. Russell, A. Cvekl, and R. G. Pestell. (2003) DACH1 inhibits transforming growth factor-beta signaling through binding Smad4. *J Biol Chem.* , **278**, 51673-51684.

Xue, Y., J. C. Canman, C. S. Lee, Z. Nie, D. Yang, G. T. Moreno, M. K. Young, E. D. Salmon, and W. Wang. (2000) The human SWI/SNF-B chromatin-remodeling complex is related to yeast rsc and localizes at kinetochores of mitotic chromosomes. *Proc Natl Acad Sci U S A.*, **97**, 13015-13020.

Yamamoto, T., and M. Horikoshi. (1996) Cloning of the cDNA encoding a novel subtype of histone H1. *Gene*, **173**, 281-285.

Yan, W., L. Ma, K. Burns, and M. Matzuk. (2003) HILS1 is a spermatid-specific linker histone H1-like protein implicated in chromatin remodeling during mammalian spermiogenesis. *Proc. Natl. Acad. Sci. U S A*, **100**, 10546-10551.

Yang, W.M., C. Inouye, Y. Zeng, D. Bearss, and E. Seto. (1996) Transcriptional repression by YY1 is mediated by interaction with a mammalian homolog of the yeast global regulator RPD3. *Proc Natl Acad Sci U S A.* , **93**, 12845-12850.

Yang, W.M., S. C.Tsai, Y. D. Wen, G. Fejer, and E. Seto. (2002) Functional domains of histone deacetylase-3. *J Biol Chem.* , **277**, 9447-9454.

Yao, Y.L., W. M. Yang, and E. Seto. (2001) Regulation of transcription factor YY1 by acetylation and deacetylation. *Mol Cell Biol.* , **21**, 5979-5991.

Yde, C.W., B. B. Olsen, D. Meek, N. Watanabe, and B. Guerra. (2008) The regulatory beta-subunit of protein kinase CK2 regulates cell-cycle progression at the onset of mitosis. *Oncogene.* , **27**, 4986-4997.

Yoon, H.G., D. W. Chan, Z. Q. Huang, J. Li, J. D. Fondell, J. Qin, and J. Wong. (2003) Purification and functional characterization of the human N-CoR complex: the roles of HDAC3, TBL1 and TBLR1. . *EMBO J.* , **22**, 1336-1346.

Yuan, Z.L., Y. Guan, D. Chatterjee, and Y. E. Chin. (2005) Stat3 dimerization regulated by reversible acetylation of a single lysine residue. *Science.*, **307**, 269-273.

Zang , W.Q., A. M. Fieno, R. A. Grant, and T. S. Yen. (1998) Identification of glyceraldehyde-3-phosphate dehydrogenase as a cellular protein that binds to the hepatitis B virus posttranscriptional regulatory element. *Virology.*, **248**, 46-52.

Zhang, C., G. Vilk, D. A. Canton, and D. W. Litchfield. (2002a) Phosphorylation regulates the stability of the regulatory CK2beta subunit. *Oncogene.* , **21**, 3754-3764.

Zhang, J., M. Kalkum, B. Chait, and R. Roeder. (2002b) The N-CoR-HDAC3 nuclear receptor corepressor complex inhibits the JNK pathway through the integral subunit GPS2. *Mol Cell.* , **9**, 611-623.

Zhang, X., Y. Ozawa, H. Lee, Y. Wen, T. Tan, B. E. Wadzinski, and E. Seto. (2005) Histone deacetylase 3 (HDAC3) activity is regulated by interaction with protein serine/threonine phosphatase 4. *Genes Dev.*, **19**, 827-839.

Zhao, J., N. Morozova, L. Williams, L. Libs, Y. Avivi, and G. Grafi. (2001) Two phases of chromatin decondensation during dedifferentiation of plant cells: distinction between competence for cell fate switch and a commitment for S phase. *J Biol Chem.*, **276**, 22772-22778.

Zheng, L., R. G. Roeder, and Y. Luo. (2003) S phase activation of the histone H2B promoter by OCA-S, a coactivator complex that contains GAPDH as a key component. *Cell*, **114**, 255-266.

Zhou, X., V. M. Richon, R. A. Rifkind, and P. A. Marks. (2000) Identification of a transcriptional repressor related to the noncatalytic domain of histone deacetylases 4 and 5. *Proc Natl Acad Sci U S A.*, **97**, 1056-1061.

Zlatanova, J., and D. Doenecke. (1994) Histone H1 zero: a major player in cell differentiation? *FASEB J*, **8**, 1260-1268.

APPENDIX

LIST OF ABBREVIATIONS

Ac-H3K9	acetylated histone H3 lysine 9
AKAP95	nuclear A-kinase anchoring protein 95
APC	anaphase promoting complex
ATM	ataxia telangiectasia mutated kinase
ATR	ataxia telangiectasia Rad3-related kinase
BAF	barrier to autointegration factor
BCoR	BCL6 co-repressor
CBFA2T3	core-binding factor, runt domain, alpha subunit 2 translocated to 3
CBP	sarcoplasmic calcium-binding protein
Cdc	cell division cycle
Cdks	cyclin-dependent kinases
CHD	chromodomain helicase DNA binding protein
ChIP	chromatin immunoprecipitation
Chk	cell cycle checkpoint kinase
CK2	casein kinase II
C-Nap1	centrosomal NeK2-associated protein 1
CORO2A	coronin, actin binding protein, 2a
CRM	chromosome region maintenance

hCTD	histone c-terminal domain
DACH1	dachshund homolog 1
DAXX	death-domain associated protein
DNA	deoxyribonucleic acid
FITC	fluorescein isothiocyanate
FRAP	fluorescence recovery after photobleaching
GAPDH	glyceraldehyde-3-phosphate dehydrogenase
GCMa	glial cells missing homolog 1
GFP	green fluorescent protein
GLIS2	glis family zinc finger 2
GPS2	G protein pathway suppressor
GPS2	G protein pathway suppressor 2
H1K26	histone H1 lysine 26
H3K14	Histone H3 lysine 14
H3K27	histone H3 lysine 27
H3K4	histone H3 lysine 4
H3K9	histone H3 lysine 9
H3S10	histone H3 serine 10
H4K12	histone H4 lysine 12
H4K16	Histone H4 lysine 16
H4K16	Histone H4 lysine 16

H4K8	histone H4 lysine 8
HA95	homology to AKAP95
HAT	histone acetyl transferase
HDAC	histone deacetylase
HDI	histone deacetylase inhibitors
HMGN	high mobility group nucleosomal protein
HP1	heterochromatin protein 1
JMJD2A	jumonji domain containing 2a
Mad	mitotic arrest deficient
MAP1B	microtubule associated protein 1B
MeCP2	methyl CpG binding protein 2
MEF2	myocyte enhancing factor 2
MMTV	mouse mammary tumor virus
MSX1	MSH homeobox 1
N-CoR	nuclear receptor co-repressor 2
NeK2	NIMA-related kinase 2
NES	nuclear export signal
NIMA	never in mitosis A
NLS	nuclear localization signal
NRIP1	nuclear receptor interacting protein 1
hNTD	histone n-terminal domain

NuRD	nucleosome remodeling and deacetylase
PBS	phosphate buffer saline
PCAF	p300/CBP-associated factor
PI	propidium iodide
Plks	polo-like kinases
PP4	protein phosphatase 4
PVDF	polyvinylidene fluoride
RIPA	radio immunoprecipitation assay
Runx2	Runt-related transcription factor 2
SDS-PAGE	sodium dodecyl sulfate polyacrylamide gel electrophoresis
shRNA	small hairpin RNA
SirT	Sirtulin
SMC	structural maintenance of chromosomes
SMRT	silencing mediator for retinoid or thyroid-hormone receptors
SNK	Student-Newman-Keuls
SRY	sex determining region y
STAT3	signal transducer and activator of transcription 3
SWI/SNF	switch/sucrose nonfermentable
TBL1	transducin beta like protein 1
TBL1	transducin beta-like protein
TBLR1	transducin beta like receptor 1

TF	transcription factor
TR	Texas-red
TSA	tricostatin A
YY1	yin-yang1